Environmental Pollutants Disrupting Nuclear Receptor Signaling and Metabolism in Zebrafish

A Dissertation

Presented to

The Faculty of the Department of Biology and Biochemistry

University of Houston

In Partial Fulfillment

Of the Requirements for the Degree of

Doctor of Philosophy

By

Sharanya Maanasi Kalasekar

August, 2015

Environmental Pollutants Disrupting Nuclear Receptor Signaling and Metabolism in Zebrafish

Sharanya Maanasi Kalasekar

APPROVED:

Dr. Jan-Åke Gustafsson, Ph.D.
Committee Chair

Dr. Maria Bondesson Bolin, Ph.D.

Dr. Robert Schwartz, Ph.D.

Dr. Joseph Eichberg, Ph.D.

Dr. Yu Liu, PhD.

Dr. Ioannis Kakadiaris, PhD.

Dr. Dan Wells, Ph.D.
Dean, College of Natural Sciences and Mathematics

ACKNOWLEDGEMENTS

First, I would like to extend my deepest gratitude to Prof. Jan-Åke Gustafsson for providing me with the opportunity to carry out my graduate work at the Center for Nuclear Receptors and Cell Signaling. He has served as an inspiration and role model, and has made possible all of my achievements over the past five years.

Dr. Maria Bondesson has been instrumental, to say the least, in my completion of this degree. I thank her for her constant encouragement and support, guidance and inspiration. I thank her profusely for the several opportunities extended to me during the course of my PhD, for which I will be eternally grateful.

I would like to extend my gratitude to the members of my PhD Committee- Dr. Robert Schwartz, Dr. Joseph Eichberg, Dr. Yu Liu and Dr. Ioannis Kakadiaris- for their time, valuable inputs, and guidance.

I would like to thank other faculty members the University of Houston's Department of Biology and Biochemistry, including Drs. Daniel Frigo, Anders Strom, Christophoros Thomas, Shaun Zhang, George Fox, Tasneem Bawa-Khalfe, Ricardo Azevedo and David Tu for their inspiring science, valuable advice and patient guidance through my years at graduate school.

I would like to thank my collaborators Dr. Eleni Zacharia and Noah Kessler from the Kakadiaris group at UH, Dr. Clifford Stephan and his team at the Institute of Biosciences and Technology, Houston, and Dr.Philip Jonsson for his help with the microarray analyses.

I would like to thank Dr. Cecilia Williams for her encouragement and guidance during my early days at the University of Houston.

I am forever grateful to Drs. Anne Riu, Catherine McCollum and Caroline Pinto for their friendship and guidance, and for their constant support through graduate school. I could not wish for better colleagues, or friends. I am forever indebted to them.

I also thank the other members of the Gustafsson/Bondesson lab (past and present), including Triet Truong, Nestor Narvaez, Juan Narvaez and Muzamil Haq for taking the best care of our zebrafish, Savini Thrikawala and Rachna Sach for their hard work, co-ordinated team efforts, and adding new zing to the lab, Stephanie Sandri, and Drs. Ruixin Hao and Nicole Ducharme.

I would like to thank my graduate advisors Amanda Paul and Rosezelia Jackson, the past and present members of the administrative team at CNRCS including Dr. Edward Kuczynski, Holly Laurenzana, Emily Merrell, Adil Alvi and Anna Garza, and Kaberi Das and Bilqees Bhatti for their support.

I would like to thank all my friends at CNRCS, and the Department of Biology and Biochemistry at UH for making my years at graduate school unforgettable. They have all inspired and supported me, through times of fun as well as distress.

I would also like to thank my many friends in Houston for making the past five years among the most memorable in my life. I would especially like to thank Aditiyaa for all his love and encouragement, faith, support and guidance. I am also profusely grateful for

the support of my family, especially Raksha and Pranav, and their love and cheerful camaraderie.

Words cannot express the extent of my love and gratitude for my parents. I thank them for their unrelenting support and unconditional love, and for always inspiring me to dream big and stay optimistic. I am eternally indebted to them for everything they've magnanimously done for me, and for encouraging me to spread my wings even at times when I didn't realize I had any.

For their infinite love, I dedicate to them, this thesis,

All, but finite.

Environmental Pollutants Disrupting Nuclear Receptor Signaling and Metabolism in Zebrafish

An Abstract of a Dissertation

Presented to

The Faculty of the Department of Biology and Biochemistry

University of Houston

In Partial Fulfillment

Of the Requirements for the Degree of

Doctor of Philosophy

By

Sharanya Maanasi Kalasekar

August, 2015

ABSTRACT

Obesity affects a large proportion of the world's population, and the alarming rates of increase in its incidence have necessitated several research efforts investigating the risk factors for the disease. Apart from genetic and lifestyle factors, environmental exposure to chemicals, such as the estrogen diethylstilbestrol and the anti-diabetic Thiazolidinediones, are known to induce weight gain in animals and humans. Estrogens and Thiazolidinediones act via the Estrogen Receptors (ERs) and the Peroxisome Proliferator-Activated receptor gamma (PPARγ), respectively. In this study, we identify environmental endocrine disrupting chemicals (EDCs), which may act through ERs or PPARγ, to affect metabolism in zebrafish. Furthermore, we investigate the mechanism by which widely prevalent flame retardants and PPARγ agonists tetrabromobisphenol A (TBBPA) and tetrachlorobisphenol A (TCBPA) induce aberrant lipid accumulation in zebrafish.

Through our studies, we have identified 32 environmental chemicals from EPA's ToxCast library of 309 chemicals as being estrogenic in zebrafish. Through extensive surveys of previously published *in vitro* and *in vivo* studies of these chemicals, we infer that *in vitro* tests for estrogenicity may not fully predict toxicity *in vivo,* and posit that zebrafish be used in whole-organism high-throughput screens to supplement *in vitro* chemical prioritization efforts for toxicological testing. We have also established a zebrafish-based quantitative phenotypic screening platform to investigate the effect of environmental chemicals on yolk utilization. Zebrafish utilize the lipid-rich yolk during

development, and, we posit that chemical disruption of yolk-lipid utilization could suggest abnormal lipid mobilization and energy demand in developing zebrafish. Using this platform we evaluated nine chemicals, and found that while pesticide prochloraz delays yolk utilization, another pesticide butralin, the mammalian obesogen tributyltin, and TBBPA and TCBPA increase yolk lipid consumption by zebrafish larvae.

Transcriptomic analysis of TBBPA, TCBPA and TBT in zebrafish showed that, just as in mammals, these chemicals induce pathways driving adipogenesis. These chemicals also induced the expression of several genes related to lipid metabolism and inflammation. Although further studies are needed to determine the sequence of molecular events triggered by these chemicals, we posit that TBBPA, TCBPA and TBT may act through these pathways to induce obesity in zebrafish, and possibly, in humans.

CONTENTS

LIST OF FIGURES

LIST OF TABLES

CHAPTER 3: ZEBRAFISH ASSAYS TO IDENTIFY ESTROGENS AND ESTROGENIC OBESOGENS

Chapter 4: A zebrafish-based screening assay to identify disruptors of whole body-energy homeostasis

Chapter 5: A transcriptomic analysis of obesogen exposures in zebrafish

ABBREVIATIONS

AAT: α1-antitrypsin, human proteinase inhibitor

BMI: Body Mass Index – accepted measure of adiposity – ratio of body weight in kg to the height in m^2

DBD: Nuclear receptor DNA Binding Domain

dpf: days post fertilization – denotes age of the zebrafish embryo/larva

ER: Estrogen Receptor, a nuclear receptor

ERK: Extracellular signal-regulated kinase.

GFP: Green Fluorescent Protein - fluorescing reporter protein

LBD: Nuclear receptor Ligand Binding Domain

mpf: months post fertilization – denotes age of juvenile/adult zebrafish

NR: Nuclear Receptor

ORO: Oil Red O – Stain used on whole zebrafish or its tissue sections to visualize neutral lipid accumulation

OVX: ovariectomized

PI3K: Phosphatidylinositol-4,5-bisphosphate 3-kinase

PPAR: Peroxisome-Proliferator Activated Receptor, a nuclear receptor

PPRE: Peroxisome Proliferator Response elements

ROS: Reactive Oxygen Species – inducers of oxidative stress

YSL: yolk syncytial layer – extra-embryonic tissue forming the interface between the lipid-rich yolk and the developing zebrafish embryo

CHAPTER 1: INTRODUCTION

1.1 THE GLOBAL OBESITY EPIDEMIC

According to the World Health Organization ((http://www.who.int), 30% of Americans and 10-20% Europeans are obese, with Body Mass Index (BMI: ratio of weight in kg to height in meters squared) greater than 30. 11-17% of American and European children are also classified as obese (Fagot-Campagna 2000). Furthermore, obesity prevalence in developing countries continues to rise.

When energy intake exceeds energy expenditure, excess nutrients (carbohydrates and lipids) are stored as fat (triglycerides) in adipose depots. A long-term, persistent imbalance in energy intake versus expenditure leads to an increase in BMI, a prolonged perturbation of neuroendocrine control of energy utilization, and subsequently, onset of obesity.

Apart from having several molecular, physiological and psychological effects, increased BMI and obesity are established risk factors for several leading causes of preventable death, including heart disease, stroke, type 2 diabetes and cancer (Calle et al. 2003; Manson et al. 1990; Reeves et al. 2007; Song et al. 2004). On average, mild obesity decreases life expectancy by 2 to 4 years, and severe obesity (BMI>40) reduces life expectancy by 10 years (Whitlock et al. 2009). Moreover, the estimated annual medical costs of obesity in the U.S., in 2008, was $147 billion, and the medical costs for obese people were, on an average, $1,429 more than those of normal weight (Finkelstein et al. 2009). These realities have justified several multipronged efforts by scientists and

clinicians to attempt to cure obesity and to better understand its origins, so that it may be prevented.

1.2 Factors Affecting Energy Homeostasis

A number of genetic, behavioral, developmental and environmental factors are associated with obesity prevalence (van der Klaauw and Farooqi 2015). Given the high variability in body weight and fat mass, it is suspected that several of these factors interact to produce a spectrum of phenotypes in human body weight within a population.

Traditionally, evidence of the role of genetic factors in determining body weight came from family studies, often involving twins or adopted children. Bouchard and colleagues showed, through two studies with mono- and dizygotic twin pairs, that weight gain induced by overfeeding correlates well within a twin pair, but vary largely between different twin pairs (Bouchard et al. 1990; Bouchard et al. 1996). These studies, among many others that followed, indicate a role for heritable genetic factors *and* the environment in an individual's propensity to become obese.

More recently, several Genome-wide Association Studies (GWAS) have been performed to identify genetic loci, which are associated with increased BMI. The first GWAS-reported genetic loci linked to increased BMI were an intronic region in *fto* (Fat mass and obesity associated), and a variant downstream of the gene for *mc4r* (melanocortin receptor 4) (Dina et al. 2007; Frayling et al. 2007; Loos et al. 2008). The *fto* locus is also associated with altered eating behavior (Cecil et al. 2008; Wardle et al. 2008). There is

also substantial experimental evidence showing that deletion or overexpression of *fto* and genes in that region (such as *irx3*) in rodents have a significant effect on energy homeostasis (Church et al. 2010; Fischer et al. 2009; Gerken et al. 2007; Smemo et al. 2014; Stratigopoulos et al. 2008).

To date, more than 80 genetic loci associated with increased BMI across several diverse populations have been identified (meta-analysis by (Locke et al. 2015)). Several GWAS-identified loci have been previously identified to be involved in maintaining energy homeostasis, such as those of the leptin receptor (*lepr*), the SH2B adaptor protein 1, the brain-derived neurotrophic factor (*bdnf*), and the melanocortin receptor (*mcr4*). Other loci/genes identified through GWAS studies could be possible biological candidates for obesity, but have not been previously explored in the context of energy homeostasis or obesity. These findings present strong evidence for the heritable nature of obesity-related phenotypes. However, given the wide spectrum of such phenotypes found, even within a given genetically similar population, behavioral and environmental factors have recently been explored as causative agents in the development of obesity.

Psychological conditions such as anxiety and depression cause significant changes in feeding behavior and energy expenditure and disrupt control of energy homeostasis by the brain and the central nervous system. In the 1900s, the first evidence that the hypothalamus is involved in maintaining energy homeostasis surfaced from clinical studies of patients with hypothalamo-pituitary tumors, who displayed signs of altered feeding behavior and obesity (van der Klaauw and Farooqi 2015). It was subsequently

established that specific parts of the medial hypothalamus are responsible for controlling food intake and body weight gain/loss (Anand and Brobeck 1951; Brobeck et al. 1943; Brobeck 1946; Brooks and Lambert 1946; Hetherington and Ranson 1983; Kennedy 1950). Since these first studies, several significant contributions investigating neural control of appetite, satiety, weight gain and loss have been published (reviewed in (Horvath 2005)).

One of the most seminal findings in this field, however, came with the discovery of the gene encoding the adipose-tissue derived leptin (Campfield et al. 1995; Halaas et al. 1995; Pelleymounter et al. 1995; Zhang et al. 1994). This finding was a long-awaited discovery following the Coleman studies from two decades earlier, where it was suggested, using experiments with severely obese (*ob/*ob and *db/*db) mice, that there existed a circulating factor that regulated weight (Coleman and Hummel 1969; Coleman 1973).

It is now known that leptin is a master regulator of human energy homeostasis. When secreted by the adipose tissue in times of increased fat storage, leptin travels to the brain to signal satiety. Falling leptin levels signal nutritional depletion, such as that which occurs during fasting or weight loss (Chan et al. 2003). A leptin-induced hypothalamus signals to the brainstem to influence metabolically active peripheral tissues like the liver and pancreas. Because it signals to the hypothalamus, which signals to the amygdala and the periaquaductal gray, leptin also modulates behavior by affecting stress, anger, aggression and anxiety.

As can be perceived from the above example involving leptin-mediated neuroendocrine control of energy homeostasis and behavior, it is possible that genetic and behavioral risk factors of obesity interact to facilitate accelerated weight gain and disease onset. In fact, from the meta-analysis of BMI-related GWAS studies by Locke et al. ((Locke et al. 2015), it is clear that genes within the BMI-associated loci are enriched for expression in the brain and the central nervous system. In the analysis, 27 out of 31 significantly enriched tissues are in the central nervous system.

Since obesity arises because of an imbalance between calories ingested and calories expended, the role of the quantity and composition of daily diet in disease etiology and management cannot be ignored. As previously mentioned, one of the well-studied causal factors of obesity, leptin resistance, affects the control of appetite and satiety. Moreover, it is known that long-term overeating and the practice of binge eating can accelerate obesity onset (Marcus and Wildes 2014). The western diet, rich in saturated fat and simple carbohydrates, affects hippocampal control of hunger and satiety (reviewed in (Kanoski and Davidson 2011). A high-fructose diet has been implicated in obesity (Rayssiguier et al. 2006). It has also been suggested that the consumption of less proteins and more lipid- and sugar-rich sources of food accelerate obesity onset (reviewed in (Raubenheimer et al. 2015).

1.3 The Environmental Obesogen Hypothesis

Although several genetic and lifestyle factors are thought to play in a role in obesity etiology, these factors cannot fully explain the alarming rise in obesity occurrence over a short period of time. In 2002, it was first proposed that chemicals in the environment, including those used in agriculture, dyes, plastics, medicines, and food preservatives, could contribute to the rise in global obesity prevalence (Baillie-Hamilton 2002). In 2006, Grun and Blumberg proposed the "obesogen hypothesis", based on previously established mechanistic evidence of the involvement of nuclear receptors and endocrine signaling in genetic programing of obesity (Grun and Blumberg 2006).

1.4 Nuclear Receptors in Lipid Metabolism and Obesity

Nuclear receptors (NRs) are transcription factors that regulate target gene expression in response to several hormones or small molecule signals. NRs form a superfamily of phylogenetically- related proteins, with more than 270 genes in *Caenorhabditis elegans*, 21 genes in *Drosophila melanogaster*, 48 genes in humans, and 49 genes in the mouse genome (Adams et al. 2000; Robinson-Rechavi et al. 2001; Robinson-Rechavi and Laudet 2003; Sluder et al. 1999). The ligand-activated NR superfamily includes receptors for steroid hormones (such as estrogens, glucocorticoids, progesterone, mineralocorticoids, androgens, vitamin D3, ecdysone, oxysterols and bile acids), retinoic acids (all-trans and 9-cis isoforms), thyroid hormones, fatty acids, leukotrienes and prostaglandins (Escriva et al. 2000). NRs have many different functions including maintaining homeostasis, and regulating development, reproduction and metabolism.

Of the several NRs known (represented in (Gronemeyer et al. 2004)), the Estrogen Receptor (ER) and Peroxisome-Proliferator Activated Receptor (PPAR) families of NRs lie directly within the scope of this study, given their integral role in metabolism and susceptibility for disruption by environmental chemicals, and are discussed in detail below.

1.4.1 ERs

The sex hormone estrogen plays a vital role in regulating organismal reproductive development and function (Eddy et al. 1996; Hess et al. 1997; Lubahn et al. 1993), and maintenance of metabolic homeostasis (Barros and Gustafsson 2011; Bryzgalova et al. 2006; Faulds et al. 2012; Heine et al. 2000; Laudenslager et al. 1980).

Naturally occurring, physiological estrogens include steroids such as estrone (E1), 17β-estradiol (E2), and estriol (E3). E2, the most predominant form of estrogen, is synthesized from testosterone, an androgen, by a Cytochrome P450, family 19, subfamily A, polypeptide 1 (*cyp19a1*) aromatase enzyme. The aromatase enzyme is expressed in several tissues including the gonads, brains, adipose tissue, placenta and bone, during normal sexual development, as well as alongside pathologies such as breast and endometrial cancer, indicating the role of estrogens in these diverse tissues during development and disease etiology.

The functions of estrogens are exerted by Estrogen Receptors (ERs). Estrogen Receptor α (ERα, NR3A1) and Estrogen Receptor β (ERβ, NR3A2) are ligand-activated nuclear receptors, which share a structural domain organization similar to other NRs (Figure 1.1). ERα and ERβ were first cloned in the rat uterus and prostate/ovary, in the 1960s and 1996, respectively (Kuiper et al. 1996; Soloff and Szego 1969; Talwar et al. 1964). The ligand-activated cytoplasmic ERs are known to function by translocating to the nucleus, binding *cis*-acting estrogen response elements upstream of hormonally regulated genes, and recruiting co-activators or co-repressors to facilitate Estrogen Receptor-mediated regulation of gene expression.

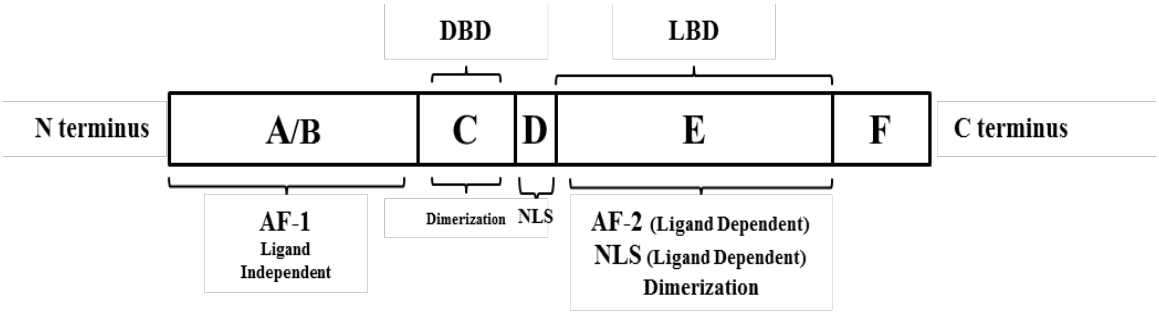

Figure 1.1. Schematic representation of the typical structural organization of NRs. The A/B domain includes the ligand independent transactivation function (AF1). Domains C and D possess the DNA binding (DBD), ligand independent nuclear localization signal (NLS) and dimerization functions. The E/F domains contain the ligand binding domain (LBD) and functions that are dependent on ligand binding, such as transactivation function 2 (AF2) and NLS.

A third estrogen receptor is membrane bound G-protein coupled receptor (GPER/GPR30). E2-activated GPER plays a significant role in various reproductive, neural and immune functions (reviewed in (Prossnitz and Barton 2011)) by transactivation of the Epidermal Growth Factor Receptor (EGFR), and activation of

cytoplasmic non-receptor protein kinase cascades (involving ERK and PI3K) and cAMP signaling.

Estrogen and estrogen receptors are known regulators of lipid and glucose metabolism (reviewed in (Barros and Gustafsson 2011; Faulds et al. 2012)). Polymorphisms in the gene encoding ERα (*esr1*) have been associated with perturbed lipoprotein metabolism (Lamon-Fava et al. 2010), type 2 diabetes (Yoshihara et al. 2009), and pathologies associated with aberrant metabolism, such as cardiovascular vascular disease (Schuit et al. 2004). Polymorphisms in the gene encoding ERβ (*esr2*) have been associated with eating disorders (Eastwood et al. 2002; Peter et al. 2005) and premature coronary artery disease (Nilsson and Gustafsson 2011).

Estrogens play a major role in regulating energy balance, appetite, fat distribution and body weight in mice (Dubuc 1985). Furthermore, in a study by Laudenslager et al. (Laudenslager et al. 1980), ovariectomized (OVX) estrogen-deficient mice showed an increase in food intake and fat mass, which was reversed on estrogen treatment. Injection of E2 into the paraventricular nucleus of the hypothalamus reduces food intake and body weight (Ahdieh and Wade 1982). Food intake also varies across women's menstrual cycle, with lowest daily food intake coinciding with the peri-ovulatory period, when estrogen levels are the highest (Asarian and Geary 2006).

As previously discussed, leptin is an important adipocyte-derived hormone, which signals suppression of appetite and satiety. Leptin levels are higher in human females relative to

males (Shimizu et al. 1997), and high levels of estrogens have been associated with increased sensitivity to leptin in the brain in rats (Ainslie et al. 2001).

Although the aforementioned studies may indicate that estrogen signaling, overall, has protective effects on obesity, no conclusions have been drawn in this regard, as estrogenic endocrine disrupting chemicals such as diethylstilbesterol (DES), described in more detail in section 1.5, act as obesogens by causing aberrant lipid metabolism and excessive fat accumulation.

1.4.2 PPARs

Peroxisome proliferators constitute a diverse class of compounds, which cause the proliferation of hepatic peroxisomes. Peroxisomes are organelles present in almost all eukaryotic cells. They play a crucial role in fatty acid catabolism, regulation of reactive oxygen species (ROS) through production of enzymes like catalase, and synthesis of plasmalogen, the most abundant phospholipid in myelin. Peroxisome proliferators, however, may also act as hepatic carcinogens, as peroxisome proliferation induces an increase in β-oxidation of fatty acids, resulting in increased, uncontrollable production of oxidative stress-inducing hydrogen peroxide.

Initial interest in studying peroxisome proliferators arose from simultaneous involvement of these compounds in lipid metabolism as well as hepatic carcinogenesis. The identification of peroxisome proliferator binding proteins in the rat liver (Lalwani et al.

1983; Lalwani et al. 1987), and the discovery that peroxisome proliferators induce specific gene transcriptional activity (Hardwick et al. 1987; Reddy et al. 1986), suggested that these compounds could act with mechanisms similar to steroid hormones like estrogen, which activate NRs (Beato 1989; Evans 1988; Green and Chambon 1988). In 1990, the first Peroxisome Proliferator Activated Receptor (PPAR, subsequently PPARα) was cloned (Issemann and Green 1990). It was later established through targeted disruption of the receptor, that the effects of peroxisome proliferators were indeed mediated by PPARα (Lee et al. 1995).

We now know of a PPAR subfamily of NRs consisting of PPARα, β/δ and γ, with each type of receptor being encoded by a distinct gene (Schoonjans et al. 1996). PPARγ was identified while cloning homologues of the NR superfamily in *Xenopus (Dreyer et al. 1992)*, and then in mice (Zhu et al. 1993). Subsequently, Spiegelman's group, in 1992, cloned the human PPARγ, when characterizing ARF6 as a factor that controlled the fat-specific enhancer of the *ap2* gene (Graves et al. 1992). Through several, extensive studies on receptor structure and function, it is now known that ligand-induced PPARγ activation plays a significant role in multiple obesity-associated pathways such as adipogenesis, lipid metabolism and inflammation (reviewed in (Tontonoz and Spiegelman 2008)).

There exist several naturally-occurring ligands for PPARγ. Multiple studies have shown that naturally-occurring polyunsaturated fatty acids such as linoleic acid and eicosapentanoic acid act as PPARγ ligands (Kliewer et al. 1997; Krey et al. 1997; Xu et

al. 1999). However, PPARγ responds poorly to physiologic fatty acids compared to the other PPARs, suggesting that PPARγ may actually be activated by modified fatty acids. Recently, it was shown that nitrated fatty acids and the growth factor-like phospholipid, lysophosphatidic acid activate PPARγ (Schopfer et al. 2005; Zhang et al. 2004). Certain J-series prostaglandins such as 15-deoxy-$\Delta^{12,14}$ – PGJ_2 (15d-PGJ2) are excellent activators of PPARγ at low micromolar concentrations *in vitro* (Forman et al. 1995; Kliewer et al. 1995). However, it is unlikely that 15d-PGJ2 is a biologically significant PPARγ ligand as it is only present at lower concentrations *in vivo*. Furthermore, human monocyte stimulation with the C-terminal fragment (C-36) of α1-antitrypsin (AAT) activates both PPARα and PPARγ (Dichtl et al. 2000). AAT is a major proteinase inhibitor found in several human tissues and blood plasma.

Although several possible naturally-occurring ligands for PPARγ have been investigated, the true endogenous PPARγ ligand produced during adipogenesis (Tzameli et al. 2004) has not yet been identified.

In addition to naturally-occurring PPARγ agonists, several synthetic ligands have been produced. Thiazolidinediones (TZDs), a chemical class of compounds with anti-diabetic activity, are well-studied PPARγ agonists (Houseknecht et al. 2002). Although TZDs such as Rosiglitazone are prescribed widely for their glucose lowering ability, they possess only a modest affinity for PPARγ. The search for more potent ligands, with half maximal effective concentrations below 50nM, has resulted in the identification of non-TZD PPARγ agonists like JTT-501, GW-7845, GW-0207, partial agonist triterpenoid-2-

cyano-3,12-dioxooleana-1,9-dien-28-oic acid (CDDO), and antagonists CDDO-Me (the methyl ester of CDDO), bisphenol A diglycdyl ether (BADGE) and acid LG-100641, among others (Cobb et al. 1998; Mukherjee et al. 2000; Shibata et al. 1999; Suh et al. 1999; Wang et al. 2000; Wright et al. 2000).

PPARγ, upon binding and activation by a ligand, undergoes a change in conformation, which facilitates its dimerization with the Retinoid X Receptor (RXR). The ligand-activated PPARγ-RXR heterodimer then, within the nucleus, binds to Peroxisome Proliferator Response Elements (PPRE) upstream of target genes, and recruits co-activators to induce gene transcription. Ligand-induced conformational change and dimerization, translocation to the nucleus from the cytoplasm, and binding to response element sequences in gene promoters is typical of canonical nuclear receptor signaling. Moreover, PPARγ contains structural domains similar in organization to other NRs (Figure 1.1). The C-terminal region of PPARγ is responsible for the receptor's interaction with RXR, and also contains the transcriptional activation domain AF2, which is important for the activation of co-activator proteins in a ligand-dependent manner. The C-terminal region also contains the receptor's Ligand Binding Domain (LBD). The N-terminal region of PPARγ contains the DNA Binding Domain (DBD), which is the part of the receptor that interacts with the promoter of the target gene. However, an interesting paradox was observed when the N-terminal of PPARγ was deleted, with the mutated receptor gaining greater transcriptional activity (Tontonoz et al. 1994). This finding is now known to be due, at least in part, to a receptor-inhibiting phosphorylation of the N-

terminal of the PPARγ protein by Mitogen-Activated Extracellular-signal Regulated Kinase 1/2 (ERK1/2) (Adams et al. 1997; Hu et al. 1996).

ERKs are activated by growth factor stimulation, and drive cell proliferation. Therefore, ERKs' inhibition of PPARγ-activity suggests a role for PPARγ in cell differentiation. In particular, PPARγ is known as the central or "master" regulator of adipogenesis – the process by which fibroblast-like preadipocytes differentiate into lipid-accumulating, mature adipocytes (reviewed in (Tontonoz and Spiegelman 2008). PPARγ expression and activation is induced during adipocyte differentiation, and is required for adipogenesis both *in vitro* and *in vivo* (Rosen et al. 1999). Rosen et al. established this fact by showing that PPARγ-null cells were unable to differentiate into adipocytes in chimeric mice despite retaining their ability to differentiate into other cell types. Moreover, expression and activation of PPARγ has been shown to be sufficient for adipogenesis (Tontonoz et al. 1994).

Apart from being critical for the formation of adipose tissue, PPARγ is involved in adipose tissue metabolic processes. Much of what is known about PPARγ's role in adipose lipid metabolism comes from studies using the TZDs as PPARγ agonists. Within adipocytes, PPARγ activation by TZDs increases lipid uptake, thereby shifting the lipogenesis (lipid synthesis) – lipolysis (lipid breakdown) balance towards lipid accumulation. Under normal circumstances, upon feeding, activation of PPARγ (by circulating free fatty acids) facilitates the storage of excess energy as lipids (triglycerides) into adipocytes. This is an essential process, as inefficiency in lipid sequestration within

adipocytes will lead to unwanted deposition of lipids into other organs (such as the liver, causing non-alcoholic hepatic steatosis, for example). However, under other conditions such as overfeeding or chronic PPARγ activation (by pharmaceutical TZDs, for example), there is an abnormal increase in the number of adipocytes (increased adipogenesis), as well as the size of the adipocytes (increased lipid accumulation) within the body, leading to increased adiposity/BMI and obesity. For example, although TZDs Rosiglitazone and Pioglitazone have proven to be effective therapy for the treatment of type 2 diabetes, an evident adverse effect from TZD treatment is weight gain (Shim et al. 2006).

1.5 The Role of Endocrine Disrupting Chemicals in Lipid Metabolic Disease

Environmental chemicals capable of disrupting hormonal signaling pathways are known as Endocrine Disrupting Chemicals (EDCs). These chemicals can act in multiple ways to alter hormone/NR signaling pathways. EDCs can act as agonists or antagonists for hormone receptors, thereby mimicking or counteracting the effects of the endogenous hormone. EDCs can also interfere with NR function by interacting with their co-activators/-repressors, affecting NR interaction with other transcription factors, or by eliciting transgenerational effects by directly affecting gene methylation patterns in germ cells (reviewed in (Tabb and Blumberg 2006)). While research on EDC effects has traditionally focused on developmental and reproductive perturbations involving the

estrogen and androgen receptors, the research focus has recently expanded to include investigation of EDCs affecting thyroid, neuroendocrine and metabolic functions.

Estrogenic chemicals such as diethylstilbesterol (DES), genistein and bisphenol A (BPA) are known to have obesogenic effects. DES is a potent estrogen, which was prescribed to pregnant women between the 1940s and 1970s, under the mistaken belief that DES could help alleviate complications related to pregnancy and miscarriages. An estimated 2-8 million pregnancies worldwide were exposed to this chemical. However, it has since then been well-established that DES exposure is carcinogenic, and that it has adverse effects on multiple generations via epigenetic mechanisms (Newbold et al. 1990; Newbold and McLachlan 1996; Newbold 2004). Neonatal exposure of mice to DES causes increased body weight, not during treatment, but in the adult animal (Newbold et al. 2008; Newbold et al. 2009), (Figure 1.2). This increase in body weight is associated with an increase in the percent of body fat and increased fat mass is observed in several locations, such as the inguinal, parametrial, gonadal and retoperitoneal fat pads (Newbold et al. 2005). DES-treated mice also have elevated levels of leptin and triglycerides, as well as increased number and size of adipocytes (Newbold et al. 2007).

Prenatal and neonatal exposures to low doses of BPA also cause increased body weight in mice and rats (Howdeshell et al. 1999; Nikaido et al. 2004; Somm et al. 2009). Numerous naturally occurring estrogens such as genistein, resveratrol and zearalonone also increase body weight in mice (Nikaido et al. 2004).

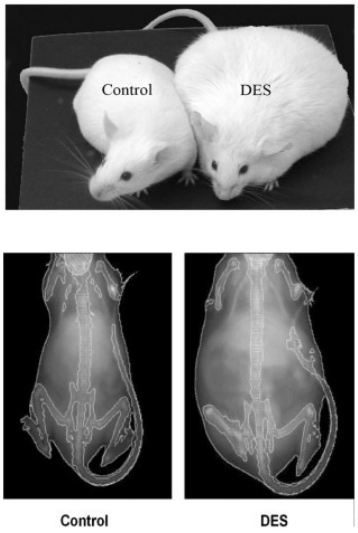

Figure 1.2. DES exposure induces body weight gain in mice. Neonatal exposure of CD-1 mice to DES caused increased body weight. Mice are approximately 6 months old. Bottom panel images are from densitometry of vehicle or DES exposed mice. Images reproduced from (Newbold et al. 2005) with permission from Elsevier.

As described in the previous section, the nuclear receptor PPARγ plays an important role in adipogenesis and adipocyte lipid metabolism and TZDs increase adiposity and cause weight gain (Shim et al. 2006). Another class of chemicals, the organotins, consists of compounds such as tributyltin (TBT), which are used for their anti-fouling properties in paints in the shipping industry, and for its anti-fungal properties on agricultural crops, wood treatments, textiles and industrial water systems. TBT is a well-known obesogen, and acts as a PPARγ/RXR agonist, inducing adipogenesis both *in vitro* and *in vivo* (reviewed in (Grun and Blumberg 2006)). Epidemiological evidence associates the levels of phthalates mono-benzyl and mono-ethyl-hexyl phthalate and their metabolites in urine with increased waist diameter and BMI (Hatch et al. 2008; Stahlhut et al. 2007). Phthalates are used as industrial plasticizers, and are ubiquitously prevalent. Mono-ethyl-hexyl phthalate (MEHP) is a known PPARγ activator, which promotes adipogenesis *in vitro* (Feige et al. 2007).

Since a large number of industrial and pharmaceutical chemicals are found in our environment, and because there is a suspicion that some of these chemicals may be contributing to rising obesity prevalence numbers worldwide, there is an undeniable need for the scientific research community to identify and investigate EDCs and their involvement in metabolic disease, and inform regulatory bodies and policy makers, in the hope that limiting the use of obesogenic chemicals may help prevent the disease.

1.6 Zebrafish Models of Metabolic Disease

Given the proliferation of metabolic pathologies such obesity, diabetes, non-alcoholic fatty liver disease and atherosclerosis worldwide, abundant research in this field has helped reveal some of the molecular pathways, which may contribute to these diseases. For instance, several genes possibly involved in obesity pathogenesis have been identified by GWAS (Locke et al. 2015), as described above.

In several other areas of research, vertebrate zebrafish have been used extensively to investigate variant function *in vivo*, using high-throughput forward, and more recently, reverse genetics. There are several advantages to using zebrafish as a model for biological research, the most important among them being that zebrafish share considerable genetic identity with humans (with approximately 70% of human genes having at least one zebrafish homologue (Howe et al. 2013)), and that several organs systems in zebrafish are similar to those in humans. There are several practical advantages to using zebrafish as well, including the translucent body of zebrafish

embryos that enables non-intrusive visualization *in vivo*, the availability of multiple genetic tools and a fully sequenced genome, their low cost, the ability to produce large numbers of offspring, which undergo rapid development.

The above advantages, while making it feasible to genetically manipulate zebrafish embryos and study them using real-time assays to visualize both development and molecular function, enable the use of zebrafish to conduct medium- to high-throughput molecular screening efforts for both drug discovery and environmental toxicology.

1.6.1 Zebrafish-Based High-Throughput Screening Assays

In environmental toxicology, traditionally, toxicological studies have involved testing a suspected toxic compound using a pre-determined set of *in vitro* and *in vivo* assays. For example, a compound would be tested by determining hepatotoxicity/kidney toxicity using cells *in vitro*, and by studying possible developmental and reproductive effects using animal models. The disadvantage of such a toxicity testing paradigm is that the chosen endpoints may not represent all the possible endpoints, which a chemical could affect. Also, the use of large animal models (rodents and rabbits) for testing means that toxicity testing is limited to a few doses and exposures. Accumulating evidence, in fact, suggests that many compounds are capable of eliciting a spectrum of effects based on the dose tested, the route of administration, the model used, the exposure window, the endpoint measured, and the timing of endpoint measurement.

Apart from the numerous variables that complicate the design of toxicological studies and the interpretation of the results from these studies, the sheer number of chemicals that need to be tested and/or regulated creates a seemingly insurmountable challenge. However, using whole organism models such as zebrafish, which can be scaled up to high-throughput testing platforms and used for studying several chemicals in multiple combinations of dose, exposure window, and endpoints being measured, can, potentially, solve the problem.

Using zebrafish to perform phenotypic screens has hastened the process of chemical discovery, for drug development as well as chemical regulation purposes. Since 2000, there have been at least 66 zebrafish-based chemical screens performed (reviewed in (Rennekamp and Peterson 2015)), with most studies using embryo/larval stage zebrafish in 96-well plates. While the early zebrafish screens used wild type zebrafish embryos and screened chemical libraries for general toxicity by looking at embryo morphology and development, more recent screens have been developed using mutant and transgenic zebrafish lines to examine many different phenotypic endpoints, such as heartbeat (Milan et al. 2003; Peal et al. 2011), cell proliferation and migration (Gutierrez et al. 2014; Liu et al. 2013; Robertson et al. 2014; Yeh et al. 2009), behavior (Baraban et al. 2013; Kokel et al. 2010; Kokel et al. 2013; Rihel et al. 2010; Wolman et al. 2011) and lipid absorption (Clifton et al. 2010).

1.6.2 Zebrafish Models for Obesity

Whole-body energy homeostasis involves a complex interplay between several metabolically active tissue/organs and the co-ordination of numerous endocrine signals. Therefore, chemical screens for metabolic endpoints using *in vitro* models, which cannot recreate the complexity that exists *in vivo,* can be supplemented or even replaced with zebrafish-based screening assays. The development of lipid staining molecules and protocols for zebrafish has enabled the study of lipid metabolism in the zebrafish (Holtta-Vuori et al. 2010).

Several zebrafish models have also been developed to better understand lipid metabolism and obesity-related pathways in the species. Since several of these pathways seem to be conserved between the zebrafish and humans, zebrafish models for obesity have been well-received (Seth et al. 2013).

1.7 PROJECT OBJECTIVES

The overall objective of the studies described in this thesis is to develop and implement zebrafish-based high-throughput screening and mechanistic models to explore the role of EDCs in lipid metabolism, and therefore, obesity. We focus our efforts specifically on EDC disruption of the ER and PPARγ signaling pathways.

In Chapter 3, our efforts to identify estrogenic environmental pollutants using a high-throughput zebrafish-based assay are described. Our findings were also compared to existing *in vitro* and *in vivo* estrogenicity studies to better understand the strengths and

setbacks of our zebrafish-based screening model. Finally, the ability of estrogens to affect lipid storage in the zebrafish model was explored.

In Chapter 4, the development of a zebrafish-based screening model to evaluate environmental chemicals for their ability to affect lipid utilization is described. This was accomplished by measuring yolk lipid consumption in developing zebrafish larvae.

In Chapter 5, I describe the elucidation of the mechanism by which PPARγ agonists tetrabromobisphenol A and tetrachlorobisphenol A affect lipid metabolism in the zebrafish.

CHAPTER 2: MATERIALS AND METHODS

2.1 ZEBRAFISH MAINTENANCE

All lines (wild-type and transgenic) of zebrafish were housed and used according to the maintenance and experimental protocols approved by the Institutional Animal Care and Use Committee at the University of Houston. Adult zebrafish were maintained in 3.5 L tanks in a Tecniplast system (Tecniplast USA Inc., West Chester, PA) supplied continuously with circulating filtered water at 28.5˚C on a 14h/10h light/dark cycle. Transgenic fish HGn50D were obtained from Dr. Kawakami, the National BioResource Project from the Ministry of Education, Culture, Sports, Science and Technology of Japan (Asakawa et al. 2008; Urasaki et al. 2008). Transgenic fish *Tg(5xERE:GFP) (Gorelick and Halpern 2011)* were obtained from Dr. Daniel Gorelick.

2.2 CHEMICALS

Prochloraz (purity 99.1%, CAS 67747-09-5), tributyltin (TBT) chloride (96%, CAS 1461-22-9), tetrabromobisphenol A (TBBPA, 2,2-bis(3,5-dibromo-4-hydroxyphenyl)propane) (97%, CAS 79-94-7), perfluorooctanoic acid (PFOA) (96%, CAS 335-67-1), imazalil (99.7%, CAS 35554-44-0), butralin (99.8%, CAS 33629-47-9), clofibrate (CAS 637-07-0), and gemfibrozil (CAS 25812-30-0) were obtained from Sigma-Aldrich (St.Louis, MO). Tetrachlorobisphenol A (TCBPA, 2,2-bis(3,5-dichloro-4-hydroxyphenyl)propane) (95%, CAS 79-95-8) was purchased from TCI America (Portland, OR). ToxCast chemicals were obtained from US-EPA, provided at 20mM concentrations in DMSO. All chemicals were dissolved and diluted in DMSO to make 1000X stock solutions.

2.3 Oil Red O Staining

The same protocol was followed for lipid accumulation studies in Chapter 3 and 4. Embryos were harvested after spawning and housed in a 28.5˚C incubator with 14h/10h light/dark cycle in embryo media E3 (5 mM NaCl, 0.17 mM KCl, 0.33 mM CaCl2, and 0.33 mM MgSO4). For yolk utilization studies, 2 and 5 dpf, larvae were euthanized in tricaine methylsulfonate (MS-222, Sigma-Aldrich), and fixed in 4% paraformaldehyde overnight at 4ºC. For lipid accumulation assays following E2 or BPA treatment, 3 dpf zebrafish larvae were treated in 3mL of E3 media containing E2/BPA dissolved in DMSO, or DMSO. The chemical solution was replenished between 6-10 dpf. The larvae were also fed with ground egg yolk for 6 hours from 6-10 dpf. Larvae were euthanized at 11 dpf with Tricaine, and fixed with 4% PFA. Fixed larvae from both experiments were then washed with 0.1% Tween-20 in PBS (PBT), and stained with a 0.3% Oil Red O (ORO) solution for 3 hours at room temperature. Staining was followed by PBT washes. Stained larvae were then stored in 90% glycerol.

2.4 Embryo Treatment and Scoring for the zfERE Assay

Tg(5xERE:GFP) embryos were harvested after spawning and allowed to develop in a Petri dish at 28.5˚C with 14h/10h light/dark cycle in E3 media. At 3 dpf, embryos were transferred into each well of a 96-well plate containing 90µL E3. The embryos were exposed to 10µL of prepared stock solutions of compounds dissolved in E3 media and dimethylsulfoxide (DMSO) or to DMSO alone (vehicle-control). The compounds were added to the plates using a Tecan liquid handler robot available at the laboratory of our collaborator Dr. Clifford Stephan, from Texas A&M IBT Institute, Houston, Texas. At 4

dpf, the larvae were anesthetized and manually scored while in 96-well plates using an Olympus IX51 inverted fluorescence microscope using a 4X objective.

2.5 EMBRYO TREATMENT AND IMAGING FOR MEASUREMENT OF YOLK UTILIZATION

HGn50D embryos were harvested after spawning and allowed to develop in a Petri dish at 28.5˚C with 14h/10h light/dark cycle in E3 media. At 2 dpf, a clutch of 20 embryos were transferred into each well of a 6-well plate containing 4 ml E3. The embryos were exposed to compounds dissolved in dimethylsulfoxide (DMSO) or to DMSO alone (vehicle-control). At 5 dpf, the larvae were transferred to 96-well plates (1 embryo/well in approximately 100 µL E3), manually imaged on an Olympus IX51 inverted fluorescence microscope using a 4X objective, and images captured using an Olympus XM10 camera with CellSens Dimension v1.9 software (Olympus). Exposures were not performed directly in 96 well plates because the small volume could result in motility restriction, thereby causing decreased yolk absorption. The larvae were not anaesthetized, and thus swam in an upright position, facilitating image capture of the ventral side of the larvae. Chemical exposure experiments for all concentrations were repeated 2-4 times, with 1-2 sets of 20 embryos per experiment. Images of ORO stained zebrafish were acquired using a Nikon AZ100M microscope with a color camera DS Fi1 (Nikon) and the NIS-Elements AR analyzing program. For confocal imaging, embryos were imaged at 72 hpf using an Olympus FluoView 1000 confocal microscope with an 800 x 800 aspect ratio at 4 µs/pixel using the default eGFP filter setting. Images were processed by Olympus Fluoview software.

To determine LC_{50} values and morphological malformations, a clutch of 20 TAB 14 embryos were exposed to a dose range of the compounds at 2 dpf, and lethality and morphology were scored at 5 dpf.

2.6 TREATMENT FOR MICROARRAY ANALYSIS

Wild-type (Tüebingen-AB; TAB) fish at two months old were isolated in Falcon tubes (Corning Life Sciences, Tewksbury, MA) with 40 mL of clean fish system water, and treated with TBBPA at 100 nM, TCBPA at 100 nM, or TBT at 1 nM (n = 5 per chemical). Control fish were treated with 0.1% DMSO (vehicle). All treatments were renewed daily after a one-hour feeding with live artemia (Brine Shrimp Direct, Ogden, UT) for a total exposure of two days. At the end of the treatments on the third day, the fish were washed multiple times with clean fish system water without chemicals and anesthetized with 0.04% MS-222 (Pentair Aquatic Eco-systems, Apopka, FL).

2.7 RNA EXTRACTION FOR MICROARRAY ANALYSIS

Each fish sample from the control and treatment groups was washed once with purified distilled, deionized water and homogenized. Total RNA was extracted using Trizol reagent (Invitrogen, Carlsbad, CA), purified using RNeasy (Qiagen, Valencia, CA) and pooled. RNA concentrations were measured with NanoDrop 1000 spectrophotometer (Agilent Technologies, Palo Alto, CA). ScDNA was synthesized using Superscript III reverse transcriptase (Invitrogen Corporation, Carlsbad, CA) with random hexamer primers were used for cDNA synthesis.

2.8 QUANTITATIVE REAL-TIME POLYMERASE CHAIN REACTION (RT-QPCR)

RT-qPCR studies were performed using the ABI 7500 Fast Real-Time PCR system (Applied Biosystems, Foster City, CA) with iTaq Universal SYBR Green Supermix (Bio-Rad, Hercules, CA) according to the manufacturer's protocol. Primers for confirmation of selected genes were designed using Primer Blast (http://www.ncbi.nlm.nih.gov/tools/primer-blast/), and synthesized by Integrated DNA Technologies, Inc (Coralville, IA). The primer sequence list used to detect zebrafish transcripts is provided in Appendix Table 5C. Transcript abundance for the zebrafish experiments was normalized to Elongation Factor 1α (*ef1α*) as the endogenous reference gene and normalization of the data was done using the ΔΔCt method.

2.9 MICROARRAY SCANNING AND ANALYSIS

Microarray analysis was conducted using Agilent zebrafish (V3) gene expression microarray 4X44K (Design ID 026437). Sample labeling, hybridization and array scanning were performed by the Genomic and RNA Profiling Core at Baylor College of Medicine (Houston, TX), as described previously (Hao et al. 2013). R environment for statistical computing using the Limma package for analysis of differential expression (Smyth et al. 2005) was executed to process the microarray data. Arrays were quantile normalized, replicated spots averaged and empirical Bayes methods applied for differential-expression analysis. Four arrays of control and TBBPA-, TCBPA-, or TBT-treated zebrafish were used for microarray data analysis. Statistical significance was assessed using false-discovery rate (FDR) at 5%. The resulting dataset with FDR-

adjusted $p<0.05$ and absolute fold-change (FC) $\geq |\pm 1.5|$ were subjected to hierarchical clustering using complete-linkage clustering of the Euclidean distance measure of the FC values in each sample, and Venn diagrams were generated to represent the overlapping genes between all three treatments. Non-annotated probes were excluded from the dataset, and probes mapped to the same gene were resolved by averaging the fold-change values to maintain a conservative analysis. The list of statistically significant genes commonly and uniquely regulated by TBBPA, TCBPA and TBT are displayed in Appendix Table 5D.

2.10 Biological function and tissue enrichment analysis

Differentially expressed zebrafish genes ($p<0.05$, FC $\geq |\pm 1.5|$) were mapped to their corresponding human homologues using Homologene (www.ncbi.nlm.nih.gov/homologene), ZFIN (http://zfin.org) and Ensembl (http://ensembl.org). Pathway Studio software 10.5 (Elsevier Inc., MD, USA) was used for the analyses of enriched biological processes for the human homologues of the zebrafish genes regulated by TBBPA, TCBPA and TBT using Gene Ontology (GO) functional annotations. Enriched subnetwork analysis was used to identify transcriptional regulators that are responsible for the gene expression profile obtained from the microarray data. Fisher Exact test was applied to determine enriched GO functional groups and subnetworks; $p<0.05$ was considered significant. REVIGO (http://revigo.irb.hr) was used to summarize the list of enriched GO terms obtained after functional analysis of the whole set of differentially expressed genes by each chemical.

GO terms with $p<0.001$ and SimRel semantic medium (0.7) similarity were used for REVIGO clustering analysis.

Tissue enrichment analysis was performed with zebrafish genes regulated by TBBPA, TCBPA, and TBT using the ZFIN_Anatomy functional category of the NIH DAVID Bioinformatic Resources database (http://david.abcc.ncifcrf.gov) to evaluate the zebrafish tissues most affected by the chemicals. Fisher Exact test was used to calculate enriched functional categories with $p<0.05$ significance.

2.11 Software Package ZebRA

A novel software package, named ZebRA, for automatically and accurately segmenting and quantifying the fluorescing yolk in images captured at the end of the treatment period was developed by our collaborators from the laboratory of Dr. Ioannis Kakadiaris at the University of Houston's Computer Science department, and can be downloaded from http://cbl.uh.edu/ZEBRAFISH/research/software/ (will be made publicly available shortly). The image processing algorithm of the software program was implemented in MATLAB 2012a with the Image Processing Toolbox. Comprehensive procedures of software features and development are described in detail in the original journal publication (Kalasekar et al. 2014).

2.12 Statistical Analysis For Yolk Utilization Studies

After image analysis, y_a ratios were computed using Microsoft Excel from Microsoft Office Professional Plus 2010. We define the y_a ratio as the ratio of the area of the yolk of

the treated larva (measured in number of pixels) to the average yolk area of the respective control group of vehicle treated-larvae. One-way ANOVA with post-hoc Dunnett's test was performed using GraphPad Prism version 5.00 for Windows (GraphPad Software, San Diego, California USA). All treatment groups were compared to the DMSO-treated control group for Dunnett's analyses for statistical significance. GraphPad Prism version 5.00 was also used to prepare graphical representations. Vertical box and whiskers plots represent the distribution of y_a ratios across doses. The box extends from the 25th to 75th percentile, with the median (the line within the box) and the mean (+) represented. The whiskers run from 10^{th}-90^{th} percentile of data points. For a given chemical, the stacked column graphs are representations of the same data values as those used to plot the box and whiskers graphs. GraphPad Prism version 5.00 was also used to plot zebrafish lethality dose curves and calculate LC_{50} values.

CHAPTER 3: ZEBRAFISH ASSAYS TO IDENTIFY ESTROGENS AND ESTROGENIC OBESOGENS

3.1 INTRODUCTION

Estrogens play a critical role in several physiological processes such as development, sexual maturation, reproduction and maintenance of metabolic homeostasis, across numerous species. The importance of estrogen signaling is evident from the high degree of evolutionary conservation of the components of the estrogen signaling pathway (the physiological hormones, the enzyme CYP19 aromatase that is involved in their synthesis and the estrogen receptors) among diverse classes of organisms, including the zebrafish, a teleost vertebrate (Callard et al. 2011).

The zebrafish genome contains three estrogen receptor (ER) genes, as opposed to the two genes in mammals (Hawkins et al. 2000). However, there exist similarities between human and zebrafish ERs with regard to protein sequences, tissue localization and mechanisms of gene regulation. Zebrafish ERα (esr1) is orthologous to the human ERα, and ERβ1 (esr2b) and ERβ2 (esr2a) are orthologous to the human ERβ (Bardet et al. 2002). The expression of zfERs partially overlaps in estrogenic tissues such as the gonads, brain, pituitary and liver, similar to ER expression patterns in mammals (Kuiper et al. 1997). Furthermore, as in mammals, the zebrafish ERs (zfERs) regulate gene expression by interacting with consensus DNA Estrogen Response Elements (EREs) within target gene promoters in an estrogen-dependent manner (Bardet et al. 2002; Lassiter et al. 2002; Menuet et al. 2002).

In addition to estrogens and ERs, hormones such as progestogens and androgens, and their receptors are fairly conserved between zebrafish and mammals (Chen et al. 2010; de Waal et al. 2008; Hanna et al. 2010; Hossain et al. 2008; Jorgensen et al. 2007) and the hypothalamo-pituitary-gonadal axis is organized similar to mammals (Abraham et al. 2010; Herzog et al. 2004; Steven et al. 2003). Furthermore, zebrafish are both cost-effective and practical to use for high-throughput reporter-based screening assays because of their ability to produce large numbers of offspring, optical transparency and small size. For all of these reasons, the zebrafish is increasingly becoming a valuable model for implementing drug screens (Gibert et al. 2013; Raldua and Pina 2014), investigating hormone function (McGonnell and Fowkes 2006), and identifying environmental chemicals involved in developmental toxicity and endocrine disruption (Ankley and Johnson 2004; Mathias et al. 2012; McCollum et al. 2011; Miscevic et al. 2012).

Unlike pharmaceutical chemicals, which are extensively tested for adverse effects before being released into the market, industrial and agricultural chemicals (such as plasticizers, food preservatives, anti-fouling agents and pesticides) are not thoroughly investigated for potential toxicities. Industries producing these chemicals are only required to notify regulatory agencies (such as the United States Environmental Protection Agency or EPA) of the chemicals produced. It is the regulatory agency's task to identify potential toxic effects of industrial chemicals. This current paradigm implies two major consequences: firstly, the population at large, and the entire ecosystem is exposed to potentially harmful, yet unidentified chemicals, which may or may not cause to human and animal life and the ecosystem, and, secondly, the regulatory agencies are faced with the Herculean task of

sifting through tens of thousands of new chemicals produced annually for ascertaining their potential adverse effects. The latter consequence is fueled by antiquated toxicity testing, which requires collecting data on one chemical at a time, using a standardized battery of tests, many of which are performed on rodents. However, more recently, higher throughput toxicity testing has been encouraged (Boekelheide and Campion 2010), which recommends the design and implementation of computational in silico modeling, in *vitro* assays and assays based on small model organisms like zebrafish to accelerate toxicological studies.

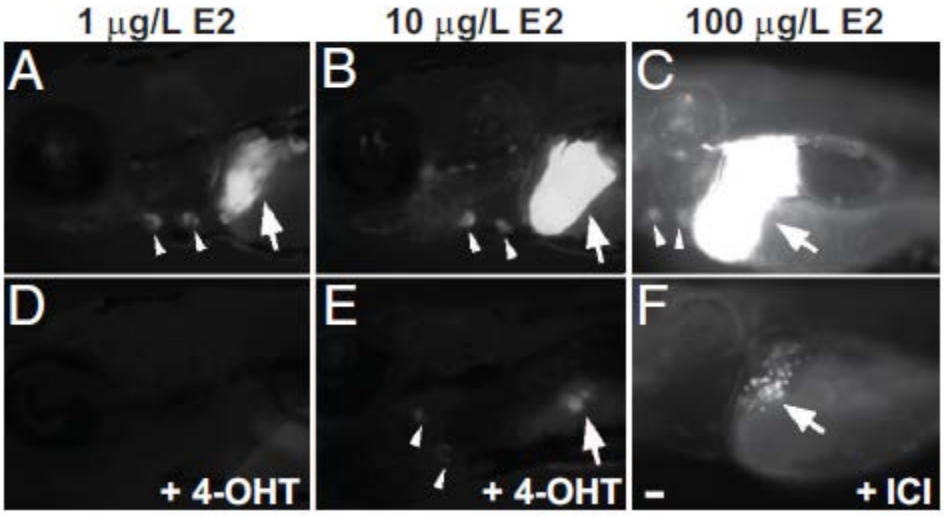

Figure 3.1. E2 induces ERE-driven GFP expression in the transgenic zebrafish *Tg(5xERE:GFP).* Figure taken from (Gorelick and Halpern 2011), available on PubMed Central freely. Lateral view of zebrafish larvae, with anterior to the left. **A-C: Fluorescence increases with dose.** E2 induced GFP expression in the heart valves (marked with arrowheads) and liver (marked with an arrow). D-F: E2 induced GFP expression is diminished in the presence of 4-hydroxytamoxifen or ICI. Scale bar: 50μm.

In order to identify environmental chemicals, which could act as estrogenic endocrine disrupting chemicals (EDCs), we sought to develop a zebrafish-based high-throughput screening assay using the *Tg(5xERE:GFP)* transgenic zebrafish line (Gorelick and Halpern 2011). This transgenic line was generated to monitor ER activation in larval and adult zebrafish, and contains a five tandem repeats of the consensus ERE sequence (5'-GGTCACAGTGACC-3') upstream of the gene for the Green Fluorescent Protein (GFP). Gorlick and Halpern have previously shown that larval *Tg(5xERE:GFP)* transgenic fish displayed induction of transgene activity in the heart valves, brain and liver upon treatment with E2 (Figure 3.1). The induction in ERE-driven GFP expression was increased with E2 dose, and repressed by ER antagonists 4-hydroxytamoxifen and ICI, indicating that transgene induction was specific to ER activation by an agonist and inhibition by an antagonist.

In the present study, we used the *Tg(5xERE:GFP)* zebrafish larvae to screen the 309 environmental chemicals of the EPA ToxCast^{TM} Phase I library. The Toxicity Forecaster or ToxCast effort was launched by the EPA in 2007 to prioritize the most biologically active chemicals for toxicity testing. The Phase I library is a compilation of mostly pesticides, herbicides or antimicrobials, and has been evaluated by EPA's Endocrine Disruption Screening Program (EDSP) using *in vitro* HTS assays already.

The positive hits from our assay were then also compared to prior literature data to investigate if rodent or other fish assays were concordant with the zfERE assay. And,

finally, we investigate if estrogens can cause aberrant lipid accumulation in larval zebrafish.

3.2 RESULTS

3.2.1 A zebrafish-based high-throughput screening platform to identify estrogenic environmental pollutants

The zfERE assay was developed to enable fast and efficient screening of ToxCast™ Phase I chemicals. In each well of a 96-well plate, one 3 days post fertilization (dpf) zebrafish larva was exposed to 100μL total volume of the chemical solution in E3. Three wells of one larva each were tested per chemical per dose. The doses tested were 0.2, 2 and 20μM. After 24 hours of exposure, the larvae were anesthetized and manually scored for lethality and GFP expression qualitatively by fluorescence microscopy.

Of the 309 chemicals in the ToxCast™ Phase I library, 32 chemicals were annotated as positive hits in the zfERE assay. To be considered positive, a chemical had to induce ERE-driven GFP expression in at least 2 larvae for at least 1 dose tested. Figure 3.2 represents the ERE-induction and mortality effects of the positive hit compounds from the screen. Control treatments were performed with 8 larvae per 96-well plate treated with the vehicle 0.1% dimethyl sulfoxide (DMSO) only. The chemical classes of the hit compounds as well as their commercial use are listed in Table 3.1. Except bisphenol A (BPA), all other compounds identified are used in pest/germ/weed control in agriculture. The chemical triclosan is used as a fungicide, but is also well-known for its ubiquitous presence as an anti-bacterial agent in hand sanitizers, soaps and household cleaners. BPA

and triclosan are different types of phenol compounds. Insecticide pyrethroids bifenthrin, cyfluthrin and esfenvalerate are also among the hits in the zfERE assay.

The widely prevalent plasticizer BPA is known to activate estrogen receptors in humans and zebrafish (Pinto et al. 2014). Accordingly, BPA was identified as a strong activator of ERE-driven GFP expression in the zfERE assay (Figure 3.2, grid 1). BPA induced GFP expression in the heart valves ("H" in Figure 3.2) at all the doses tested, liver ("L) at 2 and 20μM, and the pancreas ("P") and ears ("E") at the highest tested dose of 20μM. The identification of BPA as an activator of estrogen signaling in this model supports the reliability of the model.

Fig. 3.2. Induction of zfERE-driven GFP expression by ToxCast Phase I chemicals

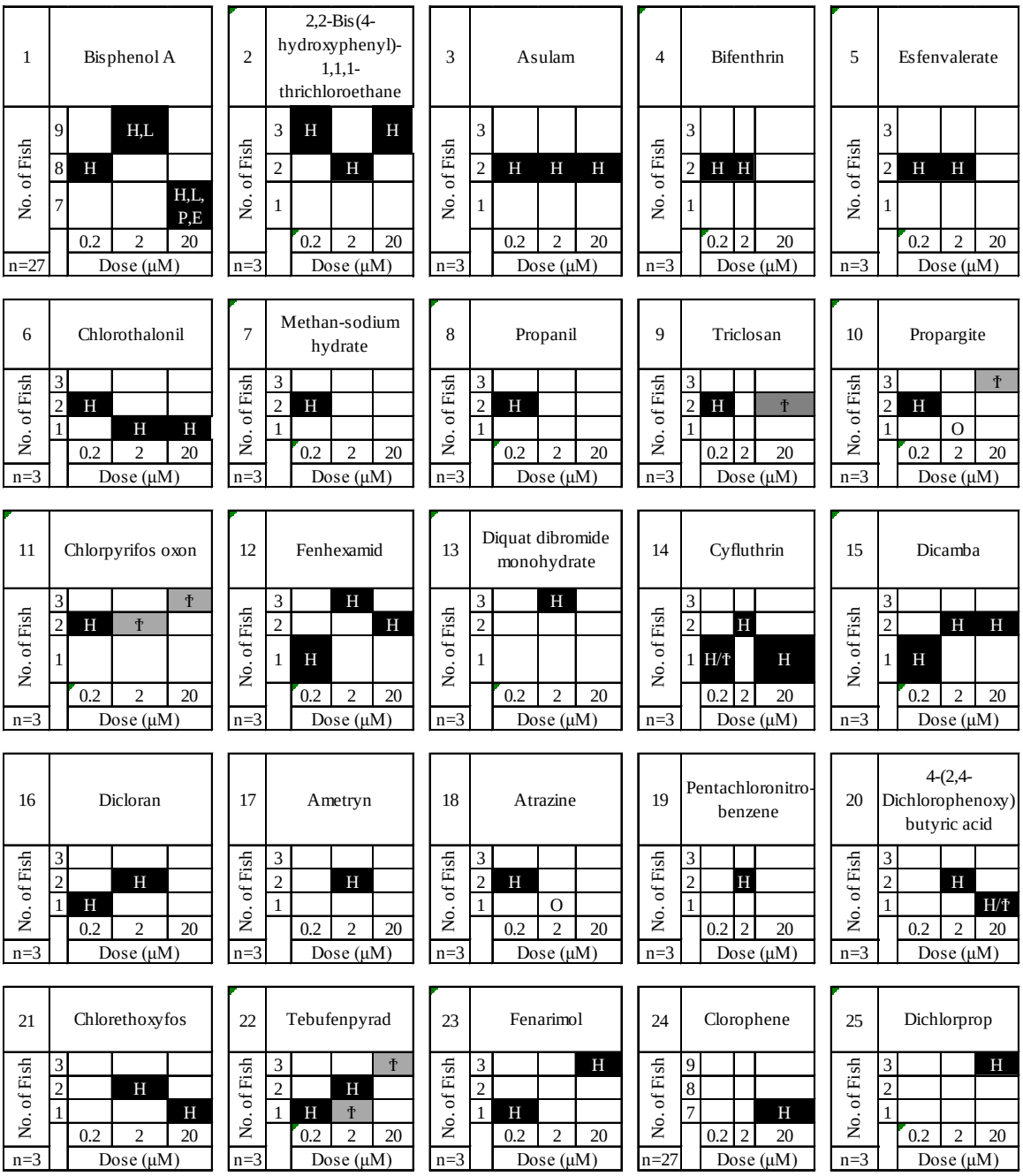

Fig. 3.2. contd.

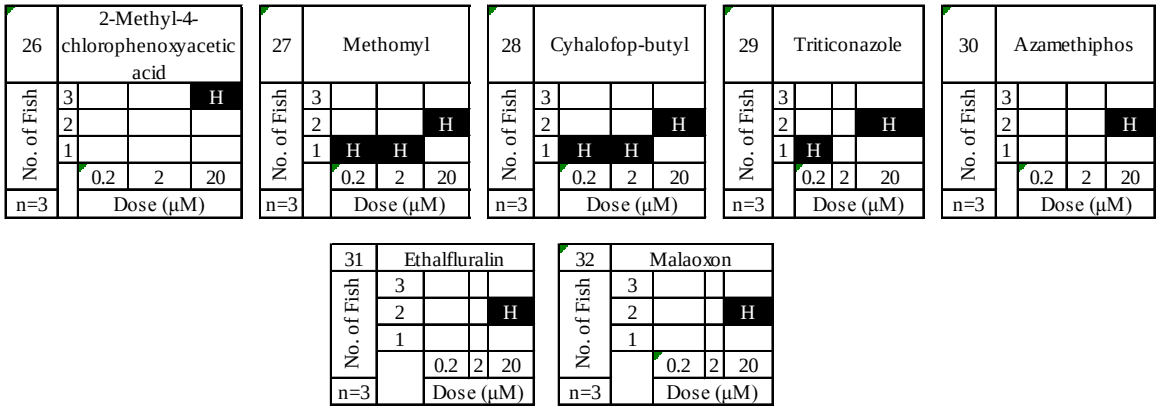

Figure 3.2. Induction of zfERE-driven GFP expression by ToxCast Phase I chemicals. Hits from the zfERE assay are depicted. For each chemical, the number of fish (1/2/3 or 7/8/9) displaying GFP expression for each tested dose (0.2µM, 2µM or 20µM) is represented. "n" is the total number of fish treated per chemical, irrespective of dose. "H", "L", "P" and "E" indicate GFP expression in the heart valves, liver, pancreas and ears, respectively. "†" indicates death. For example, for cyfluthrin (grid 14), out of 3 larvae treated at 0.2µM, 1 larva expressed GFP in the heart valves, and 1 larva was dead. At the 2µM dose, 2 out of the 3 exposed larvae possessed GFP expression in the heart valves, while 1 out 3 of exposed larvae was positive for heart valve-localized GFP expression at the 20µM dose. For BPA(grid 1) and clorophene (grid 24), the total number of fish tested were 27 across 3 doses, as there were multiple replicates of these chemicals in the library.

3.2.2 A comparison of zebrafish and *in vitro* estrogenicity assays

In order to place the zfERE screen in context with current toxicity testing standards, we compared the results from the zfERE assay to those from the EPA-EDSP's *in vitro* HTS assays (this section, in Table 3.2a).

The EPA's Endocrine Disruption Screening Program (EDSP) database (http://actor.epa.gov/edsp21/) provides data from *in vitro* high-throughput screening (HTS) assays from EPA ToxCast and federal Toxicity Testing in the 21st century (Tox21) projects. The cell- and recombinant protein-based *in vitro* assays for estrogen signaling represented within the EDSP database are summarized in Table 3.2b. All the assays (except the NoVaScreen NVS assays) are performed using human liver (HepG2), kidey (HEK293T), ovarian (BG-1) or cervical cancer (HeLa) cells. NVS assays use the wild type ERα protein extracted from bovine uterine membranes, human breast cells MCF7 or recombinantly expressed mouse ESR1 protein in a single radio-ligand binding design. NVS assays are *in vitro*, non-cell-based binding assays.

In Table 3.2a, the results from the zfERE screen are represented alongside AC_{50} values for the aforementioned *in vitro* assays. AC_{50} is the half maximal activity concentration of the chemical in a particular assay, denoted in micromolar concentration units (μM). The AC_{50} for BPA in the ATG_ERE_CIS assay, for example, is 0.098μM, indicating that the dose-response curve of BPA for this assay reaches half its maximum activation at 0.098μM. The AC_{50} concentration is determined by interpolation (purple line) of the dose-response curve (with data points denoted as circles) in Figure 3.3.

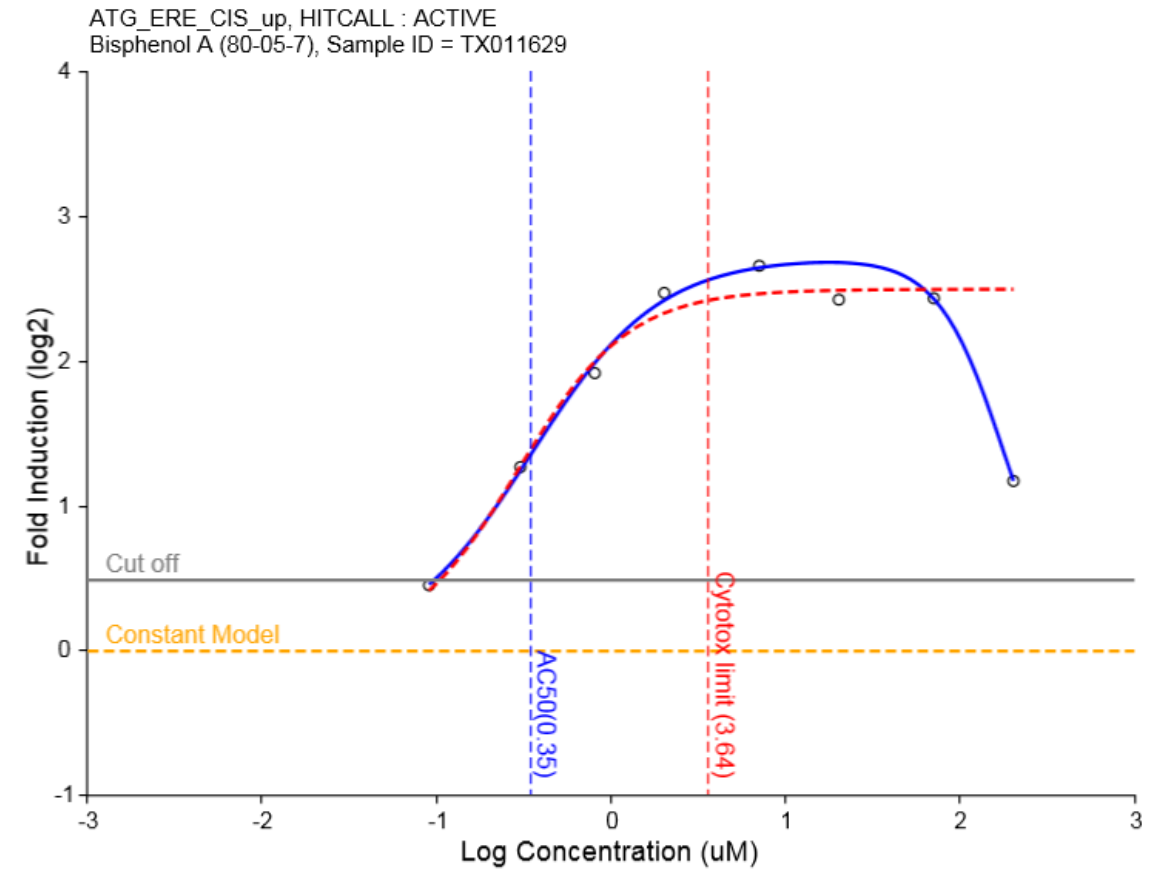

Figure 3.3. Dose response curve for BPA from the ATG_ERE_*cis* assay. Figure downloaded from EPA's Endocrine Disruption Screening Program (EDSP) database (http://actor.epa.gov/edsp21/). Freely available.

The AC_{50} values in the different agonist and binding assays for BPA are low indicating BPA is a strong agonist. In contrast, the high AC_{50} values for BPA in the Tox21_ERa_BLA_Antagonist assay show that BPA is not a good antagonist. 2,2-Bis(4-hydroxyphenyl)-1,1,1-thrichloroethane (HPTE) has agonist and antagonist values similar to BPA. Both BPA and HPTE activated zfERE at all the doses tested. Another phenol, chlorophene, has AC_{50} values from receptor dimerization assays only slightly higher than

those for BPA, and is also a weak antagonist for the estrogen receptor. Clorophene, too, activated ERE-driven GFP expression in our zebrafish assay.

Weaker agonists of ERs *in vitro* (fenarimol, fenhexamid, pentachloronitrobenzene, ethalfluralin, chlorethoxyfos, malaoxon. esfenvalerate and bifenthrin) also activated zfERE. Chlorpyrifos oxon is a weak agonist and a strong antagonist, and activated zfERE. Dicloran, propargite, terbufenpyrad, propanil and triclosan act as antagonists but not agonists in *in vitro* assays. All these chemicals were found to induce ERE-driven GFP expression in zebrafish.

The other 13 chemicals, which were positive for estrogenicity in the zfERE assay, were inactive in the ToxCast *in vitro* assays.

Table 3.2a. Comparison of zfERE assay to ToxCast in vitro HTS assays

Chemical	ZF Assay			AC50 from *in vitro* HTS assays															Comparison on ZF and *in vitro* testing
	ERE			Agonist											Binding			Antagonist	
				ERE			Receptor Dimerization						ER α		ERα			ERα	
	Zebrafish			Human											Human	Mouse	Bovine	Human	
	0.2 µM	2 µM	20 µM	ATG_ERE_CIS	OT_ERa_EREGFP_0120	OT_ERa_EREGFP_0480	OT__ER_ERaERa_1440	OT__ER_ERaERb_1440	OT__ER_ERbERb_1440	OT__ER_ERaERa_0480	OT__ER_ERaERb_0480	OT__ER_ERbERb_0480	ATG_ERa_TRANS	Tox21_ERa_LUC_BG1_Agonist	Tox21_ERa_BLA_Agonist_ratio	NVS_NR_hER	NVS_NR_mERa	NVS_NR_bER	Tox21_ERa_LUC_BG1_Antagonist	Tox21_ERa_BLA_Antagonist_ratio	
HPTE	H	H	H	0.092	0.003	0.234	0.266	0.144	0.003	0.642	0.150	0.176	0.485	0.048		0.038	0.008	0.015	59.197	0.549	R
MCPA			H														NT				N
2,4-DB		H	H														NT				N
Ametryn		H															NT				N
Asulam	H	H	H													NT	NT	NT			N

Table 3.2a. contd.

Cyhalofop-butyl	Cyfluthrin	Chlorpyrifos oxon	Chlorothalonil	Clorophene	Chlorethoxyfos	Bisphenol A	Bifenthrin	Azamethiphos	Atrazine
H	H/Ŧ	H	H			H	H		H
H	H	Ŧ	H		H	H	H		
H	H	Ŧ	H	H	H	H,L,P,E		H	
		39.825		1.839	35.989	0.098	25.181		
						0.738			
						0.822			
						3.150			
				3.672	34.544	1.883			
				9.211	58.419	0.518			
				13.891		5.323			
				22.544		1.051			
NT				15.229		0.515			
		33.818		2.176	27.286	0.119	12.148		
					65.493	0.408			
		122.275	119.858			1.368			
NT				21.854		0.608			
NT	NT	NT	NT	16.612	NT	0.871	NT	NT	
NT				23.118		0.421			
		43.699	44.272						
		1.773	27.125	79.770		84.665			
N	N	R	R	R	R	R	R	N	N

Table 3.2a. contd.

Methan-sodium hydrate	Malaoxon	Fenhexamid	Fenarimol	Ethalflurali n	Esfenvalerat e	Diquat dibromide monohydrat e	Dicloran	Dichlorprop	Dicamba
H		H	H		H		H		H
		H			H	H	H		H
	H	H	H	H				H	H
	55.920	7.830	7.027	34.283		DATA NOT AVAILABLE	28.724		
		32.931		14.964					
		41.046	18.355						
		11.839	16.446						
		20.038	14.203						
		65.898							
		26.291	11.710	57.696					
		23.138	14.268						
		6.074	4.849	27.361	6.806		44.274		
		27.535	5.557						
		42.690							
NT				NT			NT		
NT	NT	NT	NT	NT	NT			NT	NT
NT				NT			NT		
							77.379		
		70.222	39.890						
N	R	R	R	R	R	R	R	N	N

Table 3.2a. contd.

	Methomyl	Pentachloronitrobenzene	Propanil	Propargite	Tebufenpyrad	Triclosan	Triticonazole
	H	H	H	H	H	H	H
	H	H			H/Ŧ		
	H			Ŧ	Ŧ	Ŧ	H
		8.760					
		77.690					
					NT		
					NT		
					NT		
		51.209					
					NT		NT
	NT	NT	NT	NT			
					NT		NT
			52.743	11.494	0.039	72.356	
				2.913	25.290	34.534	
	N	R	R	R	R	R	N

Table 3.2a (Page 45-48). Comparison of zfERE assay to ToxCast in vitro HTS assays. "H" represents GFP expression in the heart, "Ŧ" represents death. "N" denotes chemical tested negative for estrogencity in in vitro tests. "R" indicates condcordance between zfERE and in vitro tests. For the *in vitro* assays, the value represents the AC_{50} of a chemical for the particular assay. "NT" denotes that the chemical was not tested using the assay, and the absence of a value indicates that the tested chemical was inactive for the particular assay. The *in vitro* assays used for comparison are described briefly in **Table 3.2b**. AC_{50} is the half maximal activity concentration in μM. All values have been rounded off to 3 decimal places. ToxCast HTS screening data were obtained from the EPA's Endocrine Disruption Screening Program (EDSP21) website: http://actor.epa.gov/edsp21/.

Table 3.2b. ToxCast *in vitro* HTS assays used in EDSP

Agonist	**Human**	**ERE**	ATG_ERE_CIS	Multiplexed ER reporter gene assay using full length receptor in HepG2 cells
			OT_ERa_EREGFP_0120	Fluorescence reporter readout from HeLa cells after 2h, through Erα and ERE
			OT_ERa_EREGFP_0480	Fluorescence reporter readout from HeLa cells after 4h, through Erα and ERE
		Receptor Dimerization	OT__ER_ERaERa_1440	Odyssey Thera ERα-ERα dimerization in agonist mode after 24h in HEK293T cells
			OT__ER_ERaERb_1440	Odyssey Thera ERα-ERβ dimerization in agonist mode after 24h in HEK293T cells
			OT__ER_ERbERb_1440	Odyssey Thera ERβ-ERβ dimerization in agonist mode after 24h in HEK293T cells
			OT__ER_ERaERa_0480	Odyssey Thera ERα-ERα dimerization in agonist mode after 8h in HEK293T cells
			OT__ER_ERaERb_0480	Odyssey Thera ERα-ERβ dimerization in agonist mode after 8h in HEK293T cells
			OT__ER_ERbERb_0480	Odyssey Thera ERβ-ERβ dimerization in agonist mode after 8h in HEK293T cells
		ER α	ATG_ERa_TRANS	Multiplexed GAL4 reporter construct with human ERα ligand-binding domain in HepG2 cells
			Tox21_ERa_LUC_BG1_Agonist	ERα luciferase reporter gene assay in human BG-1 ovarian cells in agonist mode
			Tox21_ERa_BLA_Agonist_ratio	ERα β-lactamase reporter gene assay in human HEK-293 cells in agonist mode
Binding	**Human**	**ERα**	NVS_NR_hER	Human ER binding assay
	Mouse		NVS_NR_mERa	Murine ERα binding assay
	Bovine		NVS_NR_bER	Bovine ER binding assay
Antagonist	**Human**		Tox21_ERa_LUC_BG1_Antagonist	ERα luciferase reporter gene assay in human BG-1 ovarian cells in antagonist mode
			Tox21_ERa_BLA_Antagonist_ratio	ERα β-lactamase reporter gene assay in human HEK-293 cells in antagonist mode

3.2.3 A comparison of zebrafish and *in vivo* estrogenicity assays

To explore the concordance between the zfERE assay and previously published data from other fish or rodent-based estrogenicity assays, we performed a literature survey. The findings from our survey have been summarized in Table 3.3a. The findings are denoted by the type of effect observed (+/-/nil) and the PubMed ID of the data source, citations of which are listed in Table 3.3b.

Estrogenic endpoints traditionally tested in rodents were surveyed. These include estrogen biosynthesis assays, female pubertal assays examining advancement or delay in sexual maturation caused by endocrine disruption, assays investigating other female reproductive endpoints such as fertility and offspring litter size, and the gold standard rodent uterotrophic assays, in which estrogenic environmental pollutants are identified by their ability to increase uterine weight in ovariectomized (OVX) rats or mice. Furthermore, several other fish species like the rainbow trout and fathead minnow have also been used to investigate endocrine disruption, and studies from these models have also been included in this survey.

HPTE is a well-studied metabolite of the insecticide methoxychlor. Methoxychlor is an insecticide known for its teratogenicity and endocrine disruption activity. Both methoxychlor and HPTE were indicated as an estrogen receptor agonists in ToxCast *in vitro* assays (Table 3.2a), and are also known to cause abnormal endocrine function *in vivo* (Table 3.3a). Methoxychlor exposure is also known to increase vitellogenin (VTG, a biomarker of estrogen signaling) concentrations in juvenile rainbow trout. In line with

previous *in vitro* and *in vivo* studies, HPTE was indicated as an inducer of ERE mediated transcription in the zfERE assay. However, methoxychlor was not indicated as positive in the zfERE assay.

Table 3.3a. (Page 52-54) Comparison of zfERE assay to other *in vivo* assays. "R" denotes estrogenicity observed in both *in vitro* EDSP and zfERE assays. "N" denotes estrogenicity observed in the zfERE assay, but not in the EDSP *in vitro* assays. References for various rodent and fish assays are indicated by their PubMed IDs, whose citations are enumerated in Table **3.3b (Page 55-56)**. For rodent estrogen steroidogenesis assays, (+) indicates an increase, and (-) indicates a decrease in estrogen synthesis and (nil) indicates there was no effect observed. For rodent uterotrophic assays, (+) indicates an increase in uterine weight and other estrogen-related parameters upon exposure of ovariectomized mice/rats to the particular chemical, a (-) indicates a decrease in these parameters, a (+/-) indicates evidence of both estrogenic as well as anti-estrogenic activity by the particular chemical, and (nil) indicates there was no effect observed. For female rodent pubertal and reproductive assays, a (+) indicates an effect was observed upon chemical exposure, whereas (nil) indicates there was no effect observed. Concordant positive effects are indicated by gray shading. Inconclusive/negative/no effects are not shaded. The absence of PMIDs indicates the lack of published data on the chosen endpoints for these chemicals.

Table 3.3a. Comparison of zfERE assay to other *in vivo* assays					
Chemical	**ZF Vs. HTS**	**Rodent Assays**			**Other Fish Assays**
		Estrogen Synthesis	**UT Assay**	**Female Pubertal/Reproductive Endpoints**	
HPTE(methoxychlor metabolite)	R		728194(+), 9118870(+), 11390168(+)	11861976(+)	Vitellogenin induction in juvenile rainbow trout (11432551)
MCPA	N			11288930(nil)	
2,4 - DB	N			12417478(+)	
Ametryn	N				
Asulam	N				
Atrazine	N	19541795(-)	8812239(nil), 7932848(-), 17190974(-), 17904329(-), 7737039(-),	12202059(+), 24797874(+), 19265281(+), 21059795(nil)	Vitellogenin and *cyp1a* induction in rainbow trout (18973769), reduction of reproduction in medaka (24929351), fathead minnow (20471700) and zebrafish (23358194). No effects on reproduction in fathead minnow in another study (15095900).
Azamethiphos	N				
Bifenthrin	R		23050436(+)		Induction of choriogenin in *Menidia beryllina* (25127356) and(23007834), increase in plasma 17β-estradiol in *Oncorhynchus mykiss* (23518481), induced vitellogenin transcription in *Pimphales promelas* (21718662)

Table 3.3a. Contd. Comparison of zfERE assay to other *in vivo* assays

Chemical	ZF Vs. HTS	Rodent Assays		Other Fish Assays	
		Estrogen Synthesis	UT Assay	Female Pubertal/Reproductive Endpoints	
Bisphenol A	R	21182934(+), 20413367(+), 23545179(+), 22687996(nil), 21055461(nil), 21722727(nil), 21285323(nil), 23512349(-), 20599497(-)	**(+):** 9417770, 10536110, 10746942, 10822019, 10839476, 10910991, 11133394, 11258963, 11552294, 11750080, 12460799, 12948896, 14689164, 15635150, 15721882, 16326438, 18079610, 21112483, 23160314; **(+/-):**23037998; **(-)**10828501, 11029274, 11606437, 11914775, 16639590, 20435109	12151630(nil),19864446(nil), 22384422(+), 19479018(+), 19535786(+), 12759096(+), 22384422(+ puberty, - reproductive parameters), 9799186(+/-, depending on dosage route)	Induction of steroidogenic genes in *Gobiocypris rarus* (25125231 and 25048937), but suppression of steroidogenesis in the same species at higher doses (25048937)
Chlorethoxyfos	R				
Clorophene	R			9719427(nil)*	
Chlorothalonil	R				
Chlorpyrifos oxon	R				
Cyfluthrin	N				
Cyhalofop-butyl	N				
Dicamba	N				
Dichlorprop	N				
Dicloran	R				

Table 3.3a. Contd. Comparison of zfERE assay to other *in vivo* assays					
Chemical	**ZF Vs. HTS**	**Rodent Assays**			**Other Fish Assays**
		Estrogen Synthesis	**UT Assay**	**Female Pubertal/Reproductive Endpoints**	
Diquat dibromide monohydrate	DATA NOT AVAILABLE				
Esfenvalerate	R		12052007(nil)	21889588(+), 18795170(+), 16005607(+)	Decreased fertilization in medaka (12408625)
Ethalfluralin	R				
Fenarimol	R	3672523(-)	16324804(+)	21722721(+)	Decreased vitellogenin and reproductive success in fathead minnow (17942165 and 15901916), and aromatase activity (15901916)
Fenhexamid	R				
Malaoxon	R				
Methan-sodium hydrate	N			17258889(+), 7935259(+)	
Methomyl	N			23033640(+)	
Pentachloronitrobenzene	R		21783589(-)		
Propanil	R				Induction of vitellogenin and aromatase in *Danio rerio* and medaka (24992288)
Propargite	R				
Tebufenpyrad	R				
Triclosan	R		22062131(+), 20562219(+), 23261820(nil)	20562219(+)	Induction of vitellogenin expression in *Gambusia affinis*(20821571)
Triticonazole	N				

Table 3.3b - List of References from Table 3.3a					
Chemical	**PMIDs from Table 3.3a**	**References**	**Chemical**	**PMIDs from Table 3.3a**	**References**
HPTE	728194	(Bulger et al. 1978)	BPA	11133394	(Yamasaki et al. 2000)
	9118870	(Shelby et al. 1996)		11258963	(Matthews et al. 2001)
	11390168	(Newbold et al. 2001)		11552294	(Kim et al. 2001)
	11861976	(You et al. 2002)		11750080	(Yamasaki et al. 2002b)
	11432551	(Thorpe et al. 2001)		12460799	(Papaconstantinou et al. 2002)
MCPA	11288930	(Bellet et al. 2001)		12948896	(Kanno et al. 2003)
2,4-DB	12417478	(Cavieres et al. 2002)		14689164	(Diel et al. 2004)
Atrazine	19541795	(Pogrmic et al. 2009)		15635150	(Kitamura et al. 2005)
	8812239	(Connor et al. 1996)		15721882	(Koda et al. 2005)
	7932848	(Tennant et al. 1994)		16326438	(Kim et al. 2005)
	17190974	(Moon et al. 2007)		18079610	(Kim et al. 2005)
	17904329	(Akahori et al. 2008)		21112483	(Yu et al. 2010)
	7737039	(Eldridge et al. 1994)		23160314	(Kendig et al. 2012)
	12202059	(Ashby et al. 2002)		23037998	(Ohta et al. 2012)
	24797874	(DeSesso et al. 2014)		10828501	(Mehmood et al. 2000)
	19265281	(Shibayama et al. 2009)		11029274	(Tinwell et al. 2000)
	21059795	(Hovey et al. 2011)		11606437	(Nagel et al. 2001)
	18973769	(Salaberria et al. 2009)		11914775	(Yamasaki et al. 2002a)
	24929351	(Papoulias et al. 2014)		16639590	(Schmidt et al. 2006)
	20471700	(Tillitt et al. 2010)		20435109	(Okuda et al. 2010)
	23358194	(Weber et al. 2013)		12151630	(Tinwell et al. 2002)
	15095900	(Bringolf et al. 2004)		19864446	(Ryan et al. 2010)
Bifenthrin	23050436	(Tan et al. 2012)		22384422	(Nah et al. 2011)
	25127356	(DeGroot and Brander 2014)		19479018	(Fernandez et al. 2009)
	23007834	(Brander et al. 2012)		19535786	(Adewale et al. 2009)
	23518481	(Forsgren et al. 2013)		12759096	(Kato et al. 2003)
	21718662	(Beggel et al. 2011)		9799186	(Ashby and Tinwell 1998)
BPA	21182934	(Xi et al. 2011)		25125231	(Liu et al. 2014)
	20413367	(Fernandez et al. 2010)		25048937	(Zhang et al. 2014)
	23545179	(Tan et al. 2013)		10746942	(Laws et al. 2000)
	22687996	(Kobayashi et al. 2012)		10839476	(Goloubkova et al. 2000)
	21055461	(Mendoza-Rodriguez et al. 2011)		10910991	(Papaconstantinou et al. 2000)
	21722727	(Rivera et al. 2011)	Esfen-valerate	12052007	(Kunimatsu et al. 2002)
	21285323	(Varayoud et al. 2011)		21889588	(Guerra et al. 2011)
	23512349	(Lee et al. 2013)		18795170	(Pine et al. 2008)
	20599497	(Berger et al. 2010)		16005607	(Moniz et al. 2005)
	9417770	(Milligan et al. 1998)		12408625	(Werner et al. 2002)
	10536110	(Ashby et al. 1999)			
	10822019	(Diel et al. 2000)			

Table 3.3b - List of References from Table 3.3a					
Chemical	**PMIDs from Table 3.3a**	**Reference**	**Chemical**	**PMIDs from Table 3.3a**	**Reference**
Methan-sodium hydrate	17258889	(Goldman et al. 2007)	Fenarimol	3672523	(Hirsch et al. 1987)
	7935259	(Goldman et al. 1994)		16324804	(Andersen et al. 2006)
Propanil	24992288	(Schiller et al. 2014)		21722721	(Park et al. 2011)
Triclosan	22062131	(Jung et al. 2012)		17942165	(Thorpe et al. 2007)
	20562219	(Stoker et al. 2010)		15901916	(Ankley et al. 2005)
	23261820	(Louis et al. 2013)	Methomyl	23033640	(Shanthalatha et al. 2012)
	21058171	(Rodriguez and Sanchez 2010)	Pentachloroni trobenzene	21783589	(Ashby et al. 2005)

Carbamate chemicals methan-sodium hydrate and methomyl were indicated as estrogenic in the zfERE assay, although there were negative for estrogenicity in the ToxCast *in vitro* assays. Prior studies have shown that both chemicals act as estrogen antagonists in rodent assays: methan sodium (or metam sodium) perturbs estrus cycles (Goldman et al. 2007) and blocks ovulation (Goldman et al. 1994) in rats, while methomyl exposure causes the loss of ovarian follicles and infertility in mice (Shanthalatha et al. 2012).

Propanil was estrogenic in the zfERE and *in vitro* assays. Although our search did not yield published literature data from rodent assays on this chemical, propanil has previously been found to induce aromatase and vitellogenin expression in zebrafish and medaka (Schiller et al. 2014).

2-Methyl-4-chlorophenoxyacetic acid (MCPA) is a powerful herbicide and plant growth hormone. Although indicated as estrogenic in the zfERE assay, it was negative in the

ToxCast *in vitro* assays. One extensive study using rats even reported that MCPA-exposed animals did not manifest any reproductive defects (Bellet et al. 2001).

In utero exposure to phenoxy herbicide 2,4 – DB causes a decrease in litter size in mice (Cavieres et al. 2002). However, ToxCast *in vitro* assays indicated 2,4-DB was negative for estrogenicity, whereas the zfERE assay was able to identify it as a positive hit.

Pyrethroids bifenthrin, cyfluthrin and esfenvalerate were positive for estrogenicity in the zfERE assay, but cyfluthrin was not detected by *in vitro* assays. Bifenthrin and esfenvalerate have been tested on animal models previously, but have yielded positive and negative results for estrogen-related endpoints. Our search for animal-based estrogenic assays for cyfluthrin yielded no results.

Herbicide atrazine was negative for estrogenicity *in vitro*, but positive in the zfERE assay. Atrazine is known to perturb sexual maturation in peripubertal female Wistar and Sprague-Dawley rats by delaying vaginal opening and gain of uterine weight (Ashby et al. 2002). Atrazine has also been shown to have anovulatory effects in rats (Shibayama et al. 2009). However, there exist rodent uterotrophic studies that indicate that atrazine may have an anti-estrogenic effect (Akahori et al. 2008; Eldridge et al. 1994; Moon et al. 2007; Tennant et al. 1994). Atrazine seems to have an anti-estrogenic effect in cell-based and rodent assays, and has been shown to reduce reproduction in the fish species medaka (Papoulias et al. 2014). However, in the fish species rainbow trout, atrazine has been

shown to increase the estrogenic marker vitellogenin (Salaberria et al. 2009). Atrazine has no effects on reproduction in the fish fathead minnow (Bringolf et al. 2004).

While studies in the rat (Hirsch et al. 1987) and fathead minnow (Ankley et al. 2005; Thorpe et al. 2007) suggest that fungicide fenarimol acts to disrupt estrogen synthesis by inhibiting the aromatase enzyme, decrease vitellogenin production and reduce reproductive success, in other uterotrophic (Andersen et al. 2006) and reproductive (Park et al. 2011) studies in rodents, fenarimol has been shown to be estrogenic. In *in vitro* studies, fenarimol has been shown to be an agonist as well as a weak antagonist (Table 3.2A).

3.2.4 Estrogens induce aberrant lipid accumulation in the zebrafish

Given the critical role of estrogen signaling in metabolism (as described previously in Section 1.4.1), and the prevalence of estrogenic endocrine disruptors such as BPA, DES and genistein, which are associated with obesity-related phenotypes in animals as well as humans, it is necessary to explore the possibility that estrogens could alter lipid metabolism in the zebrafish. We used a previously established assay (Riu et al. 2014b) for lipid accumulation in the zebrafish and tested to see if the physiological estrogen (E2) and the synthetics estrogen bisphenol A (BPA) affected this endpoint. We exposed zebrafish larvae from 3dpf to 11dpf to E2 and BPA while feeding them a lipid-rich diet, and stained the larvae at the end of the treatment protocol with the Oil Red O (ORO) stain. Accumulation and localization of neutral lipids (including triglycerides and

cholesterol) were then recorded. Doses of exposure included 0.1nM, 1nM, 10nM, 100nM, 1μM and 10μM. 0.01% of vehicle DMSO was used as a negative control.

Larval exposure to E2 and BPA caused an increase in ORO staining, implying increased lipid accumulation (Figure 3.4). The E2-induced increase in lipid accumulation was highest at the lowest dose of E2 tested with 42.9% of E2 exposed larvae displaying increased lipid staining, indicating that the obesogenic effect of estrogen happens at very low concentrations. BPA induced lipid accumulation at both low and high doses, but not in the intermediate doses of 1nM or 10nM.

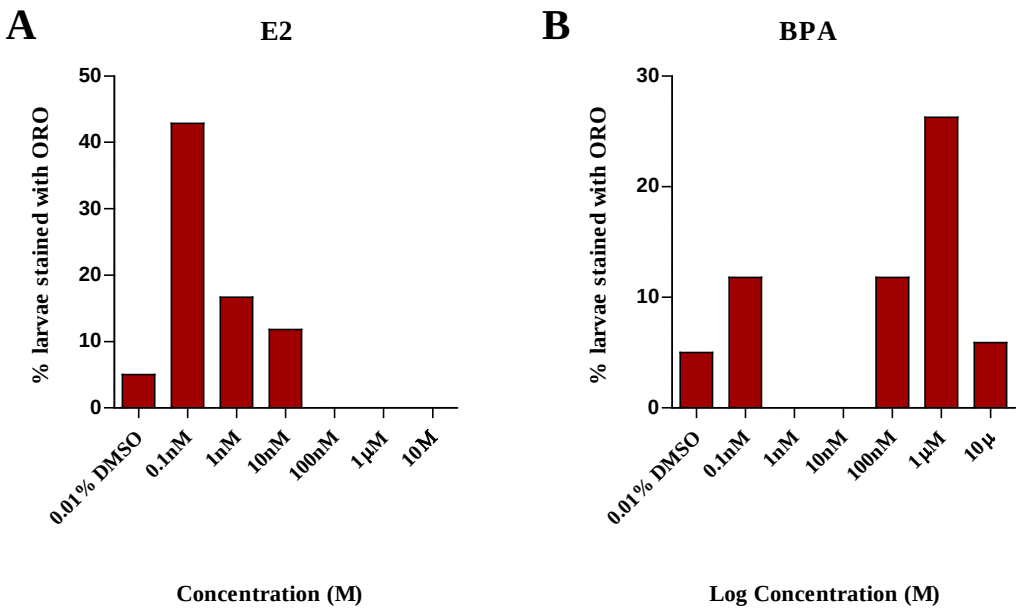

Figure 3.4 Estrogens induce lipid accumulation in the zebrafish. Bar graph represents percentage of chemical-exposed larvae that were stained for lipids in E2 and BPA.

3.3 DISCUSSION

Xenoestrogens are environmental, non-physiological chemicals, which are capable of eliciting estrogen-like effects within the body. Unnatural and untimely exposure to these chemicals is known to cause deficiencies in sexual maturation and reproduction. Furthermore, xenoestrogens such as DES, genistein and BPA have been shown to perturb metabolic homeostasis. Given the steep rise in obesity prevalence over recent years and the abundance of industrial chemicals that pollute the environment, it is most essential that we gain a better understanding of the mechanisms by which chemicals in the environment, particularly xenoestrogens, contribute to obesity-related phenotypes. Towards this goal, the objectives of the studies in this chapter were to (i) develop a high-throughput zebrafish-based screening platform to enable screening of large libraries for estrogenic chemicals, and (ii) to investigate whether estrogens can alter lipid accumulation in the zebrafish.

We first developed a high-throughput screening amenable platform using the *Tg(5XERE:GFP)* zebrafish (Gorelick and Halpern 2011) to identify estrogenic chemicals from the ToxCast chemical library. The small size of zebrafish larvae enabled chemical screening in a 96-well plate format. Larvae were exposed for a 24 hour period to 309 chemicals. 3 doses were tested for each chemical, and there were 3 larvae tested per dose per chemical. Accurate stock solution preparation, chemical aliquoting and zebrafish dosing were made possible by automated liquid handling (see Section 2.4). Post

treatment, the larvae were scored manually using an inverted microscope with fluorescence.

Of the 309 pesticides, herbicides, insecticides and bactericides tested, 32 were determined to be positive hits. Except for BPA, for which zfERE driven GFP expression was localized to the heart valves, liver, pancreas and ears, all other positives from the assay induced GFP expression only in the heart valves. BPA has been shown to induce GFP in only the heart valves at 1μM, and heart and liver at higher doses (Gorelick and Halpern 2011). Accordingly, in our assay BPA induces GFP expression in the heart valves at 0.2μM, 2μM and 2μM doses, and heart and liver at 2μM and 20μM doses. In addition to these tissues, BPA induces GFP expression in the pancreas and ears at the 20μM dose. E2 has been shown to induce GFP expression in the pancreas at 1μM in the *Tg(5xERE:GFP)* transgenic line (Hao et al. 2013), indicating that the pancreas is an estrogen-responsive tissue, and that BPA probably acts through ER signaling in the pancreas. Furthermore, in cell-based zfER-reporter assays, it has been shown that BPA activates zfERα-driven transcriptional activity at doses lower than 1μM, but also activates zfERβ1- and zfERβ2-driven transcription at higher doses (Pinto et al. 2014). These studies indicate that the primary zfERα responsive tissues are the heart valves. zfERβ1 and zfERβ2 seem to more specifically target EREs in the liver and pancreas. It therefore follows, that all positive hits from the zfERE screening effort probably induce ERE-driven GFP expression primarily via zfERα at the tested doses.

Among the 32 hits from the assay, there were chemicals that induced zfERE-driven GFP expression only at the highest (20μM) dose. This category of chemicals includes clorophene, dichlorprop, MCPA, azamethiphos, ethalfluralin and malaoxon.

Clorophene is a strong agonist of ER signaling *in vitro,* whereas *in vivo*, in rodents, it does not seem to elicit a significant effect on reproductive endpoints (Stouten and Bessems 1998). The lack of reproductive toxicity upon clorophene exposure in rodents could be due to rapid metabolism and inactivation of the chemical *in vivo*. This would explain an estrogenic effect for clorophene *in vitro*, but not in rodents. This could also explain why clorophene fails to induce zfERE at low doses, and, suggests incomplete clorophene metabolism at 20μM as a potential cause for estrogenicity at that dose. For ethalfluralin, which is a very weak ER agonist *in vitro*, the lack of rodent-based studies makes it hard to speculate estrogenicity.

Herbicide MCPA failed to activate ERs *in vitro*. The available *in vivo* study for MCPA did not observe any reproductive effects. This could mean that MCPA is estrogenic only in zebrafish, by being a zf-ERα specific agonist. For dichlorprop, azamethiphos and malaoxon, which did not activate estrogen signaling *in vitro*, there were no rodent studies, making it hard to speculate estrogenicity.

2,4-DB and chlorethoxyfos induce zfERE-driven GFP expression in the heart valves at the higher doses tested - 2μM and 20μM. This result could mean that these chemicals activate zfERE through zfERα signaling. As 2,4-DB has been shown to affect litter size

and embryo implantation in studies with mice (Cavieres et al. 2002), it is possible that 2,4-DB is indeed estrogenic at 2μM and 20μM concentrations in the zebrafish. As 2,4-DB is not estrogenic *in vitro*, it is tempting to speculate if it is a metabolite of 2,4-DB, which acts as an estrogen *in vivo.*

Although it acts as an estrogen (albeit at high doses) *in vitro*, the lack of *in vivo* studies for chlorethoxyfos deems its estrogenic potential uncertain.

Chemicals that induce zfERE-driven GFP expression at only the lower doses, without causing toxicity (death) at higher doses may be considered potent zfERα agonists. These include atrazine, methan-sodium hydrate and propanil, which induce GFP only at 0.2μM, and bifenthrin, dicloran and esfenvalerate, which induce GFP expression at 0.2μM and 2μM. While *in vitro* studies for atrazine are negative, conflicting results from several rodent and fish studies make its true estrogenic potential difficult to ascertain. Methan-sodium hydrate is negative for estrogenicity *in vitro*, but is positive *in vivo*, in rodent assays. For propanil, both *in vitro* and zfERE assays predict estrogenicity.

Chemicals that induce zfERE-driven GFP expression in the lower tested doses, but animal death in the higher doses include chlorpyrifos oxon, propargite, tebufenpyrad and triclosan. Chlorpyrifos oxon induces GFP expression in the zebrafish heart at 0.2μM, but is lethal to larvae exposed to higher concentrations. Chlorpyrifos oxon is a very weak agonist and strong antagonist *in vitro.* Since there were no published animal studies available, it remains to be seen if chlorpyrifos oxon acts through ERs *in vivo.*

Propargite and tebufenpyrad induce zfERE-driven GFP expression at 0.2μM, have no effect at 2μM, and cause larval death at 20μM. Although these chemicals might need to be tested with more doses within the 0.2 to 20μM range to explain this pattern, it can be speculated that the chemicals are toxic at high doses, but act specifically through zfERα at lower doses. Both propargite and tebufenpyrad act as antagonists *in vitro*, suggesting that the chemicals probably bind to mammalian estrogen receptors to inhibit E2 action, but because of the lack of rodent studies, it is difficult to ascertain actual their estrogenic potential or mechanism of action.

A few chemicals tested positive across all three doses tested in the zfERE assay. Among these, HPTE, BPA, chlorothalonil and fenhexamid tested positive for estrogenicity in *in vitro* assays as well, with HPTE, BPA being indicated as agonists, fenhexamid as a weak agonist, and chlorothalonil as an antagonist. No rodent studies were found for chlorothalonil and fenhexamid, but HPTE had concordance *in vivo* studies, and BPA had inconclusive studies. The results for HPTE suggest that it is a possible agonist of estrogen signaling across species.

Asulam, cyfluthrin, cyhalofop-butyl, dicamba and methomyl tested positive across the dose range tested in the zfERE assay, but were negative in *in vitro* assays. Methomyl has been found to be estrogenic in rodents. Since this chemical has been found to be estrogenic in animal (rodent and zebrafish) assays, but not *in vitro*, it is possible that the mechanism of action of this chemical requires its metabolism, or the involvement of multiple tissues in eliciting its effects. For asulam, cyfluthrin, cyhalofop-butyl and

dicamba, such assumptions cannot be made, as it is not known whether these chemicals are inactive as estrogens in mammalian animal models.

Taken together, results from the zfERE assay indicate the ability of widely prevalent environmental chemicals to disrupt estrogen signaling in various *in vitro* and animal models, including the zebrafish. In several instances, chemicals that test positive in the *in vivo* zebrafish assay, test negative in *in vitro* assays, indicating that the physiological context provided by a whole-organism model for EDC action (such as EDC metabolism, for example) are necessary factors that cannot be ignored by extrapolating false negative results from *in vitro* assays to humans. Given the many strengths of the zebrafish model, we suggest that zebrafish-based HTS models be incorporated into current prioritization screens, to supplement *in vitro* assays, so as to more accurately predict EDC action in rodent models, and in humans. Moreover, since estrogens E2 and BPA seem to have effects on lipid metabolism in the zebrafish, we also suggest that the alteration of lipid-related endpoints by estrogens be further investigated.

CHAPTER 4: A ZEBRAFISH-BASED SCREENING ASSAY TO IDENTIFY DISRUPTORS OF WHOLE BODY-ENERGY HOMEOSTASIS

4.1 INTRODUCTION

Optimal nutrition is essential for embryonic growth and development (Wu et al. 2006). Insufficient or excess nutrition during development can cause permanent endocrine and metabolic changes, and these alterations leave “imprints”, which can manifest in adult life as diseases such as hypertension, obesity and diabetes (McMillen et al. 2008). For instance, both fetal under- and over-nutrition increase the risk of future diabetes (Yajnik and Deshmukh 2008).

Environmental factors, such as exposure to industrial chemicals, can affect the nutritional status of a developing embryo. Therefore, identifying chemicals capable of altering nutrient uptake and utilization during development can prove critical in preventing the developmental origins of adult disease. As zebrafish have been extensively used as animal models to study developmental toxicity, we sought to develop a zebrafish-based screening model to identify chemicals disrupting nutrient uptake.

The zebrafish is a suitable model for studying nutrient mobilization during development. The oviparous zebrafish’s embryo carries its own lipid-rich yolk. The yolk serves as the sole nutritional source for the developing embryo, from zygote formation up to 5 dpf, when it can ingest exogenous nutrition (Ng et al. 2005; Poupard et al. 2000). In the embryo, the yolk is surrounded by the yolk syncytial layer (YSL), an extra-embryonic tissue formed during the blastula stage (reviewed in (Carvalho and Heisenberg 2010)). One of the yolk syncytial layer’s functions throughout early embryonic development is to

hydrolyze yolk materials and transport them from the yolk to the embryonic cells and larval tissues. Knock-down of the microsomal triglyceride transfer protein (MTP), a protein involved in lipid transport and normally expressed in the yolk syncytial layer of the zebrafish embryo, results in decreased yolk consumption and loss of lipid staining of the embryo in other locations than of the yolk (Schlegel and Stainier 2006). In addition, the Mtp knock-down embryos are small and die by 6 dpf with pronounced edema. Thus, it has been shown that the lack of nutrients during development may lead to embryonic malabsorption syndrome in zebrafish.

Exposure to certain drugs or environmental chemicals has been shown to induce malabsorption. For example, both cholesterol lowering drugs and the pesticide prochloraz decrease yolk absorption (Domingues et al. 2013; Raldua et al. 2008). It is possible that many more chemicals could induce embryonic malabsorption syndrome, but due to the lack of high throughput assays for yolk absorption, few chemicals have been investigated for this effect.

In the present study, we describe the development of a screening model to examine nine chemicals' effect on zebrafish yolk uptake. The model is based on the transgenic zebrafish (HGn50D) expressing the Green Fluorescent Protein (GFP) in the yolk syncytial layer. We developed a software package named ZebRA to automatically and accurately segment and quantify the yolk in HGn50D embryos imaged by fluorescent microscopy. Given the number and variety of industrial chemicals in commerce today, the development of an automated software package for the segmentation and

quantification of biological effects is an important step for enabling high throughput screening to identify adversely acting chemicals because: (i) it will allow fast performance, (ii) it will allow accurate quantification of biological effects and (iii) it will enhance reliability and reproducibility of the experiments.

Using our software package, the yolk size was examined in embryos that had been exposed to chemicals from 2 dpf, when morphogenesis of organ rudiments is almost complete (Kimmel et al. 1995), to 5 dpf, when the endotrophic period ends. The findings from this study (as describes below) have been published (Kalasekar et al. 2014). Our method of automated image analysis will allow for future high throughput screening for developmental toxicants causing yolk malabsorption.

4.2 RESULTS

4.2.1 GFP is expressed in the zebrafish yolk syncytial layer in the transgenic *HGn50D* line

Traditionally, lipid distribution in zebrafish has been investigated by using the Oil Red O stain, which stains neutral lipids deposited throughout the body of fish. However, the ORO stain was ill-suited for measuring the yolk size in our experiments, because of the following reasons: (i) the computational algorithm used for high-throughput image analysis required high intensity signals for automated identification of the zebrafish yolk, but the intensity of ORO stains in zebrafish can vary from one individual to the other, and (ii) ORO staining for yolk-size analysis was both cumbersome and labor-intensive, and thus, will not be efficient enough for scaling the assay up to high-throughput formats.

Apart from being advantageous in these aspects, high-intensity GFP-expressing transgenic zebrafish were easy to image and did not require orienting. Live, free-swimming zebrafish were imaged using an inverted microscope, and their ventral position could be easily captured.

The transgenic zebrafish line *HGn50D* was generated by *Tol2*-mediated transposition and random insertion of a GFP expressing construct (Asakawa et al. 2008; Urasaki et al. 2008). Embryos from this transgenic line fluoresce in the yolk, the eye lenses, and the heart. Within the yolk, the GFP is expressed in the yolk syncytial layer, as shown by confocal microscopy scanning through the yolk (Figure 4.1A). The size of the yolk determined by GFP expression of live embryos correlates with the yolk size determined by ORO staining, and this correlation exists irrespective of the time point of imaging or orientation of the zebrafish (Figure 4.2B).

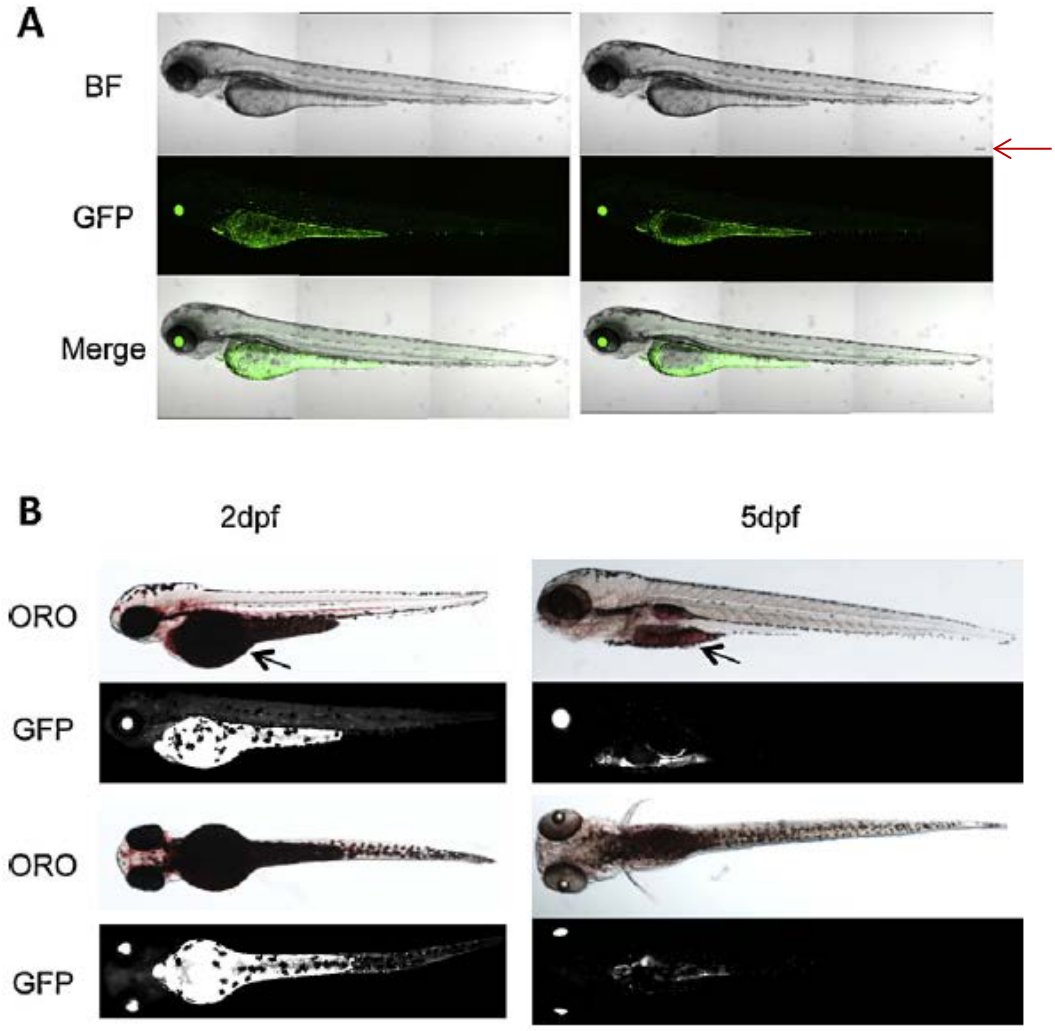

Figure 4.1. Zebrafish as a model to investigate yolk malabsorption. **(A)** Images from confocal microscopy depicting a 3 dpf HGn50D larva expressing GFP in the YSL, the heart and the eye lens, as viewed using different channels (bright field or GFP). Left panel: Z projection of 46 slices (5µm/slice) shows GFP expression in the aforementioned tissues/organs. Right panel: Z projection over 26 slices (5µm/slice) shows that GFP expression is restricted to the yolk syncytial layer surrounding the yolk mass. Scale bar on the top right panel (red arrow) indicates 90µm in length. (B) Oil Red O stained and GFP-fluorescent larvae at 2 and 5 dpf. For each time point, the top panel depicts the lateral view, and the bottom panel depicts the ventral view. The yolk (indicated by arrows) is rapidly used up between 2 and 5 dpf. These time points are depicted to represent the larvae at the beginning and end of the treatment period, respectively.

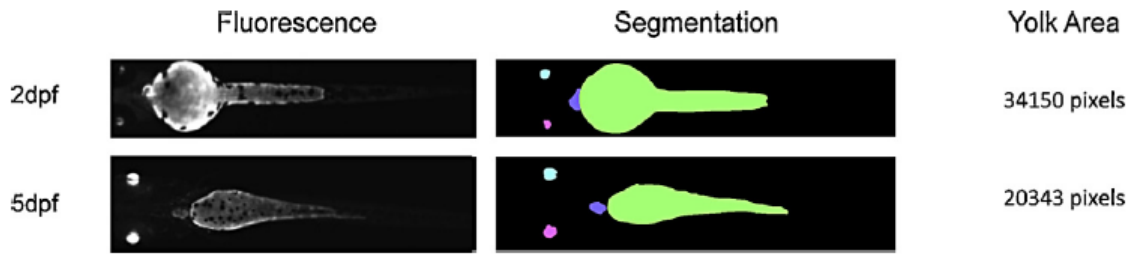

Fig. 4.2. Automatic segmentation and quantification of yolk area. Left panel: Images of 2 and 5 dpf larvae obtained on an Olympus IX51 inverted fluorescence microscope were cropped and oriented using the algorithm developed. Right panel: The processed images were automatically segmented. Representative output images depict the yolk in green, the heart in purple, and the eyes in pink and blue. Values indicate the number of pixels in the annotated yolk, as quantified by the algorithm.

4.2.2 Automated quantification of yolk size using the ZebRA software package

To develop a high throughput screening assay capturing the dynamics of yolk utilization of live fish, we utilized the *HGn50D* transgenic line. We imaged live fish at 5 dpf by fluorescence microscopy. The fish were imaged ventrally to by-pass any mounting of the fish. The acquired images depicted the fish's yolk, heart, and eyes with higher fluorescence intensity than the rest of the fish.

To facilitate quantification of chemicals' effects on yolk absorption, we developed an automated image processing algorithm for the segmentation and quantification of the yolk. The algorithm was developed by Dr. Eleni Zacharia, Noah Kessler and Dr.Ioannis Kakadiaris from the Department of Computer Science, University of Houston, Houston,

Texas. All algorithm-related information can be found on the onlinve version of the published version of this work (Kalasekar et al. 2014). The developed algorithm automatically performs the following tasks: (i) the input image is rotated so that the fish is depicted in horizontal orientation and is cropped so that only the fish and its immediate vicinity remain in a small rectangular image, (ii) an iterative procedure is performed to continually increase the brightness of the image based on an intensity transformation, and segment the image based on a thresholding technique until the components corresponding to the yolk, eyes and heart are identified, (iii) the an image of the fish with each anatomical feature highlighted is produced, along with the area (in pixels) of each feature (Figure 4.2).

The accuracy of the image analysis algorithm was evaluated by calculating the Dice similarity coefficient between the segmented regions provided by the automated image processing algorithm of the software package and manual annotations. A manual annotation tool was developed in MATLAB to help validate the accuracy of the automated segmentation algorithm Using this tool, the user could open an image which was displaying a horizontally oriented fish as described above, and click on points around the edges of each yolk, heart, and eyes. Then, a curve was interpolated using those points and was filled in to show the shapes of each region. As a result, the anatomical regions of the yolk, heart and eyes were segmented and depicted with different colors. A reference set of images was selected that contained images with a variety of distinguishing qualitative characteristics (e.g., yolks with low intensity fluorescence, narrow-shaped yolks, small eyes, etc.). Noah Kessler (collaborator from the lab of Dr.Ioannis Kakadiaris,

UH Dept. of Computer Science) and I used the manual annotation tool on the reference set, and their annotations were compared to the segmentation results of the automated algorithm. The similarity between the manual annotations and the automated segmentations was quantified by Dice's similarity coefficient (Zou et al. 2004). Of the 320 images annotated manually, 309 (96.6%) were successfully segmented by the automated algorithm. The average Dice similarity coefficient was 0.932, with a standard deviation of 0.0476.

4.2.3 Screening of chemicals for effects on yolk utilization

After establishment of the quantitative assay for screening of chemicals affecting yolk utilization, we exposed zebrafish larvae from 2 to 5 dpf to a set of chemicals. Prochloraz, a chemical previously shown to cause yolk malabsorption, was selected as a positive control. We then tested two pharmaceuticals, clofibrate and gemfibrozil, two flame retardants, tetrabromobisphenol-A (TBBPA) and tetrachlorobisphenol-A (TCBPA), the biocide tributyltin (TBT), the surfactant perfluorooctanoic acid (PFOA), and two pesticides, imazalil and butralin. The embryos were treated in 6-well plates, allowing for unrestricted embryo motility. At the end of the treatment period, larvae were transferred into 96-well plates (1 larva/well) for imaging. We measured the dissolved oxygen levels in the E3 of untreated and treated larvae at the end of the exposure period, and in E3 incubated without larvae. There were no differences in the levels of oxygen in the different samples (results nor shown). Images were fed into the segmentation algorithm for processing and analysis. Next, the computed yolk area for each larva was used to

calculate a "y_a ratio", defined as the ratio of the area of the yolk of the treated larva (measured in number of pixels) to the average yolk area of the control group of vehicle treated-larvae.

Prochloraz treatment from fertilization to 5 dpf has been shown previously to cause yolk malabsorption at 1.2 mg/L (approx. 3.18μM) (Domingues et al. 2013). To validate our model and assay, we treated the HGn50D transgenic fish with different concentrations of prochloraz. In line with the previous study, treatment with prochloraz resulted in a significant delay in yolk absorption (Figure 4.3 A). Larvae treated with 100nM, 1μM and 10μM of the prochloraz displayed significantly larger yolk sizes than those of the vehicle-treated control group. Larvae treated with 10μM prochloraz suffered a severe malabsorption phenotype, causing most of the larvae to remain on their lateral sides, making imaging difficult. We also analyzed the proportion of larvae that exhibited a larger yolk size than the control group, and found that even at the lowest concentration tested (10nM), slower yolk uptake was observed for around 60% of the embryos (Figure 4.3 B).

In zebrafish, the blood lipid lowering pharmaceuticals clofibrate and gemfibrozil have been shown to cause an embryonic malabsorption syndrome. Larvae treated with 0.5 and 0.75 mg/L (approx. 2μM and 3μM) clofibrate, and 5 mg/L (approx. 20μM) gemfibrozil during early development display larger yolk sizes than vehicle-treated larvae (Raldua et al. 2008). While our experiments showed that there were no significant changes in yolk sizes after exposure to gemfibrozil (Figure 4.3E) at 1nM, 10nM and 100nM

concentrations, clofibrate-treated larvae exhibited a smaller yolk sizes compared to vehicle-treated larvae at 100nM (Figure 4.3C and 4.3D).

Fig. 4.3. (Page 77) Effect of prochloraz, clofibrate and gemfibrozil on yolk resorption. (A) Boxplot of the y_a ratios of prochloraz-treated larvae. **(B)** Stacked-column representation of the proportion of larvae within each prochloraz treatment group with y_a ratios less than or greater than 1. **(C)** Boxplot of y_a ratios of clofibrate-treated larvae. **(D)** Stacked-column representation of the proportion of larvae within each clofibrate treatment group with y_a ratios less than or greater than 1. **(E)** Boxplot of the mean of y_a ratios of gemfibrozil-treated larvae. Statistical evaluation was performed using one-way ANOVA. Asterisks indicate p values from a post-hoc Dunnett's Multiple Comparison test between each dose and the vehicle-treated group, with * indicating $p < 0.05$, and *** indicating $p < 0.001$.

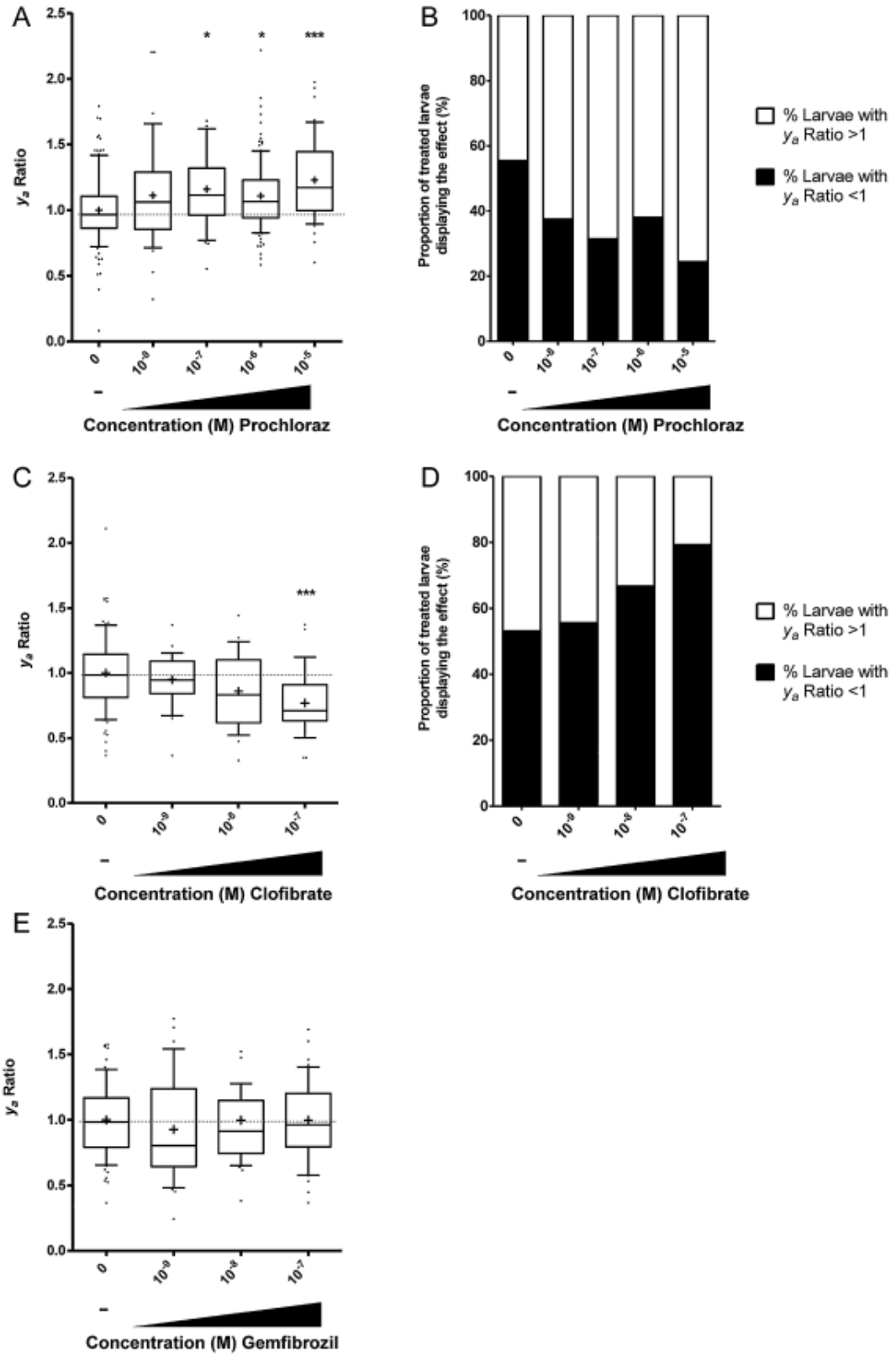
A
B
C
D
E
y_a Ratio
Proportion of treated larvae displaying the effect (%)
% Larvae with y_a Ratio >1
% Larvae with y_a Ratio <1
Concentration (M) Prochloraz
Concentration (M) Clofibrate
Concentration (M) Gemfibrozil

TBT, an antifouling agent used in paints in the shipping industry, and the flame retardants TBBPA and TCBPA have been shown to act as obesogens in the zebrafish (Riu et al. 2011; Tingaud-Sequeira et al. 2011). We investigated whether these environmental obesogens, which induce lipid accumulation in 11 dpf zebrafish at 1μM concentration for TBBPA and TCBPA and 1nM for TBT, could cause abnormal mobilization of the lipid-rich yolk. In our assay, TBBPA and TCBPA, and TBT at 1nM induced faster uptake of the yolk, with treated 5 dpf-larvae possessing smaller y_a ratios than those in the vehicle-treated control group (Figure 4.4). Exposure to 10 and 100pM TBT resulted in decreased yolk absorption.

We also treated the larvae with PFOA, a persistent organic pollutant with many industrial applications. In zebrafish, PFOA toxicity has been suggested to be mediated by mitochondrial dysfunction, causing an "energy drain" (Hagenaars et al. 2013). When treated with PFOA at 10nM, 100nM or 1μM, there was no significant effect on the y_a ratio (Figure 4.5A).

Finally, we exposed the embryos to the pesticides imazalil (a fungicide) and butralin (a herbicide). No significant effects were observed with imazalil (Figure 4.5B). Larvae treated with 10nM, 100nM and 1μM butralin displayed significantly smaller y_a ratios, implying faster consumption of the yolk than larvae in the control group (Figure 4.5C). More than 70% of larvae treated with 10nM, 100nM or 1μM butralin displayed a reduced yolk area compared to controls (Figure 4.5D).

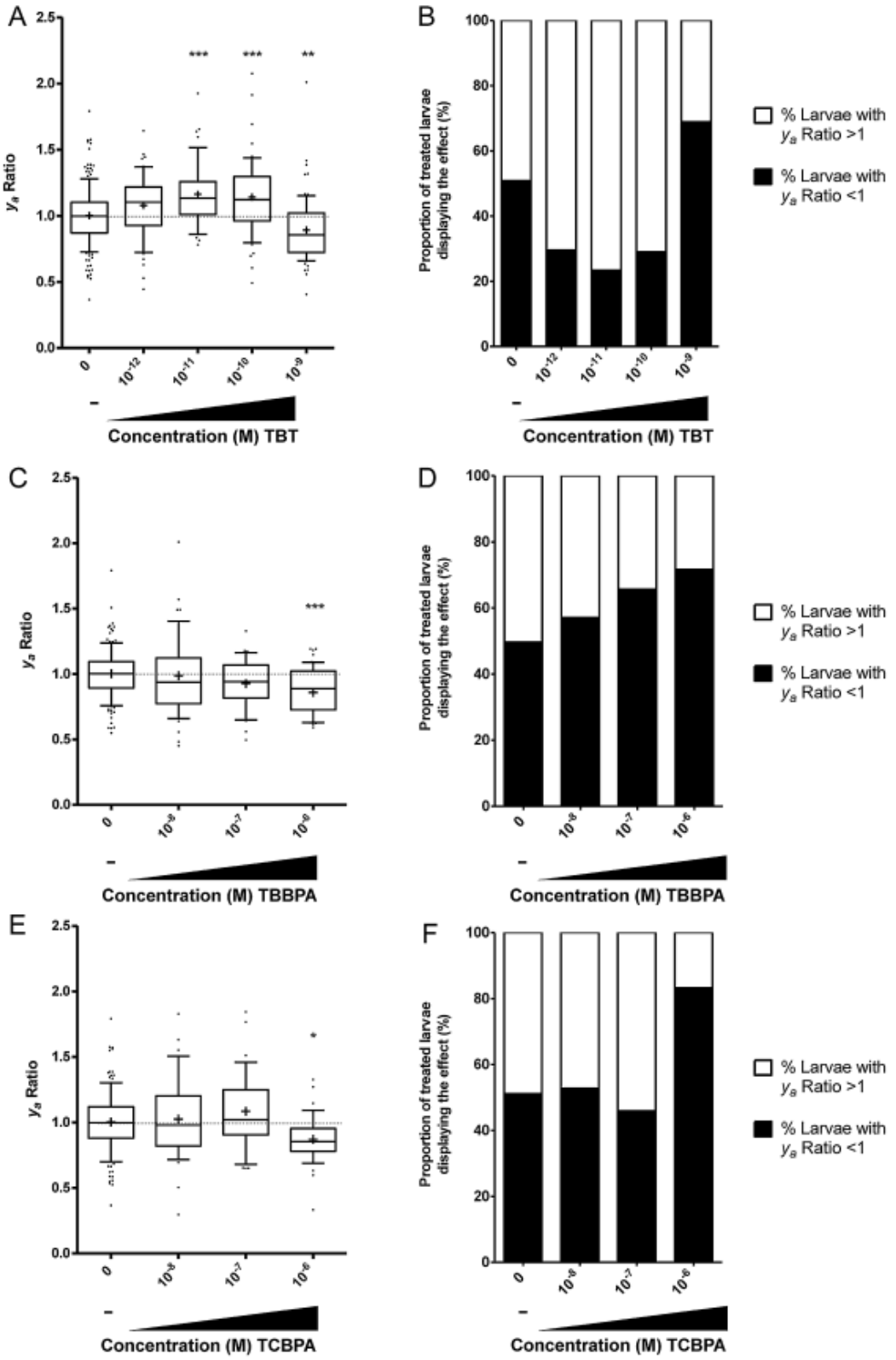
A
B
C
D
E
F
y_a Ratio
Proportion of treated larvae displaying the effect (%)
% Larvae with y_a Ratio >1
% Larvae with y_a Ratio <1
Concentration (M) TBT
Concentration (M) TBBPA
Concentration (M) TCBPA

Fig. 4.4 (Page 79) Effects of obesogens on yolk resorption. Box plots of y_a ratios against different concentrations of TBT **(A)**, TBBPA **(C)** and TCBPA **(E)**. Stacked-column representation of the proportion of larvae within each treatment group with y_a ratios less than or greater than 1 for TBT **(B)**, TBBPA **(D)** and TCBPA **(E)** respectively. Statistical evaluation was performed using one-way ANOVA. Asterisks indicate p values from a post-hoc Dunnett's Multiple Comparison test between each dose and the vehicle-treated group, with *indicating $p < 0.05$, ** indicating $p < 0.01$ and *** indicating $p < 0.001$.

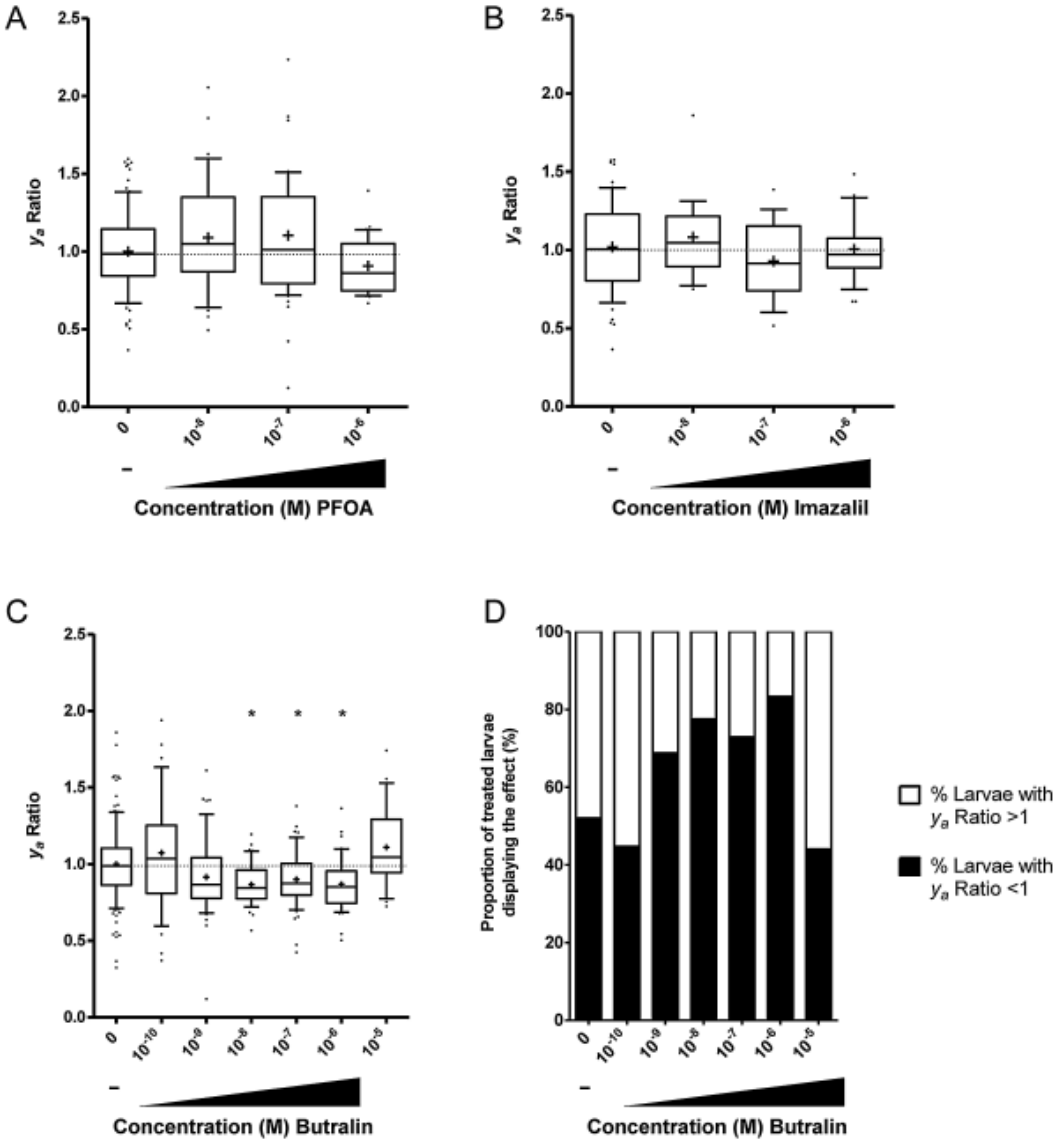

Fig. 4.5. Effects of endocrine disruptor PFOA and pesticides on yolk resorption. Box plots of y_a ratios against treatment concentration for PFOA **(A)**, imazalil **(B)** and butralin **(C)**. **(D)** Stacked-column representation of the proportion of larvae within each treatment group with y_a ratios less than or greater than 1 for butralin. Statistical evaluation was performed using one-way ANOVA. Asterisks indicate p values from a post-hoc Dunnett's Multiple Comparison test between each dose and the vehicle-treated group, with *indicating $p < 0.05$.

Table 4.1: LC_{50}, LEL and Effect Ratio for test chemicals

Chemical	LC50 (M)	LEL (M)	Effect Ratio (LC50/LEL)	Median y_a Ratio at the LEL
Prochloraz	3.6×10^{-5}	1×10^{-7}	360	1.11
Clofibrate	3.1×10^{-7}	None	NA	NA
Gemfibrozil	3.4×10^{-6}	None	NA	NA
TBT	3.4×10^{-7}	1×10^{-11}	34,400	1.13
TBBPA	3.6×10^{-6}	1×10^{-6}	3.6	0.89
TCBPA	3.6×10^{-6}	1×10^{-6}	3.6	0.85
PFOA	3.8×10^{-4}	None	NA	NA
Imazalil	6.6×10^{-5}	None	NA	NA
Butralin	9.5×10^{-5}	1×10^{-8}	9,500	0.84

We also determined the LC_{50} of the chemicals, and their capacity to induce morphological malformations. Table 4.1 summarizes the chemicals' effects on yolk absorption measured as Lowest Effect Level (LEL) and the concentration required to cause 50% lethality (LC_{50}). An effect ratio was calculated by dividing the LC_{50} by the LEL. By the LEL the compound ranking from largest to lowest effect on yolk absorption is TBT > butralin > prochloraz, clofibrate > TBBPA, TCBPA. No significant morphological malformations other than altered yolk sizes were observed at the concentrations tested.

4.3 DISCUSSION

In this study, we have designed and optimized a high-throughput zebrafish-based screening assay for yolk malabsorption. Environmental chemicals that alter the availability of nutrients to embryos during their development, across different species, can have important consequences for organogenesis, and also affect long-term risk of disease onset (reviewed in (Gluckman et al. 2007)). Given the number and variety of

industrial chemicals in commerce today, the need for developing large-scale screening models to identify such chemicals is evident.

We used the transgenic line HGn50D, which fluoresces in the yolk syncytial layer, heart, and eye lens. HGn50D was generated by *Tol2*-mediated transposition and random insertion of the GFP expressing construct (Asakawa et al. 2008; Urasaki et al. 2008), and the promoter driving the expression of GFP in the transgenic line is not known. Therefore, we have not considered the intensity of the fluorescence in yolk syncytial layer, and have only quantified the area within boundaries of the fluorescing yolk syncytial layer after chemical exposures. The effects of the chemicals on the other fluorescing tissues (heart and eyes) have not been assessed here.

Chemical exposures in our studies were restricted to 2-5 dpf. We chose the 2 dpf time point because this is after most organ rudiments have developed. An earlier exposure window might lead to developmental perturbations that could indirectly affect yolk absorption. We tested a dose range of exposures for all the chemicals. The low doses tested allowed for identification of yolk malabsorption in larvae that otherwise appeared normal morphologically, suggesting that chemicals, which impacted yolk absorption in our studies, can have effects at low doses even if there are no other observable gross morphological abnormalities. These results, therefore, underline the need for toxicological testing to assess less obvious endpoints at low doses.

The toxic effects of chemicals depend on their stability, uptake, metabolism, and elimination. Most of the chemicals analyzed in this study are stable in aquatic solutions. For prochloraz, the half-life in water has been measured to be 22.6 days at pH 7 (Aktar et al. 2008). Tributyltin is susceptible to biodegradation in water with a half-life of between 6 days and 35 weeks reported (search term "tributyltin" at https://pubchem.ncbi.nlm.nih.gov). The half-life of PFOA is measured in years rather than in days (Vierke et al. 2012). Imazalil is stable for at least eight weeks at 40 degrees (Food and Agriculture Organization of the United Nations 1978). Butralin has a half-life ranging from 21-52 days in water soil mixtures indicating its biodegradation is slow (search term "butralin" at https://pubchem.ncbi.nlm.nih.gov). We previously examined the fate of TBBPA and TCBPA in zebrafish larvae (Riu et al. 2014a). Both TBBPA and TCBPA are efficiently taken up by 3 dpf zebrafish larvae - within 24 h more than 80% of TBBPA is taken up and metabolized to sulfated-TBBPA, which retains biological activity. Being drugs, clofibrate and gemfibrozil are rapidly taken up and metabolized in humans. A linear range uptake following exposure to increasing doses in zebrafish has been reported (Brox et al. 2014), however the stability of the compounds in fish are not known.

Using our novel method, we first confirmed that prochloraz induces yolk malabsorption. Prochloraz is an imidazole fungicide used widely in Europe, Australia, Asia and South America, in both agricultural and gardening practices. It acts as an endocrine disruptor via multiple modes of action. *In vitro*, it antagonizes the androgen and estrogen receptors, inhibits aromatase and activates the aryl hydrocarbon receptor (Andersen et al. 2002;

Laignelet et al. 1992; Long et al. 2003; Vinggaard et al. 2000). *In vivo,* prochloraz acts as an anti-androgen in adult and developmental stages in rodents (Vinggaard et al. 2002; Vinggaard et al. 2006). In zebrafish, prochloraz exposure causes metabolic alterations in exposed zebrafish larvae (Domingues et al. 2013), which is in line with our results, and in adults (Biales et al. 2011). Spine malformation, pericardial edema and yolk malabsorption are observed when embryos/larvae are treated from 0 to 3 or 0 to 4 dpf, at concentrations of 1.2 mg/L (approx. 3.18μM) or higher (Domingues et al. 2013). However, in our studies, we observed a significant yolk malabsorption effect at lower concentrations (as low as 100nM), possibly indicating the high sensitivity of our quantification method.

The pharmaceutical fibrates clofibrate and gemfibrozil have previously been suggested to induce yolk malabsorption, albeit at concentrations higher than tested here. For clofibrate, Raldua et al. showed that yolk malabsorption occurred at 0.75-1.00 mg/L (approx. 3 - 4μM), with affected embryos displaying a larger yolk than control embryos (Raldua et al. 2008). However, at the highest concentration we tested (100nM), treated larvae have significantly smaller yolk sizes than vehicle-treated larvae, with more than 75% of the embryos displaying a y_a ratio less than 1. This result highlights the importance of testing low concentrations using sensitive and quantitative endpoints. Raldua et al. also showed that gemfibrozil at 5 mg/L (approx. 20μM) caused yolk malabsorption. In our study, however, we did not observe significant changes in yolk absorption at low concentrations of gemfibrozil (1nM, 10nM and 100nM), and the larvae did not survive in concentrations of 1μM or higher. It is worth noting here, that there were important differences in our

experimental design. We treated the fish only from 2 dpf, and not from 4 hours post fertilization (hpf), and only with lower concentrations of the chemicals. This might explain why we did not see drastic effects, as it is possible that these chemicals induce a stronger effect earlier during development. Mortality at 1μM concentrations may be due to the fact that we did not replace the treatment solutions each day of the treatment. It is possible that accumulation of toxic metabolites of these chemicals were highly toxic to the larvae.

Using our assay, we observed an increased uptake of the yolk in larvae treated with the flame retardants TBBPA and TCBPA, and with TBT, an antifouling agent used in paints in the shipping industry. These compounds have been suggested to be obesogens, environmental chemicals that can cause obesity. Given the steep rise in obesity prevalence in recent years (Ogden et al. 2012, 2014), the putative role of chemicals in inducing obesity is an active area of research (reviewed in (Baillie-Hamilton 2002)). TBT induces adipogenesis *in vitro* (Inadera and Shimomura 2005; Li et al. 2011) and causes obesity or lipid accumulation *in vivo,* in mice (Zuo et al. 2011), and in zebrafish (Tingaud-Sequeira et al. 2011). Recent studies by us and others have shown that TBBPA and TCBPA can act as obesogens *in vitro* (Riu et al. 2011) and *in vivo* in zebrafish (Riu et al. 2014a). TBBPA and TCBPA are ligands for the zebrafish peroxisome proliferator-activated receptor gamma (PPARγ) (Riu et al. 2014a). Whether or not PPARγ is involved in yolk absorption, however, is not known. Larvae treated with PFOA, an endocrine disruptor (Du et al. 2013) and a chemical associated with mitochondrial dysfunction in zebrafish (Hagenaars et al. 2013), did not show significant effects on yolk utilization in

our study. However, approximately 60% of 1μM treated larvae displayed smaller yolk sizes as compared to controls, indicating that perhaps a stronger effect can be seen at higher doses.

As our assay was able to detect the altered yolk consumption rates of known disruptors of energy/lipid metabolism, we suggest that our assay may be used to supplement other screening efforts designed to identify chemicals altering metabolic endpoints.

We also analyzed the effects of two pesticides from the ToxCast phase I chemical library, imazalil, and butralin, on yolk absorption. Imazalil, which is a fungicide and food contaminant, is known to induce cytochrome P450 isoforms in the mouse intestine (Muto et al. 1997), and alter developmental endpoints, including cardiac edema, and deformations in the notochord and tail in the zebrafish (Sisman and Turkez 2010). In our experiments, we did not see significant effects of imazalil, possibly because of the low concentrations tested.

Butralin, on the other hand, significantly increased yolk uptake, with y_a ratios across four different concentrations being less than the average of the control group. Butralin, a dinitroaniline compound, is an herbicide used on agricultural crops, including tobacco. Very little is known about its potential other biological effects. In a retrospective epidemiological study conducted on tobacco farmers, exposure to the pesticide Tamex, containing butralin, was found to significantly correlate to low maximal motor nerve conduction velocity, indicating a possible effect on the nervous system (Kimura et al.

2005). As little is known about the chemical's mechanism of toxicity, it is not possible to speculate on how butralin causes yolk malabsorption, although its potential effects on the nervous system could be worth investigating.

In conclusion, we have established an assay for the quantification of yolk size in zebrafish larvae exposed to different environmental chemicals and showed that several chemicals alter yolk absorption. Although elucidation of the mechanisms through which the chemicals impacting our assay elicit their effect on yolk absorption is beyond the scope of this study, it would be interesting to differentiate a chemical's effect on the chosen endpoint as being a direct or an indirect effect. It will also be interesting to investigate long-term effects of the chemicals that disturb nutritional balance during zebrafish development. Moreover, chemicals causing alterations in this assay could be tested on other animal models to ascertain their relevance, perhaps, in a mammalian context.

CHAPTER 5: A TRANSCRIPTOMIC ANALYSIS OF OBESOGEN EXPOSURES IN ZEBRAFISH

5.1 INTRODUCTION

As previously described in Chapter 1, the nuclear receptor PPARγ is involved in the regulation of adipose tissue development and lipid metabolism in the adipose tissue. Because of its role in adipose tissue function, PPARγ has been implicated in the etiology of lipid metabolic disease and obesity. For example, clinical use of a mammalian PPARγ agonist (Rosiglitazone) for diabetes patients has proved effective, but has been shown to cause weight gain over long periods of use (Shim et al. 2006). Among other chemicals known to induce weight gain in animal studies is BPA, a synthetic estrogen. BPA induces adipogenesis in 3T3-L1 cell lines and weight gain in mice and rats (Howdeshell et al. 1999; Nikaido et al. 2004; Somm et al. 2009). However, BPA, does not act activate PPARγ to induce these obesity-related phenotypes (Riu et al. 2011).

In contrast, halogenated analogs of BPA, tetrabromobisphenol A (TBBPA) and tetrachlorobisphenol A (TCBPA) activate mammalian PPARγ and induce adipogenesis *in vitro* in murine preadipocytes NIH3T3-L1 cells (Riu et al. 2011). In zebrafish, exposure of larval zebrafish for 3 days to TBBPA, TCBPA, and the well-known mammalian obesogen and activator of PPARγ/RXR signaling tributyltin (TBT), results in increased uptake of the lipid-rich yolk relative to controls (Chapter 4, and (Kalasekar et al. 2014)). Moreover, exposure of larval zebrafish to these chemicals for 8 days increases lipid deposition in the larvae, and also result in increased BMI in exposed fish three weeks after treatment withdrawal (Riu et al. 2014b). Given that TBBPA and TCBPA are used ubiquitously as flame retardants in household plastics and electronics, and that TBBPA

has been detected in human tissues such as adipose tissue, umbilical cord blood as well as breast milk (Cariou et al. 2008; Fernandez et al. 2007), a better understanding of the potentially obesogenic effects of TBBPA and TCBPA is essential.

Although it is possible that the activation of PPARγ/RXR signaling by TBBPA, TCBPA and TBT (Figure 5.1) causes the phenotypes of aberrant lipid accumulation and weight gain in the zebrafish, the precise mechanisms by which these chemicals act remains to be elucidated. Since zebrafish share several similarities with mammalian models, particularly with regards to metabolism (see Chapter 1, reviewed in (Seth et al. 2013)), the objective of the following study was to explore the gene expression changes associated with exposure of juvenile zebrafish to these chemicals. Juvenile zebrafish were chosen for their small size and well-developed hypothalamus-pituitary-gonadal axis. The fish were exposed DMSO (vehicle-control), 100nM TBBPA, 100nM TCBPA or 1nM TBT for 48 hours. Following exposure, the fish were sacrificed, and RNA was extracted from the whole fish. Transcriptomic analysis was then performed, the results of which are described and discussed below.

5.2 RESULTS

5.2.1 TBBPA/TCBPA/TBT-induced gene expression changes in zebrafish

Analysis of the gene expression data following exposure of juvenile zebrafish to TBBPA, TCBPA or TBT showed that the expression of several genes was regulated by exposure to these chemicals. The total number of gene probes found to be regulated by the chemicals was 1209 for TBBPA, 983 for TCBPA and 2178 for TBT. Most, but not all,

of these probes (approximately 92% for TBBPA, 88% for TCBPA and 90% for TBT) had gene symbols. Hierarchical clustering of genes regulated at least 1.5-fold is depicted by a gene expression heat map (Figure 5.2A). Although TBBPA, TCBPA and TBT function through PPARγ/RXR signaling and TBBPA and TCBPA are highly similar structurally, the three chemicals exhibit diverse gene expression profiles with only a few genes being regulated commonly by all three chemicals. The number of genes commonly regulated by the chemicals is depicted in Figure 5.2B. Of all the annotated zebrafish genes with fold-induction (FI) greater than or equal to 1.5 in either direction (up-regulation or down-regulation), approximately 69% (TBBPA), 67% (TCBPA) and 73% (TBT) possessed annotated human homologs (Figure 5.2C). All subsequent functional analyses were carried out using the annotated human homologues of the zebrafish genes.

Functional tissue enrichment analysis using the NIH DAVID online tool (Figure 5.2D) indicates that the tested chemicals target genes in several tissues, including the somites (which are paraxial mesoderm present in the zebrafish), liver, skeletal tissues, eyes, the yolk syncytial layer (YSL), gut, heart, gonads, muscles and the heart and cardiovascular system.

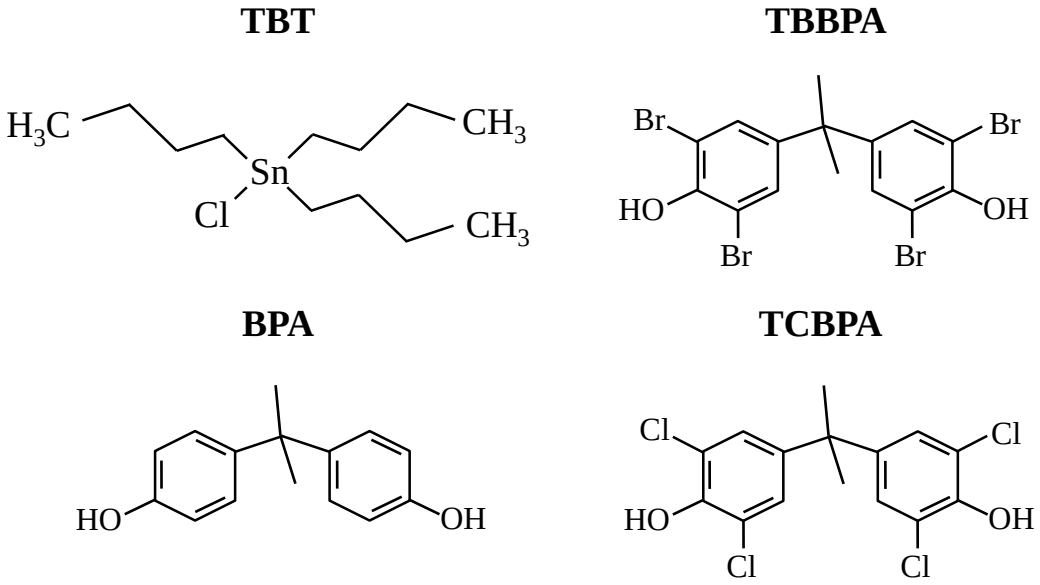

Figure 5.1 Chemical structures of tested obesogens.

Figure 5.2. (Page 94) Hierarchical clustering and Venn diagram representing differentially expressed genes determined by microarray analysis in zebrafish larvae treated with TBBPA, TCBPA or TBT. (A) Heat map of differentially expressed genes in juvenile zf exposed to TBBPA, TCBPA or TBT as determined by microarray analysis (absolute fold change $\geq |\pm 1.5|$, FDR-adjusted p-value ≤ 0.05). **(B)** Venn diagram illustrating the number of genes that were significantly regulated in zebrafish treated with TBBPA, TCBPA or TBT. **(C)** Venn diagram illustrating the number of zebrafish genes with known human homologues. **(D)** Tissue enrichment analysis using the NIH DAVID. Enriched tissues with $p<0.05$ are represented. YSL: yolk syncytial layer. Figures by Drs. Philip Jonsson and Catherine McCollum, compiled by the author.

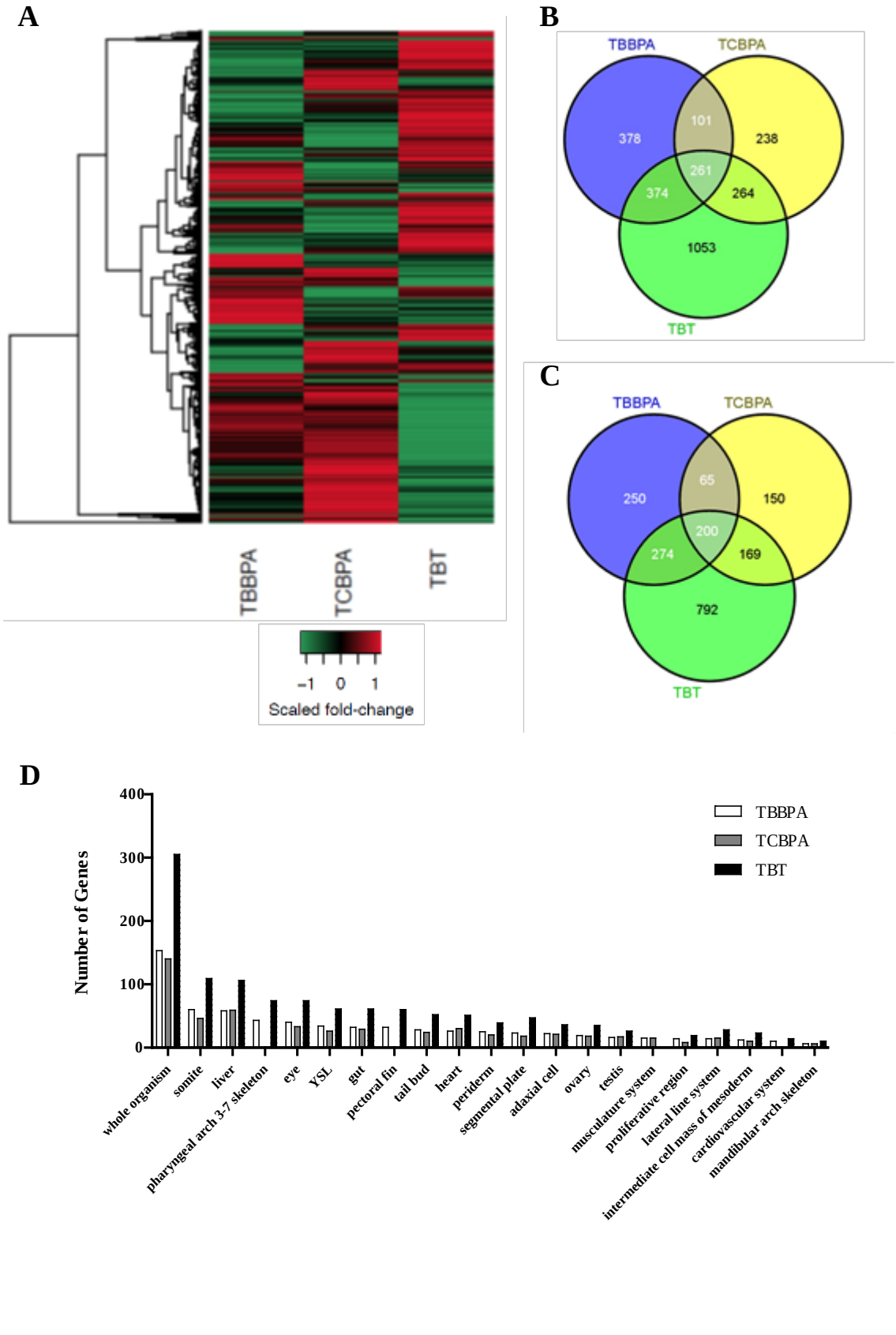
A
TBBPA
TCBPA
TBT
−1 0 1
Scaled fold-change
B
TBBPA
TCBPA
TBT
378
101
238
261
374
264
1053
C
TBBPA
TCBPA
TBT
250
65
150
200
274
169
792
D
Number of Genes
400
300
200
100
0
TBBPA
TCBPA
TBT
whole organism
somite
liver
pharyngeal arch 3-7 skeleton
eye
YSL
gut
pectoral fin
tail bud
heart
periderm
segmental plate
adaxial cell
ovary
testis
musculature system
proliferative region
lateral line system
intermediate cell mass of mesoderm
cardiovascular system
mandibular arch skeleton

The genes most regulated by exposure to the toxicants are listed in Table 5.1. These genes were co-regulated to the highest extent by all three chemicals. Although phosphoenolpyruvate carboxykinase 1 (*pck1),* which is a PPARγ target gene, was among the most up-regulated genes, genes belonging to other pathways were also affected by chemical exposure. Some of these include the genes for Mediator complex subunit 13 (*med13*), which plays an integral role in WNT signaling, Supressor of cytokine signaling 3 (*socs3),* which is involved in inflammation. The most regulated genes for each chemical are listed in Appendix Table 5A.

As indicated above, there were only about 200 genes, which were co-regulated by TBBPA, TCBPA and TBT. As all three chemicals increased lipid accumulation in the zebrafish, we chose to focus our subsequent analyses on the commonly regulated 200 genes in order to investigate the mechanism by which the chemicals affect lipid homeostasis.

Table 5.1. Most-Regulated Genes			
	Gene ID	**Gene**	**Avg. FI**
Down-regulated Genes	MED13	Mediator complex subunit 13	-10.72
	EXOC1	Exocyst complex component 1	-4.56
	PCNA	Proliferating cell nuclear antigen	-3.63
	HAPLN4	Hyaluronan and proteoglycan link protein 4	-2.77
	CYP11A1	Cytochrome P450, family 11, subfamily A, polypeptide 1	-2.72
	DHX32	DEAH box polypeptide 32	-2.59
	GNMT	Glycine-N-methyltransferase	-2.55
	GPNMB	Glycoprotein (transmembrane) nmb	-2.35
	MYH4	Myosin,heavy chain 4, skeletal muscle	-2.29
	DHX33	DEAH box polypeptide 33	-2.21
	HSPA9	Heat shock 70kDa protein 9 (mortalin)	-2.18
	FUNDC2	Fun14 domain containing 2	-2.13
	CSRP2BP	Cysteine and glycine-rich protein 2 binding protein	-2.12
	CLCNKB	chloride channel, voltage sensitive Kb	-2.09
	DNMT1	DNA(cytosine-5)-methyltransferase 1	-2.05
Up-regulated Genes	CHRNB3	Cholinergic receptor, nicotinic, beta 3 (neuronal)	2.62
	FOXQ1	Forkhead box Q1	2.63
	GGACT	Gamma-glutamylamine cycletransferase	2.67
	CEBPB	CCAAT/enhancer binding protein, beta	2.88
	C8orf4	Chromosome 8 open reading frame 4	2.91
	PCK1	Phosphoenolpyruvate caboxykinase 1 (soluble)	3.03
	JUNB	Jun B proto-oncogene	3.41
	EGR4	Early growth response 4	3.82
	FOS	FBJ murine osteosarcoma viral oncogene homolog	3.85
	HBE1	Hemoglobin, epsilon 1	4.09
	JDP2	Jun dimerization protein 2	4.16
	NPAS4	Neuronal PAS domain protein 4	5.09
	SOCS3	Suppressor of cytokine signaling 3	5.11
	TCTEX1D2	Tctex1 domain containing 2	5.50
	FOSB	FBJ murine osteosarcoma viral oncogene homolog B	6.27

Table 5.1. List of gene most- altered by exposure to TBBPA, TCBPA or TBT. Genes co-regulated by the three chemicals were selected, and the average of fold-induction by each chemical was computed. The Average FI was then used to determine 15 of the most up- and down-regulated genes.

Table 5.2 Functional Analysis of Commonly Regulated Genes		
Enriched Biological Process	***p* -value**	**Overlapping Entities**
acute-phase response	4.06E-06	*fn1, saa1, ahsg, a2m, apcs, cebpb*
response to nutrient	6.47E-06	*alox5, cyp11a1, a2m, slc6a19, lct, cp, mgp, cubn, col1a1*
polysaccharide digestion	7.77E-06	*lct, amy2a, mgam*
platelet degranulation	1.03E-05	*fn1, f5, app, a2m, serping1, fga, ttn*
regulation of complement activation	1.56E-05	*cfb, c4b, cfh, c3*
skeletal muscle thin filament assembly	2.68E-05	*tcap, actc1, ttn*
muscle filament sliding	3.30E-05	*mybpc2, myh4, tcap, actc1, ttn*
osteoblast differentiation	3.68E-05	*bglap, jonb, mef2d, igfbp5, gpnmb, col1a1*
amino acid transmembrane transport	4.21E-05	*slc38a2, slc1a2, slc43a2, slc6a19, slc43a1*
positive regulation of transcription from RNA polymerase II promoter	5.05E-05	*med13, app, six2, myod1, abra, egr4, junb, cebpd, mef2d, npas4, nkx3-1, fos, mafa, hif3a, foxq1, vgll2, cebpb, nfix, nr5a2, klf4*
metabolic process	5.76E-05	*mgam, ntan1, mmp14, ptprc, atp2a1, bmp1, myh4, peli3, uchl1, qdpr, tph1, dhrs13, aloxe3, amy2a, lct, proz, agxt, gstk1, g6pc, dnmt1, ace, slc27a2, atp2b1, enpp6*
ossification	5.95E-05	*bglap, fn1, ahsg, mmp14, mgp, bmp1, col1a1*
response to light stimulus	6.61E-05	*syne1, junb, slc1a2, fos*
negative regulation of complement activation, lectin pathway	8.58E-05	*a2m, serping1*
blood coagulation	0.000146	*app, atp2a1, prox, fga, c3, col1a1, ttn, fn1, f5, atp2b1, a2m, esam, serping1, hbe1*

Table 5.2. List of biological processes most regulated by exposure to TBBPA, TCBPA and TBT. Analysis by Dr.Catherine McCollum.

Table 5.2 lists the top 15 biological processes most represented among genes whose expression was co-regulated by TBBPA, TCBPA and TBT. Analysis were done using the REVIGO online database for mammals, using the annotated human homologues of regulated zebrafish genes and REVIGO (http://revigo.irb.hr) was used to summarize the list of enriched GO terms. Although genes involved in metabolism were indeed among the top regulated processes ("Response to nutrient" and "Metabolic process" categories), several processes related to inflammation ("Acute-phase response" category, and complement activation –related genes) were also regulated. The biological processes enriched by each chemical are listed in Appendix Table 5B.

To validate the gene expression data obtained from the microarray, we carried out Real-time Quantitative Polymerase Chain Reaction (qPCR) assays with optimized primer sets specific for a subset of genes, chosen to represent the different aspects of gene regulation discussed within this chapter. qPCR analyses were performed on top–regulated genes (*jdp2* and *npas4*) and genes involved in adipogenesis (*cebpa*, *cebpb* and *cebpd*), lipid metabolism (*cd36*, *pck1* and *fasn*) and inflammation (*ptgs2* and *socs3*). The FIs from microarray as well as qPCR methods of gene expression are tabulated in Figure 5.3A, and the correlation plot in Figure 5.3B indicates correlation between the two methods for all three chemicals. The correlation was significant for all three chemicals, with the Pearson coefficient of correlation being 0.7462 (p=0.03) for TBBPA, 0.9532 (p=0.0002) for TCBPA and 0.7029 (p=0.02) for TBT. Appendix Table 5C lists the primer sequences used for the qPCR assays. Appendix Table 5D contains the list of all genes regulated by each chemical individually, as well as those that were co-regulated by all three chemicals.

A

Genes	FI from qPCR	FI from Microarray		
		TBBPA	TCBPA	TBT
cd36	1.14			
	1.29		1.54	
	1.43			1.70
cebpa	1.40			
	1.30			
	1.68			1.57
cebpb	1.87	1.87		
	2.09		2.79	
	3.54			3.98
cebpd	1.56	1.73		
	2.49		2.36	
	3.91			3.07
fasn	1.53	2.06		
	1.30			
	1.48			1.70
jdp2	0.23	2.53		
	3.49		3.16	
	1.89			6.78
npas4	5.64	3.97		
	6.23		5.29	
	8.91			6.00
pck1	1.93	1.73		
	4.39		2.96	
	10.41			4.41
ptgs2	1.56	1.95		
	1.67		1.94	
	2.76			2.33
socs3	3.05	2.15		
	5.85		5.12	
	12.48			8.05

B

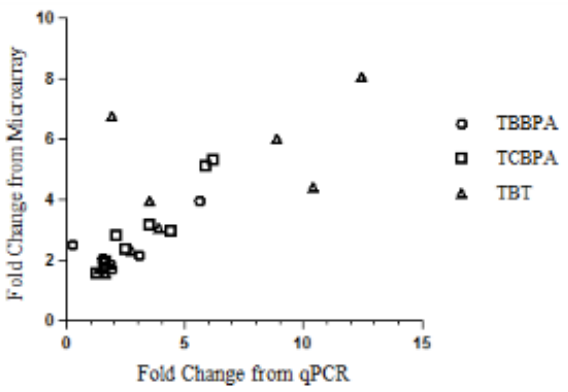

Figure 5.3. Correlation between gene expression analysis methods. A subset of genes identified as being regulated by TBBPA, TCBPA or TBT were picked for validation by RT-qPCR. **(A)** Fold inductions (FIs) obtained from qPCR and microarray profiling are listed. **(B)** Correlation plot of the FIs from microarray (y-axis) and qPCR (x-axis). Correlation between gene expression methods was significant, with the Pearson coefficient of correlation being 0.7462 (p=0.03) for TBBPA, 0.9532 (p=0.0002) for TCBPA and 0.7029 (p=0.02) for TBT.

5.2.2 TBBPA, TCBPA and TBT regulate genes involved in Adipogenesis in zebrafish

Although not among the top 15 biological process regulated by TBBPA, TCBPA and TBT, the process of fat cell differentiation appeared among the significantly enriched biological processes co-regulated by the three chemicals (p=0.02). Genes annotated to be involved in adipogenesis are listed in Figure 5.4A. To gather information on the regulation of adipogenic genes regulated by the tested chemicals, we extended our search

to include genes involved in adipogenesis that were regulated by at least one of the tested chemicals. Among the genes co-regulated by TBBPA, TCBPA and TBT are *cebpb*, *cebpd*, *ucp1* and *klf4*. The CCAAT Enhancer Binding Proteins (C/EBPs) are proteins known to be canonical markers of preadipocyte differentiation into mature adipocytes (Wu et al. 1999). The Krüppel-like family of transcription factors is also known to be an early regulator of adipocyte differentiation (Birsoy et al. 2008). The up-regulation of *ucp1*, which is activated in the absence of PPARγ in mammals and known to induce brown fat cell differentiation, however, is interesting, and will be discussed in the next section. The chemicals TBBPA, TCBPA and TBT also up-regulated the expression of other genes involved in adipogenesis, such as PPARγ target genes *cd36* and *pck1*, and down-regulated activators of the WNT signaling pathway such as *med13* (Carrera et al. 2008), *wnt8a* and *wnt11* (WNT ligands), which suppress adipogenesis (Tontonoz and Spiegelman 2008). The relationship between the different genes related to adipogenesis is represented schematically in Figure 5.4B.

Adipogenesis-related genes were then analyzed using Pathway Studio to determine possible effectors of chemical-induced gene expression changes leading to fat cell differentiation (Figure 5.4C). Regulators predicted in common for all three chemicals included CEBPB and the glucocorticoid receptor (GR), both of which are known inducers of adipogenesis (Tang and Lane 2012; Wu et al. 1999).

A

TBBPA	TCBPA	TBT	Genes
■	■	■	CEBPB
■	■	■	CEBPD
■	■	■	UCP1
■	■	■	KLF4
■			MB
■			PPARGC1A
	■	■	ARL4A
	■	■	EGR2
	■	■	LPIN1
	■	■	STEAP4
	■	■	BBS4
	■		PTGS2
		■	ADRB2
		■	AKT2
		■	ARID5B
		■	CEBPA
		■	ERAP1
		■	ERO1L
		■	PLAC8
		■	RGS2
		■	WNT11
■		■	WNT 8A
■	■	■	MED13

B

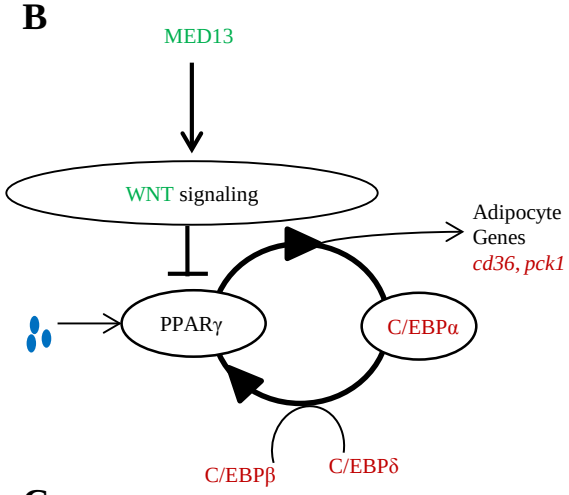

C

Predicted Regulators of Toxicant-Induced Adipogenesis		
TBBPA	**TCBPA**	**TBT**
ACVR1	ADCYAP1	ADRB2
CAMKK2	CEBPB	CEBPB
CEBPB	CREB1	CREB1
CEBPD	CREM	KLF4
KLF11	CRHR2	NNAT
KLF2	KLF4	GR
MEF2C	NFKBIZ	PLAC8
GR	GR	PTGIR
SH3PXD2B	NUR77	STAT3
WNT10B	PTGIR	TRIB2

Figure 5.4. Regulation of adipogenesis by TBBPA, TCBPA and TBT. (A) Representation of gene expression changes induced by tested chemicals on adipogenesis-related genes. Red block indicates up-regulation and green block indicates down-regulation. **(B)** Schematic representation of the relationship between canonical regulators of adipocyte differentiation in mammals, adapted from (Wu et al. 1999). Entities with transcripts up-regulated (red) and down-regulated (green) in the present study are indicated. Blue circles indicate ligands. Arrows indicate activation and inhibition is indicated by "---|". "WNT" refers to ligands *wnt8a* and *wnt11*, which were both down-regulated. **(C)** List of top regulators of adipogenesis-related genes, as predicted by Pathway Studio. Entities in green are in common across all chemicals tested.

5.2.3 TBBPA, TCBPA and TBT regulate genes involved in lipid metabolism in zebrafish

One of the biological processes most regulated by TBBPA, TCBPA and TBT was metabolism (Table 5.2). Within the broad category of metabolism, lipid metabolic processes such as lipoprotein and cholesterol metabolism were most affected (Table 5.3). In order the understand the toxicant-induced gene expression changes, which could have caused increased lipid accumulation in previous studies (Riu et al. 2014b), the gene expression changes associated with genes annotated in lipid metabolism (Pathway Studio), and other lipid metabolism-related genes (following a literature survey) were compiled (Figure 5.5A). Genes up-regulated by all three chemicals included those of the bone morphogenetic protein 1 (*bmp1*) and *pck1*. *bmp1* is known to activate apolipoprotein A1 (apoA1) and high-density lipoprotein (HDL) formation (Chau et al. 2007), and induction of *pck1* gene expression by PPARγ in adipocytes is known to induce lipid accumulation (Hallakou et al. 1997). Another PPARγ target gene, *cd36* (cluster of differentiation 36 or fatty acid translocase), which functions in fatty acid uptake into adipocytes, is also upregulated. Several other genes whose expression was induced by at least one of the toxicants are involved in reverse cholesterol transport and triglyceride synthesis in the liver (Figure 5.5B). Reverse cholesterol transport is the process by which cholesterol from peripheral tissues is carried in lipoprotein particle back to the liver, where it can be recycled or used in bile acid synthesis. Transcripts of several proteins involved in this process, including the ATP-binding cassette, sub-family A (ABC1), member 1 cholesterol transporter (*abca1*), apolipoprotein (*apoE*), plasma cholesteryl ester transfer protein (*cetp*), another cholesterol transporter scavenger receptor

class B, member 1 (*scarb1*), and sterol-O-acyltransferase1 (*soat1*) were all up-regulated by at least one of the toxicants. Genes involved in hepatic triglyceride synthesis were also up-regulated, including the acyl-CoA synthetase family member 3 (*acsf3*) and diacylglycerol O-acyltransferase 2 (*dgat2*). The relationship between the lipid metabolism-related genes regulated by TBBPA, TCBPA and TBT is schematically represented in Figure5.4B, and discussed in the following section.

Pathway Studio was then used to predict the possible regulators of toxicant-mediated effects on genes related to lipid and cholesterol metabolism (Figure 5.5C). As expected, the PPAR receptors PPARα and PPARγ, their obligate heterodimer RXR, and the liver X receptor (LXR), which has been shown to regulate cholesterol homeostasis in mammals, were all predicted regulators of the chemicals' effect on lipid metabolism.

A

TBBPA	TCBPA	TBT	Genes
■	■	■	BMP1
■	■	■	CUBN
■	■	■	ENPP6
■	■	■	PCK1
■	■	■	PTGS2
■	■	■	SLC27A2
■		■	ASPG
■		■	CYP7A1
■		■	FASN
■		■	HSD17B7
■			SCARB1
■			ACSF3
■			ACSL1
■			PPARA
■			PTGES
■		■	SULT2B1
	■	■	ABCA1
	■	■	CETP
	■	■	CD36
	■	■	FA2H
	■	■	LCN15
	■	■	LPIN1
	■	■	MID1IP1
	■	■	SRD5A2
	■		DGAT2
	■		SLC27A1
	■		SOAT2
	■		SPTSSB
	■		SREBF2

TBBPA	TCBPA	TBT	Genes
		■	APOE
		■	AGPAT9
		■	CYP51A1
		■	LPIN2
		■	PLAGL2
		■	PPP1CB
		■	PTEN
■		■	UCP3
■	■	■	LIPI
■		■	APOA4
■		■	CPT1C
■		■	LPCAT4
■		■	TECRL
		■	CBR4
		■	ELOVL3
		■	GPAT2
		■	HRASLS
		■	LDLRAP1
		■	MVK
		■	P4HB
		■	PLCD1
		■	PLCXD1
		■	PTGS1
■	■	■	CYP11A1

Down-regulated

Up-regulated

B

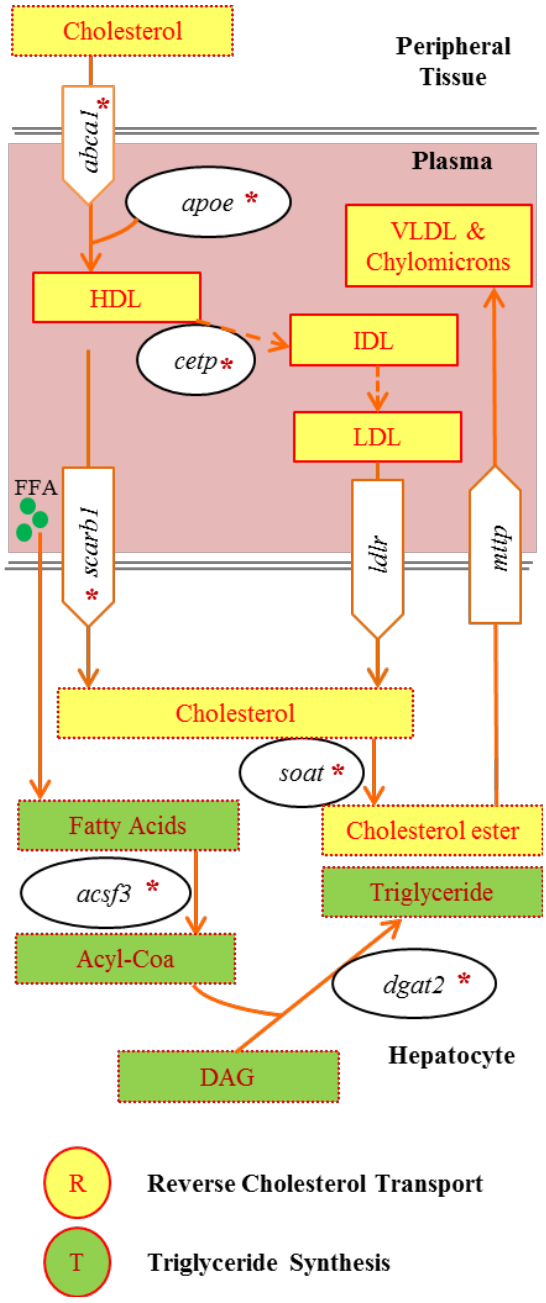

C

Predicted Regulators of Toxicant-Induced Lipid Accumulation		
TBBPA	**TCBPA**	**TBT**
LXR	SREBF1	SREBF1
PPARG	SHP1	LXR
SREBF1	LXR	SREBP
PPARA	RXR	RXR
RXR	LEP	PPARG
PXR	SREBP	SREBF2
NUR77	PPARA	PPARA
AMPK	PPARG	NR1H4

Figure 5.5. Regulation of lipid metabolism by TBBPA, TCBPA and TBT. (A) Representation of gene expression changes induced by tested chemicals on lipid metabolism-related genes. Red block indicates up-regulation and green block indicates down-regulation. (B) Schematic representation of the functional context for lipid-metabolism-related genes regulated by TBBPA, TCBPA and/or TBT. A red asterisk within the entity denotes up-regulation in the microarray. **(C)** List of top regulators of lipid metabolism-related genes, as predicted by Pathway Studio. Entities in green are in common across all chemicals tested.

Table 5.3 below represents the sub-categories of processes within metabolism, which were affected by chemical exposure. Processes indicated in red are statistically significant with $p<0.05$.

Table 5.3. Metabolic Process Sub-categories			
Biological Process	***p*-value**	**Biological Process**	***p*-value**
Metabolic process	5.76E-05	Glycogen metabolic process	5.32E-02
Lipid metabolic process	8.26E-02	Glucose metabolic process	1.13E-01
Cellular lipid metabolic process	1.57E-01	Fructose metabolic process	-
Fatty acid metabolic process	1.61E-01	Cholesterol metabolic process	2.02E-03
Triglyceride metabolic process	3.25E-01	Steroid metabolic process	1.09E-01
Lipid biosynthetic process	-	Hormone metabolic process	-
Lipid glycosylation	-	Small molecule metabolic process	2.86E-02
Phospholipid metabolic process	8.85E-01	Drug metabolic process	2.86E-01
Lipoprotein metabolic process	9.47E-03	Phthalate metabolic process	7.19E-02
Carbohydrate metabolic process	1.81E-01	Biphenyl metabolic process	7.19E-02

5.2.4 TBBPA, TCBPA and TBT regulate genes involved in inflammation in zebrafish

The genes regulated by the TBBPA, TCBPA and TBT were most significantly enriched in the category involved in the acute-phase response (Table 5.2). The genes in this category (depicted in Figure 5.6A) include the cell adhesion glycoprotein fibronectin 1 (*fn1*), serum amyloid A1 (*saa1*), alpha-2-HS-glycoprotein (*ahsg*) and the serum amyloid P component (*apcs*), which are up-regulated, and alpha-2-macroglobulin (*a2m*), which was down-regulated by chemical exposures. Other inflammation-related transcripts, which were regulated in response to obesogen exposures include *socs3*, *ptgs2*, signal transducer and activator of transcription 5B (*stat5b*), interleukin 15 (*il15*), interleukin enhancer binding factor 2 (*ilf2*) and the C-reactive protein (*crp*). *socs3* functions in mammals as a suppressor of inflammation. *saa1*, *a2m* and *crp* are establish biomarkers of acute phase reaction onset and inflammation (reviewed in (Cray et al. 2009). *il15* is a pro-inflammatory cytokine, while *ilf2* encodes for a transcription factor required for the expression of interleukin 2, another cytokine. *ptgs2*, also known as cyclooxygenase-2 (*cox-2*) is involved in prostaglandin synthesis, and is a viable target for non-steroidal inflammatory drugs that are used clinically. Taken together, TBBPA, TCBPA or TBT exposure seems to cause an inflammatory reaction in zebrafish.

The predicted regulators of toxicant-induced transcription of inflammation-related genes are listed in Figure 5.6C. These include CEBPB and CEBPD, and the STAT signaling pathway, and pro-inflammatory cytokines interleukins 1 and 6, among others.

A

TBBPA	TCBPA	TBT	Genes	Annotated Biological Process
			FN1	Acute Phase Response
			SAA1	
			AHSG	
			A2M	
			APCS	
			CEBPB	
			STAT5B	Other inflammation-related genes
			SOCS3	
			PTGS2	
			ILF2	
			IL15	
			CRP	

B

Predicted Regulators of Toxicant-Induced Inflammation
CEBPB
STAT
IL6
A2M
IL1 family
STAT3
OSM
LIF
CEBPD
AMPK

C

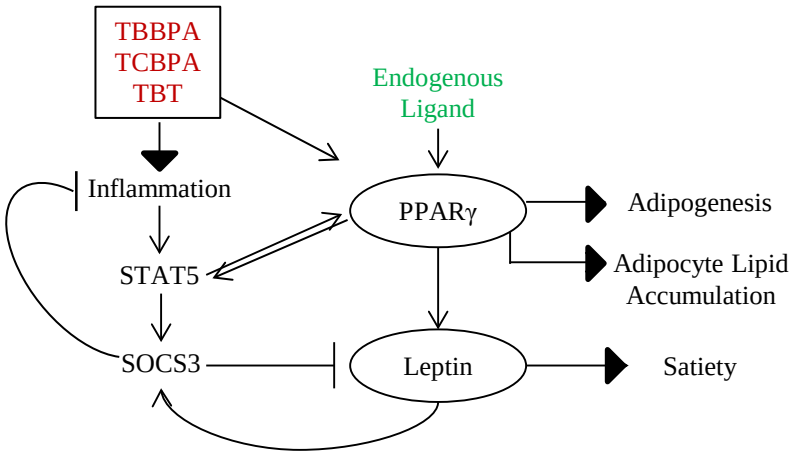

Figure 5.6. Regulation of inflammation by TBBPA, TCBPA and TBT. (A) Representation of gene expression changes induced by tested chemicals on inflammation-related genes. Red block indicates up-regulation and green block indicates down-regulation. **(B)** Predicted regulators of chemical-induced genes related to inflammation, predicted by Pathway Studio. **(C)** Schematic representation of an example of association between obesity and inflammation, and the role of TBBPA/TCBPA in driving both pathologies.

5.3 DISCUSSION

In the present study, the mechanisms of action of the halogenated bisphenol A analogs TBBPA and TCBPA, and the mammalian obesogen TBT have been investigated. Previous studies from our research group have indicated that in zebrafish, TBBPA, TCBPA and TBT increase lipid utilization from the maternally derived yolk in developing larvae(Chapter 4 and (Kalasekar et al. 2014)), and increase the storage of lipid within the larvae (Riu et al. 2014b). In order to better understand the effects of these chemicals on lipid metabolism, we performed a transcriptomic analysis of juvenile zebrafish following exposure to these "obesogens". In addition to the known obesogen TBT, the chemicals TBBPA and TCBPA are being referred to as obesogens here since, together with fundamentally altering lipid mobilization in developing zebrafish, exposure to these chemicals during development has been shown to cause significantly higher BMIs later in the life of exposed zebrafish (Riu et al. 2014b). Furthermore, TBBPA and TCBPA act as ligands to both zebrafish and human PPARγ (Riu et al. 2011; Riu et al. 2014b). Since Rosiglitazone, which is a human PPARγ agonist, has been shown to induce weight gain in humans after long-term exposure (Shim et al. 2006), it is, perhaps, not unreasonable to suggest that TBBPA and TCBPA too might act as obesogens in humans. For the same reason, a better understanding of the obesogenic effects of these chemicals is necessary.

From our transcriptomic analyses thus far, we have been able to identify that obesogens TBBPA, TCBPA and TBT activate pathways which could contribute the development of aberrant lipid metabolism and, perhaps, obesity.

From the overall gene expression patterns, it was seen that the three chemicals regulate very few genes in common (Figure 5.2). This is very interesting, as all three chemicals activate the PPARγ/RXR signaling pathway. This result suggests that there could be multiple pathways activated by these chemicals. Furthermore, from the tissue enrichment analysis, it is evident that the tested obesogens target multiple tissues. Apart from metabolically active tissues like the liver and the yolk syncytial layer (YSL), the chemicals were predicted to affect the expression of genes expressed in multiple tissues, including those of the mesoderm (somites, musculature system, intermediate cell mass of the mesoderm, pharyngeal and mandibular arch skeleton). Obesogen effects on genes of the YSL can be appreciated from the fact that these chemicals caused abnormal lipid uptake through the YSL in young larvae (Chapter 4, and (Kalasekar et al. 2014)), but the function of the YSL-specific obesogen regulated genes in juvenile fish, which have no obvious function for the YSL, is interesting. The effects of obesogens on cells of the mesoderm is also worth further investigation as adipocytes, myocytes, chondrocytes and osteocytes all arise from this germ layer.

The effects of TBBPA, TCBPA and TBT on several tissue types highlights the need for whole organism-based transcriptomic analysis. By using zebrafish for our studies, we have retained the inter-organ complexity of rodent-based *in vivo* models as well as the small scale of *in vitro* models.

The obesogens TBBPA, TCBPA and TBT seem to activate multiple pathways in juvenile zebrafish. The genes up-regulated in common by the three obesogens include the transcripts for transcription factors *npas4* and *jdp2*, the PPARγ target gene *pck1*, *cebpb*

and *socs3*. The neuronal PAS domain protein 4 (*npas4*) is known to play an important role in brain development and cognitive function (Coutellier et al. 2012). With regards to metabolism, *npas4* has been shown to improve pancreatic β-cell function in response to stress (Sabatini et al. 2013). It is possible that toxicant-induced stress in exposed zebrafish caused up-regulation of *npas4* in our study. The transcript for Jun dimerization protein 2 (*jdp2*) was up-regulated by all three chemicals. JDP2 has been shown to inhibit adipogenesis by regulating the expression of *cebpd* (Nakade et al. 2007). However, since the tested obesogens cause an up-regulation of both *jdp2* and *cebpd* in our study, it is, perhaps, possible that up-regulation of *cebpd* and a subsequent increase in adipogenesis induces *jdp2* expression as negative feedback. The C/EBP proteins are canonical markers of adipocyte differentiation, and are required for the same (Wu et al. 1999). Obesogen exposure did, indeed, cause upregulation of *cebpa*, *cebpb* and *cebpd*, with *cebpb* being among the most highly regulated genes. Activation of PPARγ in the adipocyte induces the expression of several genes, one among them being the rate-limiting enzyme in gluconeogenesis, phosphoenolpyruvate carboxykinase (*pck1*). Within the adipocyte, PPARγ activation induces triglyceride synthesis and lipid accumulation via the induction of the *pck1* gene (Hallakou et al. 1997). *pck1* was highly up-regulated by obesogen exposure, although whether this activation was restricted to adipocytes is not known. The gene for the suppressor of cytokine signaling 3 (*socs3*) was also highly up-regulated by the three obesogens. This gene is generally induced in response to inflammation and is known to be involved in PPARγ's regulation of feeding behavior (reviewed in (Lubis et al. 2008)). The relationship between *socs3* and PPARγ activation is discussed further on in this section.

The gene for the cytochrome P450, family 11, subfamily A, polypeptide 1 enzyme (*cyp11a1*), which converts cholesterol to pregnenolone as the first step in steroidogenesis, was among the most down-regulated genes in the microarray. The inhibition of this gene's expression by the tested obesogens probably suggests an accumulation of the enzyme's substrate cholesterol. Various other genes, which were related to cholesterol transport and metabolism, were also affected by the obesogens, and these are discussed later in this section. The gene for myosin heavy chain 4 (*myh4*) was also down-regulated by the obesogens. Since this gene is a marker for stem cell differentiation into skeletal muscle cells (Kang and Krauss 2010), and because adipocytes and myocytes arise from the same precursors (mesenchymal stem cells or MSCs), the down-regulation of *myh4* may indicate the differentiation of MSCs into adipocytes at the expense of myocytes. Another gene down-regulated by the obesogens was that of the DNA methyltransferase 1 enzyme (*dnmt1*). This enzyme is involved in the transfer of methyl groups to CpG islands of promoters of genes, thereby silencing them epigenetically. The down-regulation of this enzyme by the tested obesogens indicates a decrease in gene silencing, or the activation of gene expression. Obesogen-induced epigenetic activation of genes (involved in adipogenesis, for example) may explain the increased BMI of juvenile zebrafish following obesogen exposure in the larval stages.

Functional analysis of the genes co-regulated by all three obesogens was carried out to determine the biological processes enriched (Table 5.2). Several obesogen-affected biological processes were related to inflammation and innate immune responses. Entities in some of the other enriched biological processes were also involved in inflammation, suggesting the interplay between chemical-induced acute-phase response and, for

example, platelet degranulation. There is a high degree of overlap between the genes assigned to these two biological processes, and conceptually, both these processes can cause, or occur as a result of, inflammation. Other processes enriched in obesogen-regulated genes include muscle assembly and bone formation. However, there is some ambiguity in whether these processes are induced or inhibited, as a few genes are up-regulated while others are down-regulated in these processes.

As previously discussed, zebrafish larvae exposed to TBBPA, TCBPA or TBT for 8 days during development accumulated more lipid than vehicle-treated control group larvae (Riu et al. 2014b). We hypothesized that the increase in lipid accumulation was a result of either increased number of fat cells in obesogen-exposed zebrafish (due to increased adipogenesis), or an increase in the amount of fat stored in the adipocytes or other tissues. Both these effects could be the consequences of obesogen activation of zfPPARγ. From the transcriptomic data following obesogen exposures, we observed that genes involved in both adipogenesis and lipid metabolism were indeed regulated by these chemicals.

Ligand-induced activation of PPARγ is known to drive preadipocytes' differentiation into mature lipid droplet-accumulating adipocytes by activating a continuous feed-forward loop involving activation as well as expression of the CEBPs (Wu et al. 1999) (Figure 5.4B). In our study, we show for the first time that the tested obesogens induce the expression of these canonical markers of mammalian adipocyte differentiation in zebrafish. Chemical exposure also results in downregulation of WNT ligands *wnt8a* and *wnt11*, and the *med13* mediator complex, which is essential for WNT signaling (Carrera et al. 2008). It is known that WNT signaling mediated, likely by mammalian Wnt-10b,

maintains preadipocytes in an undifferentiated state by inhibiting the CEBPs and PPARγ in mammalian 3T3 cells, and inhibits adipogenesis (Ross et al. 2000). Therefore, this result indicates the regulation of multiple pathways by obesogens to facilitate adipogenesis.

Zebrafish exposure to the tested obesogens also results in activation of *cd36* and *pck1* genes, which are known to be induced by PPARγ activation in mammalian adipocytes (Hallakou et al. 1997; Silverstein and Febbraio 2009). *cd36*, also known as fatty acid translocase, is a cell surface glycoprotein expressed in several cell types, including adipocytes, muscle cells and enterocytes. *cd36* binds long chain fatty acids and facilitates their transport into these cell types (reviewed in (Silverstein and Febbraio 2009)). *pck1* expression in adipocytes is also known to stimulate triglyceride formation in the adipocyte (Hallakou et al. 1997; Tordjman 2003). Therefore, the up-regulation of *cd36* and *pck1* by the tested obesogens suggests a possible increase in PPARγ-activated lipogenesis in the zebrafish adipocyte.

In the previous study by Riu et al. (Riu et al. 2014b), increased lipid accumulation in obesogen exposed zebrafish larvae was visualized by Oil Red O (ORO) staining. The ORO stain binds to all neutral lipids, and therefore ORO staining in obesogen-exposed larvae could indicate accumulation of any kind of neutral lipid, including triglycerides and cholesterol. From Table 5.3, it can be seen that the tested obesogens significantly affected cholesterol and lipoprotein metabolism. In line with this observation, we found that several genes belonging to these metabolic processes were, indeed, regulated by TBBPA, TCBPA and TBT.

As mentioned earlier, *cyp11a1* was among the most down-regulated genes in the microarray, suggesting obesogen-induced down-regulation of cholesterol utilization for steroidogenesis and, perhaps, accumulation of cholesterol. Figure 5.5A lists several other obesogen-regulated genes involved in lipid metabolism. *bmp1*, as previously discussed, activates apolipoprotein A1 (apoA1) and high-density lipoprotein (HDL) formation (Chau et al. 2007). Up-regulation of *bmp1* by obesogens, therefore, might indicate increased transport of cholesterol from peripheral tissues in HDL particles. This is supported by the observation that the cholesterol transporter *abca1* is also up-regulated by obesogen exposure. Obesogen-induced increase in cholesterol transport is also indicated by the up-regulation of several genes involved in the transport of cholesterol from peripheral tissues into the liver (reverse cholesterol transport, Figure 5.5B). Among these are the genes for another apolipoprotein (*apoe*), plasma cholesteryl ester transfer protein (*cetp*, which transports cholesterol from HDL to lower density lipoproteins), scavenger receptor class B member 1 (*scarb1*, a receptor for cholesterol from HDL particles) and sterol-O-acyltransferase1 (*soat1*, which converts cholesterol to cholesterol esters). While the up-regulation of these genes indicates a possible increase in shuttling of cholesterols to the liver, there was no up-regulation of genes, such as *mttp* (microsomal triglyceride transfer protein), which transport lipids out of the liver by packaging them into Very Low Density lipoprotein particles (VLDLs). Also, the genes involved in hepatic triglyceride synthesis such as acyl-CoA synthetase family member 3 (*acsf3*) and diacylglycerol O-acyltransferase 2 (*dgat2*) were up-regulated by the tested obesogens. Taken together, the above described gene expression patterns indicate a possible accumulation of cholesterol and triglycerides in the liver of obesogen-exposed zebrafish.

This observation is in line with results from the previous study by Riu et al (Riu et al. 2014b), in which ORO staining localized to the liver in response to the chemicals TBBPA, TCBPA and TBT.

Several genes involved in inflammation were regulated by zebrafish exposure to TBBPA, TCBPA and TBT. Transcripts of proteins involved in inflammation-induced acute phase response such as serum amyloid A1 (*saa1*), alpha-2-HS-glycoprotein (*ahsg*), serum amyloid P component (*apcs*) and the C-reactive protein (*crp*) were all up-regulated. The acute phase response is usually initiated in response to a localized inflammation, which produces pro-inflammatory cytokines in order to "attract" immune cells to the site of inflammation (reviewed in (Cray et al. 2009)). In our studies, obesogen exposure induced the expression of several pro-inflammatory cytokines and enzymes such as interleukin 15 (*il15*), *ptgs2*/*cox*-2 and signal transducer and activator of transcription 5B (*stat5b*). Furthermore, increase in protein level expression of these pro-inflammatory cytokines is, perhaps, indicated by obesogen-induced induction of the suppressor of cytokine signaling 3 (*socs3*) transcripts. *socs3* is a major regulator of inflammation, and is known to be induced in response to activation of the STAT signaling pathway by pro-inflammatory cytokines (reviewed in (Carow and Rottenberg 2014)).

The interplay between PPARγ signaling and obesogen-induced inflammation is represented in Figure 5.6C. Under normal conditions, in response to endogenous ligands, such as circulating free fatty acids from digested food following a meal, PPARγ activation leads to lipogenesis within the adipocyte and the secretion of the peptide hormone leptin, which functions by signaling via leptin receptors in the brain to control

appetite. The effect of continuous secretion of leptin is controlled by a leptin-induced mechanism of its own inhibition via the SOCS3 protein. The balance between leptin secretion and socs3-mediated regulation of leptin activation of its receptors is responsible for the maintenance of energy homeostasis with respect to feeding behavior and energy intake. However, obesogen-induced inflammation could possibly perturb this balance in many ways. The production of pro-inflammatory cytokines in response to obesogen exposure triggers several defense mechanisms and molecular pathways, including the STAT signaling pathway. Activation of STAT signaling (*stat5b* is up-regulated in the microarray) induces the expression of *socs3* to control cytokine-mediated inflammation (reviewed in (Linossi et al. 2013). The inflammation-induced continuous activation of *socs3* causes leptin resistance, and results in increased synthesis of leptin in adipocytes. Furthermore, STAT5B is known to induce adipogenesis via activation of PPARγ, and PPARγ ligands are known to activate STAT signaling in adipocytes (Gesta et al. 2006; Newbold and McLachlan 1996).

Taken together, the regulation of these inter-linked pathways (adipogenesis, lipid metabolism and inflammation) by chemicals TBBPA, TCBPA and TBT indicates the ability of these obesogens to act through multiple pathways to contribute to obesity pathogenesis. Further validation of the effects of these chemicals on mammalian models will help predict their effects in humans, and establish the evolutionary conservation of processes such as adipogenesis between zebrafish and mammals.

CHAPTER 6: CONCLUSIONS AND FUTURE DIRECTIONS

Through the studies described in this thesis, we have explored the ability of environmental chemicals to act, via the estrogen or PPARγ nuclear receptors, as "obesogens". The environmental obesogen hypothesis suggests that prenatal or early life exposure to endocrine disrupting chemicals (EDCs) can predispose exposed individuals to increased fat mass and obesity later in life. Given the critical role played by the significant roles played by the estrogen and PPARγ nuclear receptors in processes relating to lipid metabolism and adipose tissue function, we posit that the discovery and investigation of novel EDCs disrupting metabolic homeostasis can accelerate our understanding of the environmental factors, which contribute to obesity pathogenesis.

Towards the same goal, we have developed zebrafish-based screening (Chapters 3 and 4) and mechanistic (Chapter 5) models to explore EDC-induced disruption of nuclear receptor signaling (estrogen receptors in Chapter 3 and PPARγ in Chapter 5) and lipid metabolism.

In Chapter 3, we developed a zebrafish-based screening assay and identified 32 environmental chemicals that disrupt estrogen signaling. Of these, 13 chemicals were identified as EDCs in the zfERE assay but not in the *in vitro* assays complied by the EPA's EDSP Database. Of these 13 chemicals, only 3 (2,4-DB, methan-sodium hydrate and methomyl) had at least one study indicating an estrogenic effect in rodents. For these chemicals, it can be reasoned that the *in vivo* zebrafish model was a better predictor of rodent toxicity than mammalian *in vitro* studies, suggesting that these chemicals could disrupt estrogen signaling by complex mechanisms only observable in an intact animal

model and not by acting as ligands interacting directly with the receptor. This result indicates the need for whole-animal models in toxicity testing. The need for zebrafish-based small animal screening in toxicity is evident from the various practical advantages that this model has to offer when compared to rodents with regards to high-throughput screening (see section 1.6).

The chemical atrazine was not indicated as an estrogen in *in vitro* assays, but was identified as an estrogen in the zebrafish assay. However, in rodent assays, atrazine has been shown to have an anti-estrogenic effect. This result indicates that there could be species-specific effects of EDCs that cannot be ignored while drawing comparisons from assays conducted across species. The same line of reasoning can be adopted for MCPA, which had no estrogenic effects in mammals either *in* vitro or *in vivo,* in rodents.

Therefore, we suggest that high-throughput *in vitro* assays be supplemented with high-throughput zebrafish-based *in vivo* screens to prioritize chemicals for rodent testing (which remains the gold standard in toxicology), and posit that using only either one of these approaches might result in undesirable identification of false positives or false negatives. For example, 8 chemicals (ametryn, asulam, azamethiphos, cyfluthrin, cyhalopfop-butyl, dicamba, dichlorprop, dicloran and triticonazole) did not act as estrogens *in vitro,* but induced zfERE driven GFP expression. This could either mean that these chemicals are not estrogens in the mammalian context, or that they require a whole-animal context to elicit their adverse effects. Further investigation using zfER-reporter cell lines will help clarify some of these questions. Also, the finding that E2 and BPA

induce lipid accumulation in the zebrafish underlines the need for further research in this area.

Oftentimes, in environmental toxicology, the molecular target of the environmental pollutant is not known. Therefore, using molecular endpoints to identify toxicity can be analogous to looking for a needle in a haystack. In these situations, it can be more efficient to conduct phenotypic screens, particularly, if an animal model is used for testing. By developing a quantifiable zebrafish-based assay to identify chemicals disrupting yolk utilization in the zebrafish (Chapter 4), we have identified several advantages and salient features of phenotype-based screens in toxicology. Firstly, by looking at a phenotypic endpoint such as yolk utilization, we showed that chemicals belonging to diverse chemical classes (and therefore, possibly having different molecular targets) can significantly affect development. Secondly, by using a sensitive and quantifiable method to identify chemical-induced perturbations in yolk consumption, we showed that environmental chemicals can be biologically active at very low doses. This result underlines the need for toxicological testing to include low doses in the study design. And finally, this model serves another important example of the need for toxicity testing to involve whole-animal models, especially for the accurate modeling of EDC disruption of metabolism.

Apart from chemical screening assays, whole-animal modeling of EDC disruption of metabolism is also necessary for mechanistic studies. The zebrafish model shares several similarities with mammals, especially with respect to metabolism. In Chapter 5, zebrafish

were used to explore the systemic effects of chemicals TBBPA, TCBPA and TBT via whole-animal transcriptomic analyses. From the results of these studies, it was observed that PPARγ agonist functions are, to some extent, conserved between mammals and zebrafish. For instance, TBBPA and TCBPA are human- and zebrafish-PPARγ agonists, and they induce adipocyte differentiation in both models (Chapter 5, and (Riu et al. 2011)). Although there seems to be a conservation of PPARγ related pathways between the zebrafish and mammals, it is important to note that structural differences between the human- and zebrafish- PPARγ receptors do exist, and that this is evident from the fact that TZDs, while acting as good agonists for human PPARγ, do not activate its zebrafish counterpart (Riu et al. 2011; Riu et al. 2014b). Therefore, care should be taken while using zebrafish-based chemical screens to identify cross-species PPARγ agonists, but a zebrafish-based phenotypic screen to identify environmental inducers of adipogenesis might yield relevant results.

The focus of the studies in this thesis has remained on lipid metabolism. Although not within the scope of this thesis, the close relationship between lipid and glucose metabolism, and the already known involvement of both ERs and PPARγ in regulating glucose–stimulated insulin secretion and insulin sensitivity, respectively, cannot be ignored, and the effects of obesogens on these processes warrant further investigation.

Other members in our research group initially observed TBBPA/TCBPA-induced lipid accumulation in larval fish at 11dpf (days post fertilization). Although our transcriptomic analysis was performed in juvenile fish, it would be interesting to see whether chemical-

induced gene expression changes are conserved between different developmental stages. Different transgenic zebrafish lines can also be utilized to visualize TBBPA/TCBPA-induced changes in zebrafish during developmental stages – for example, it can be investigated if the chemicals cause alteration in neutrophil migration indicating inflammation, or a decrease in the appearance of fluorescence driven by skeletal, cartilage or muscle-derived markers to indicate increase in adipogenesis.

Furthermore, the impact of developmental exposure to TBBPA/TCBPA on the onset of obesity/lipid-related disease in adulthood might be worth examining. Given that these chemicals do regulate genes involved in epigenetically silencing DNA (*dnmt1*), and that larval exposure to these compounds increases BMI of zebrafish later in life, it is not unreasonable to expect that these chemicals might be reprogramming fundamental metabolic parameters in young fish to cause disease later in life. An examination of genome-wide methylation patterns in exposed larvae might also yield insightful results.

APPENDIX

Table A: List of genes most regulated by obesogens

	TBBPA		TCBPA		TBT	
	Gene	**FI**	**Gene**	**FI**	**Gene**	**FI**
Down-regulated Genes	MED13	-13.821047	FAT3	-4.9643562	MED13	-15.953665
	MPZL1	-10.221164	CYP11A1	-3.7177054	CSF3	-5.6589058
	EXOC1	-8.4196442	KIF7	-3.5108404	IQCA1	-5.6290475
	HAPLN4	-5.1374244	NOS2	-3.4234959	PCNA	-5.6085608
	FKBP5	-3.9981048	SYPL2	-3.3022724	FAT3	-5.115215
	B3GNTL1	-3.8586337	SLC2A7	-3.2302693	NOA1	-5.0041978
	CPT1C	-3.5645217	GNMT	-2.8477846	GTF2A2	-4.7407986
	ZMAT5	-3.5197255	ZC3H7B	-2.7909844	WNT8A	-4.0955513
	SSX2IP	-3.3983494	PCNA	-2.6900432	UFL1	-3.7804116
	TRIM47	-3.3932859	AMOTL2	-2.6461521	EXOC1	-3.7090576
	DHX32	-3.0552332	GH1	-2.4680789	ALDH3A1	-3.7041781
	RAB15	-2.9834818	MED13	-2.3836521	PANX1	-3.6073034
	AHSA1	-2.9329655	GLRX	-2.3444884	CPT1C	-3.5939928
	LIPI	-2.8351364	HEATR5A	-2.2919426	PDLIM2	-3.515049
Up-regulated Genes	ATP5J2	-2.763824	B3GNT5	-2.2791891	GPNMB	-3.1823032
	JDP2	2.5339306	C8orf4	2.8219822	SFXN2	3.8699205
	DNM2	2.5579139	PBDC1	2.8910957	CEBPB	3.9848901
	ALDOB	2.6767657	PCK1	2.9560894	JUNB	4.1525723
	SAMD7	2.703851	JDP2	3.1572527	CYP8B1	4.3320412
	CHRNB3	2.9336171	FKBP5	3.2778342	PCK1	4.410965
	ID1	3.2009267	FOS	3.463822	KLF2	4.8809995
	TCTEX1D2	3.3205847	ALDH2	3.4933755	FOS	5.5531142
	EGR4	3.573809	LCT	3.5101117	HBE1	5.7506559
	JUNB	3.6797927	SLC44A5	3.6551666	NPAS4	5.9993928
	NPAS4	3.9738535	EGR4	4.0958339	ITIH2	6.7819414
	HBE1	4.61548	SOCS3	5.1163886	JDP2	6.7819414
	RBBP8	5.7358438	NPAS4	5.2857605	FOSB	7.4048821
	FOSB	5.9869126	FOSB	5.428486	TCTEX1D2	7.749889
	FAT3	9.7106966	TCTEX1D2	5.4320336	SOCS3	8.0475663
	MARCKS	324.21802	MPV17	130.36658	MPV17	414.89701

Table B: List of biological processes most regulated by obesogens

TBBPA		TCBPA		TBT	
Enriched Biological Process	***p*-value**	**Enriched Biological Process**	***p*-value**	**Enriched Biological Process**	***p*-value**
platelet degranulation	2.38E-08	metabolic process	2.25E-08	small molecule metabolic process	9.05E-10
acute-phase response	5.17E-08	small molecule metabolic process	9.69E-08	positive regulation of transcription from RNA polymerase II promoter	2.15E-08
small molecule metabolic process	6.95E-07	response to nutrient	2.18E-07	DNA replication	2.40E-07
cell adhesion	2.04E-06	response to progesterone stimulus	4.60E-07	aging	5.65E-07
blood coagulation	3.57E-06	response to mechanical stimulus	3.91E-06	metabolic process	6.65E-07
regulation of transcription involved in G1-S phase of mitotic cell cycle	5.51E-06	complement activation	5.27E-06	acute-phase response	7.65E-07
extracellular matrix organization	5.82E-06	response to food	1.39E-05	cellular nitrogen compound metabolic process	2.46E-06
platelet activation	8.13E-06	complement activation, alternative pathway	1.46E-05	positive regulation of transcription, DNA-dependent	2.75E-06
cell cycle	1.85E-05	skeletal muscle thin filament assembly	1.68E-05	mitotic cell cycle	3.18E-06
ossification	2.53E-05	positive regulation of transcription from RNA polymerase II promoter	2.28E-05	transcription from RNA polymerase II promoter	9.34E-06
cellular response to hormone stimulus	3.10E-05	acute-phase response	2.69E-05	response to organic cyclic compound	1.08E-05
regulation of cell proliferation	3.47E-05	ossification	2.71E-05	extracellular matrix organization	1.11E-05
positive regulation of peptidase activity	3.74E-05	cholesterol homeostasis	4.35E-05	response to nutrient	1.17E-05
oxidation-reduction process	4.18E-05	carbohydrate metabolic process	4.69E-05	cell differentiation	1.19E-05
positive regulation of transcription from RNA polymerase II promoter	4.19E-05	regulation of complement activation	6.43E-05	oxidation-reduction process	1.32E-05

Table C: List RT-qPCR primers used

Primer	Sequence
cd36 - F	TCGCTCAACCTTGCTGTCGCA
cd36 - R	TGGAAGAGTGAGGAACCGGAG
cebpa - F	GCGCCGCATCTGTCCTACCT
cebpa - R	CGTCGGGGGAGGTGTGGGAT
cebpb - F	CCGTCGATTGGAAAAACGGG
cebpb - R	TACCAGAGCTGTACCGAGCA
cebpd - F	GCACGAGAAACTTTTAGCACCT
cebpd- R	TGGCTGTCCCAAGGAAAGTG
fasn - F	CGCTTGTCCTACTTCTTTGATT
fasn - R	TTCCAGTGCCAGCAGACTAGA
jdp2 - F	CGCTGTCGGTCTGAGAAACT
jdp2 - R	CGCTCAACAGACACATTAGGA
npas4 - F	AGCTAGGCATGATGCGGAAT
npas4 - R	ATGCCTCTGTTTTGACGACCA
pck1 - F	GAGAATTCTCACACACACACACACACACGTGA
pck1 - R	GTAAAAGCTTTCCGCCATAACATCTCC
ptgs2 - F	AAGCCCTACTCATCCTTTGAGG
ptgs2 - R	AGTTGGGTCTGGATTTCTCCAC
socs3 – F	ACCAACACGGGTCTTCTGTG
socs3 - R	ACGAGTCACATCCATCGTCAA

Table D: List of all genes regulated by obesogens

Arranged from most down-regulated to most up-regulated. "FI" indicates "Fold Induction".

TBBPA	FI	TBBPA	FI	TBBPA	FI
MED13	-13.82	PTGES	-2.25	ATP8B5P	-1.89
MPZL1	-10.22	ATHL1	-2.25	RPUSD4	-1.89
EXOC1	-8.42	GTF2A2	-2.23	PHOX2A	-1.89
HAPLN4	-5.14	ACRC	-2.22	PDRG1	-1.89
FKBP5	-4.00	SRSF5	-2.20	HAUS1	-1.88
B3GNTL1	-3.86	GRAP	-2.18	CUZD1	-1.88
CPT1C	-3.56	CYP11A1	-2.17	SHD	-1.87
ZMAT5	-3.52	C8orf33	-2.16	NR1D2	-1.87
SSX2IP	-3.40	NOS2	-2.15	USP16	-1.86
TRIM47	-3.39	CPEB1	-2.15	TBC1D19	-1.85
DHX32	-3.06	CXXC1	-2.15	SCLT1	-1.84
RAB15	-2.98	CHCHD3	-2.15	ADNP	-1.84
AHSA1	-2.93	WDR6	-2.14	MSRA	-1.83
LIPI	-2.84	TDRKH	-2.14	ADCK2	-1.83
ATP5J2	-2.76	MTFR1	-2.12	ABRACL	-1.82
DCLRE1A	-2.75	FUNDC2	-2.10	VSIG10	-1.82
SYCE3	-2.73	HSPA9	-2.10	RNMTL1	-1.82
CENPM	-2.70	EFCAB4A	-2.09	KNOP1	-1.82
ALOX5	-2.70	SYNE2	-2.08	ACOT6	-1.82
UBXN2A	-2.67	SCARB1	-2.07	USH1C	-1.82
MYH4	-2.67	FTMT	-2.07	CDC45	-1.82
SH2D4B	-2.66	P2RY11	-2.06	MED28	-1.81
STIM2	-2.65	UCHL1	-2.05	UCHL5	-1.81
C5orf22	-2.64	KLHL35	-2.04	C11orf24	-1.81
RPP25	-2.62	TRIM13	-2.03	NSF	-1.81
PCNA	-2.58	C2orf44	-2.01	MCM3	-1.80
DNMT1	-2.46	PRKG1	-2.00	PDLIM7	-1.80
GNMT	-2.46	CC2D1B	-2.00	NRN1	-1.80
MOB1B	-2.43	CLCNKB	-1.99	COX11	-1.80
NTMT1	-2.42	DDX55	-1.98	CDCA8	-1.80
TRAM1	-2.42	GTPBP2	-1.97	MPI	-1.80
SWI5	-2.40	PIGP	-1.97	PLXNB2	-1.80
CSRP2BP	-2.39	ANKRD16	-1.96	ODAM	-1.79
DHX33	-2.35	LPAR2	-1.93	SPATA18	-1.79
RWDD2B	-2.34	UCP3	-1.93	RPS6KA2	-1.78
AP4B1	-2.32	DHFR	-1.92	ALDH18A1	-1.78
KCNG4	-2.31	THTPA	-1.91	H2BFWT	-1.78
GPNMB	-2.30	PTGER4	-1.90	THY1	-1.78
WNT8A	-2.29	HEATR5A	-1.90	AMD1	-1.77
MEGF10	-2.26	IMPA1	-1.90	PANX1	-1.77

TBBPA	FI	TBBPA	FI	TBBPA	FI
UGDH	-1.76	TRIP13	-1.69	SNX9	-1.63
PRPF19	-1.76	SLBP	-1.68	LAMP2	-1.63
VDAC3	-1.76	RASSF8	-1.68	SPEF1	-1.63
OLFM4	-1.76	TEKT3	-1.68	LBR	-1.63
PDXK	-1.76	TATDN2	-1.68	ZP3	-1.62
FAM58A	-1.76	CCKAR	-1.68	GIMAP7	-1.62
CCDC125	-1.75	ADAT2	-1.67	OR2AT4	-1.62
SLC6A16	-1.75	SCO2	-1.67	ABCF2	-1.62
GTF2F1	-1.75	EARS2	-1.67	CHST2	-1.62
ACYP1	-1.74	MGST2	-1.67	LSM14B	-1.62
SASH1	-1.74	TNNT1	-1.67	KRT8	-1.62
RAD51	-1.74	HIP1R	-1.67	DRD4	-1.62
RUNDC3A	-1.74	PDILT	-1.67	CDK4	-1.62
TYW5	-1.74	RCCD1	-1.67	CD97	-1.62
CYP3A7	-1.73	RSPH10B	-1.67	GALNT18	-1.62
TOMM20	-1.73	FERMT1	-1.66	KPNA2	-1.62
BMS1	-1.73	SMPDL3A	-1.66	DNAJC21	-1.61
GTF2A1L	-1.73	CEP72	-1.66	NXPH1	-1.61
RRS1	-1.72	DCTN6	-1.66	GPC2	-1.61
PIWIL2	-1.72	MFAP4	-1.66	CCNA1	-1.61
LPCAT4	-1.72	C4orf29	-1.65	NHP2L1	-1.61
MRPS35	-1.72	TMA16	-1.65	PFKFB4	-1.61
PDLIM2	-1.71	NDRG3	-1.65	PABPC1L	-1.61
ACSL1	-1.71	NPAT	-1.65	SYPL2	-1.61
A2M	-1.71	ZNF131	-1.65	GTF3C2	-1.61
DNMT3B	-1.71	TDGF1	-1.65	CDC6	-1.61
MRPL43	-1.70	SUV39H1	-1.64	CIRH1A	-1.60
ESCO2	-1.70	CCNA2	-1.64	NF2	-1.60
GPR21	-1.70	CCRN4L	-1.64	TECRL	-1.60
ASB2	-1.70	C1orf112	-1.64	GRIK1	-1.60
USP14	-1.70	TFB1M	-1.64	SOX21	-1.60
POLE3	-1.70	ZNF740	-1.64	HENMT1	-1.60
PHOX2B	-1.70	NPTN	-1.64	DDX56	-1.60
C17orf104	-1.69	PSME3	-1.64	SFT2D2	-1.60
CCM2L	-1.69	C11orf63	-1.63	TMEM14C	-1.60
CHTF18	-1.69	SLC2A3	-1.63	DCAF4	-1.59
F2RL1	-1.69	ATIC	-1.63	TRIP10	-1.59
NID2	-1.69	SLC46A1	-1.63	FBXO16	-1.59
KCTD14	-1.69	HMHA1	-1.63	SMU1	-1.59
TPH1	-1.69	PTTG1	-1.63	OCLN	-1.59

TBBPA	FI	TBBPA	FI	TBBPA	FI
ADCY8	-1.59	TSGA10	-1.56	ELAVL2	-1.53
MOV10L1	-1.59	FKBP6	-1.56	CPSF3	-1.53
QDPR	-1.59	METTL25	-1.56	NIPSNAP1	-1.53
ACP5	-1.59	OPA3	-1.56	CCNB2	-1.53
SPO11	-1.59	NAA40	-1.55	CUEDC2	-1.53
ITM2C	-1.58	CTNNBIP1	-1.55	PON3	-1.53
MCMBP	-1.58	CWF19L1	-1.55	IPO5	-1.53
STAB2	-1.58	PYGO1	-1.55	FBXL14	-1.53
SFI1	-1.58	MPL	-1.55	HSDL1	-1.52
PIGA	-1.58	ARMC1	-1.55	XPO5	-1.52
STX3	-1.58	BORA	-1.55	CENPT	-1.52
KPNA7	-1.58	CDC34	-1.55	TRIM14	-1.52
USP39	-1.58	ALOXE3	-1.55	EXD1	-1.52
QRICH1	-1.58	TDRD7	-1.55	HAUS7	-1.52
ZCCHC4	-1.58	SLC5A6	-1.55	CTNNA1	-1.52
PRDX1	-1.58	CTSS	-1.55	KIF2C	-1.52
SLC16A12	-1.58	CMSS1	-1.55	SYNE1	-1.52
RAD21L1	-1.58	RPP30	-1.55	PCM1	-1.52
NCAPH2	-1.57	B4GALNT1	-1.55	ACSF3	-1.52
MAPRE1	-1.57	ANP32B	-1.54	ZBTB8A	-1.52
ENTPD1	-1.57	PEX2	-1.54	KLF9	-1.52
PIWIL1	-1.57	OARD1	-1.54	RRM2	-1.52
GNS	-1.57	RBM44	-1.54	HEATR1	-1.52
RNF144A	-1.57	CST7	-1.54	OXR1	-1.52
MCOLN3	-1.57	EMC9	-1.54	NASP	-1.52
BBIP1	-1.57	TXNRD3	-1.54	C18orf25	-1.52
GJB6	-1.57	MLPH	-1.54	INTS5	-1.52
C8orf76	-1.57	ARHGAP11A	-1.54	TLK1	1.50
SLC25A25	-1.57	RNF38	-1.54	SMAD9	1.50
GLUL	-1.57	UBA2	-1.54	NPC1	1.50
GGT1	-1.57	MCM4	-1.54	NLK	1.50
TRRAP	-1.57	APOA4	-1.53	PRTG	1.50
CENPP	-1.56	DPH3	-1.53	DUSP16	1.50
TAC4	-1.56	WDR25	-1.53	MPP1	1.50
MTFR1L	-1.56	FANCE	-1.53	CRHBP	1.50
GDF3	-1.56	TXNDC5	-1.53	C6	1.50
SLC5A5	-1.56	CLDN7	-1.53	PAN3	1.50
NOC2L	-1.56	DHRS7C	-1.53	OAZ2	1.50
YIPF1	-1.56	CCNB1	-1.53	SKI	1.50
MS4A8	-1.56	THG1L	-1.53	PTPRC	1.50

TBBPA	FI	TBBPA	FI	TBBPA	FI
ITM2B	1.51	MYOZ3	1.53	WNK1	1.55
VWA5A	1.51	IGFN1	1.53	MYOD1	1.55
BOLA1	1.51	IGFBP5	1.53	RPL14	1.55
OMG	1.51	SAT1	1.53	SETD1B	1.55
NFIA	1.51	UFL1	1.53	HPS5	1.55
SLC26A6	1.51	TRIB3	1.53	KLHDC3	1.55
AHSG	1.51	CDH18	1.53	DNALI1	1.55
SLC6A19	1.51	APLP1	1.53	TUFT1	1.55
PRR12	1.51	CYR61	1.53	ZSWIM8	1.55
HLX	1.51	CREG1	1.53	SOX6	1.55
PHKG1	1.51	TAF3	1.53	SLC6A3	1.55
FBLIM1	1.51	TMEM27	1.53	CDHR2	1.55
STAT5B	1.51	PTPRD	1.54	MYOG	1.55
STXBP1	1.51	TAB2	1.54	CYP2D6	1.55
MSTN	1.51	ADAMTS5	1.54	ATP5J	1.55
OBSCN	1.51	SIX4	1.54	ANXA4	1.55
ATF6B	1.51	C7	1.54	SEC23B	1.55
STIM2	1.51	PROZ	1.54	SLC38A2	1.55
MYL7	1.51	BIRC6	1.54	CLPX	1.56
COMMD5	1.51	ADCK3	1.54	PAPLN	1.56
CUEDC1	1.51	HOXB1	1.54	ROBO1	1.56
SPINT1	1.51	GFRA4	1.54	NFIX	1.56
SLC10A3	1.51	HSD17B7	1.54	OGDH	1.56
C10orf107	1.51	SERPINA9	1.54	PPARA	1.56
PHC1	1.51	HIF3A	1.54	MICA	1.56
RAB36	1.52	HIST2H2BE	1.54	G0S2	1.56
NRXN1	1.52	STOM	1.54	CCNG2	1.56
ANGPTL1	1.52	ATP2B1	1.54	SYNPO2L	1.56
TCF7L1	1.52	PPARGC1A	1.54	MYBPH	1.56
SAA1	1.52	SLC30A10	1.54	ZNF703	1.57
HERC2	1.52	PABPC1	1.54	RBM47	1.57
PLEC	1.52	FSTL1	1.54	ELL	1.57
TGFB1	1.52	PDLIM5	1.54	ABRA	1.57
HDGFRP3	1.52	CREM	1.55	RSG1	1.57
ZFR2	1.52	SLC1A2	1.55	UCKL1	1.57
MTMR4	1.52	L3MBTL2	1.55	RTKN2	1.57
PRKCB	1.52	NRP2	1.55	SLC20A2	1.57
SLC44A5	1.52	RPLP0	1.55	BNIP3L	1.57
SLC30A4	1.52	UROC1	1.55	FAM160B2	1.57
ACY1	1.53	KLF4	1.55	STAC3	1.57

TBBPA	FI	TBBPA	FI	TBBPA	FI
RHO	1.57	CLDN6	1.60	WBP11	1.63
LRTM1	1.57	ZFP36L1	1.60	APP	1.63
HIC1	1.57	CFL2	1.60	RREB1	1.63
COL6A1	1.57	CAPN5	1.60	COX8BP	1.63
SIX1	1.57	AR	1.60	ATP11B	1.63
ASPDH	1.57	F7	1.60	PPAP2C	1.63
BHLHE40	1.58	KLHL21	1.60	MB	1.63
APLP2	1.58	METTL9	1.60	SERPINF2	1.63
PTH	1.58	COL2A1	1.60	SLC15A1	1.63
ANPEP	1.58	TSC2	1.61	VSTM2L	1.64
CAMSAP1	1.58	CFHR2	1.61	LPHN2	1.64
SLC16A10	1.58	HECTD1	1.61	HLA-DMB	1.64
TRIM29	1.58	SIK3	1.61	TLN1	1.64
COL6A3	1.58	TGM1	1.61	SUMF1	1.64
COL8A1	1.58	STOML3	1.61	TMEM230	1.64
ZNF850	1.58	TF	1.61	RIN2	1.64
ROM1	1.58	ILF2	1.61	SLC25A34	1.64
LECT2	1.59	HAMP	1.61	CHST14	1.64
PI16	1.59	KDM7A	1.62	KMT2E	1.65
ENDOD1	1.59	TWSG1	1.62	COL11A1	1.65
SEC16A	1.59	CLIC5	1.62	FGA	1.65
DDIT3	1.59	MEF2D	1.62	TMEM37	1.65
ELMO2	1.59	FAM96A	1.62	AGXT	1.65
VEGFA	1.59	SPIRE1	1.62	MYO7B	1.65
LRIT2	1.59	PBDC1	1.62	DNASE1L3	1.65
CPEB4	1.59	APCS	1.62	NDFIP2	1.65
EXOC3L2	1.59	BTG1	1.62	CDH6	1.65
COL6A2	1.59	COL1A1	1.62	BFSP2	1.65
CAV1	1.59	COL11A2	1.62	FGB	1.65
GPD1	1.59	CELA1	1.62	PBLD	1.65
PLXND1	1.59	AMH	1.62	REM1	1.65
SEC24D	1.59	ACTC1	1.62	THBS2	1.65
RBM39	1.59	SYNPO	1.62	ENPP6	1.66
MGAM	1.60	MMP14	1.62	CLDN5	1.66
ABHD14B	1.60	CSDC2	1.63	TCAP	1.66
CLEC4M	1.60	HHEX	1.63	AGT	1.66
PTPRS	1.60	TEK	1.63	F13A1	1.66
MYCBPAP	1.60	SQRDL	1.63	F9	1.66
CFHR1	1.60	TMEM70	1.63	NDRG2	1.67
LRP1	1.60	USP28	1.63	MIOX	1.67

TBBPA	FI	TBBPA	FI	TBBPA	FI
CSF1	1.67	CEBPD	1.73	VGLL2	1.81
SH3GL3	1.67	COL1A2	1.73	PLOD1	1.81
TNS1	1.67	USP2	1.73	OGFR	1.81
GBX1	1.67	HTATIP2	1.73	TRIM35	1.82
CYP7A1	1.67	PCK1	1.73	IFI4LL	1.82
MLF1	1.67	CCR9	1.74	C4A	1.82
NOTCH1	1.68	BGLAP	1.74	COL4A1	1.82
NR5A2	1.68	C1RL	1.74	P4HA1	1.82
GP1BB	1.68	IGFBP7	1.74	KRT18	1.82
HDAC4	1.68	IGFBP1	1.74	EVA1C	1.82
CYP2J2	1.68	SMTNL1	1.74	SCRN3	1.83
ZNF277	1.68	TMED1	1.74	HLA-DQA2	1.83
GNE	1.68	G6PC	1.74	METTL11B	1.83
NUAK1	1.68	SLC27A2	1.75	CCL19	1.83
CITED2	1.68	GATM	1.75	SMYD2	1.83
FETUB	1.69	SERPING1	1.75	ITIH4	1.83
RANGAP1	1.69	CLDN1	1.75	PFKFB3	1.84
ORAOV1	1.69	FLT1	1.75	SNX19	1.84
CCDC40	1.69	TCEB3	1.76	CUBN	1.84
ESAM	1.69	AMY2A	1.76	P4HA2	1.84
CFB	1.69	ZNF385B	1.76	DYNC1H1	1.85
USP13	1.69	TTN	1.76	PRX	1.85
TMPRSS2	1.69	JPH1	1.76	KRAS	1.85
SLC4A2	1.69	NMRK2	1.76	TXLNB	1.85
C1orf53	1.69	RAB11FIP1	1.76	SLC25A10	1.86
PHLDA1	1.69	LCT	1.76	SRP68	1.87
CGA	1.70	CYP2W1	1.77	CEBPB	1.87
WBP2	1.70	MYBPC3	1.77	GSTK1	1.87
HSPB11	1.70	DUSP27	1.77	CALCOCO2	1.88
CFH	1.70	F5	1.77	C6orf58	1.88
KIAA1279	1.70	LGALS3BP	1.77	EGLN3	1.88
NKX3-1	1.70	MGP	1.77	TMEM59L	1.89
SIX2	1.71	BMP1	1.78	GPR156	1.91
SLC13A2	1.71	GLB1L	1.79	DLL4	1.91
SLC43A1	1.71	ASPG	1.79	UCP1	1.92
PDZK1IP1	1.72	GADD45B	1.79	ZNF609	1.92
C8orf82	1.72	CYP19A1	1.80	MGRN1	1.93
ADAL	1.73	C11orf80	1.80	GCH1	1.93
FN1	1.73	FBXO36	1.81	DESI1	1.93
PELI3	1.73	SLC6A8	1.81	PYCRL	1.94

TBBPA	FI	TBBPA	FI
ATP2A1	1.94	ECHDC1	2.30
SLC5A12	1.95	INSC	2.31
PTGS2	1.95	KEAP1	2.32
BRF2	1.96	C4B	2.32
HSPB9	1.97	ACE	2.33
METTL20	1.97	CP	2.33
TTC18	1.98	TSPAN17	2.34
CYB5B	1.98	XYLB	2.34
MYBPC2	1.98	ACBD4	2.35
SLC43A2	2.00	GGACT	2.39
CRYGS	2.01	IARS	2.42
DNAJC16	2.02	PODNL1	2.45
C3	2.03	FOXQ1	2.48
TTYH3	2.05	FOS	2.52
IER2	2.05	JDP2	2.53
SULT2B1	2.05	DNM2	2.56
SIK1	2.05	ALDOB	2.68
FASN	2.06	SAMD7	2.70
RNF4	2.06	CHRNB3	2.93
MIDN	2.07	ID1	3.20
HOXC6	2.08	TCTEX1D2	3.32
ADD1	2.08	EGR4	3.57
MS4A4	2.09	JUNB	3.68
DNAI1	2.10	NPAS4	3.97
ANKAR	2.10	HBE1	4.62
CAPN8	2.11	RBBP8	5.74
DUSP11	2.11	FOSB	5.99
BLVRB	2.12	FAT3	9.71
TEKT4	2.13	MARCKS	324.22
C8orf4	2.14		
MAFA	2.15		
SOCS3	2.15		
KANK2	2.16		
HIGD2A	2.16		
NTAN1	2.16		
NOTCH3	2.18		
DNAJC19	2.18		
DHRS13	2.22		
ZNRF2	2.24		
CDK5	2.27		

TCBPA	FI	TCBPA	FI	TCBPA	FI
FAT3	-4.96	PTGER3	-1.95	OPA3	-1.77
CYP11A1	-3.72	KCNN1	-1.94	CLCNKB	-1.77
KIF7	-3.51	SLC46A1	-1.93	DENND4A	-1.76
NOS2	-3.42	FBXO31	-1.92	UGDH	-1.76
SYPL2	-3.30	HSD17B13	-1.92	TPH1	-1.76
SLC2A7	-3.23	HSF2BP	-1.91	UCHL1	-1.74
GNMT	-2.85	ZPR1	-1.91	RLBP1	-1.74
ZC3H7B	-2.79	DNMT1	-1.91	SYNE2	-1.73
PCNA	-2.69	VMO1	-1.90	RELL1	-1.73
AMOTL2	-2.65	KIAA1324L	-1.90	SERPINH1	-1.72
GH1	-2.47	TBL3	-1.90	HYOU1	-1.72
MED13	-2.38	FRRS1	-1.89	KCNG4	-1.72
GLRX	-2.34	NANS	-1.89	ZNF740	-1.71
HEATR5A	-2.29	HES7	-1.89	LIPI	-1.71
B3GNT5	-2.28	FAU	-1.88	TMEM60	-1.71
ECHDC3	-2.27	ST8SIA2	-1.88	BCL7B	-1.70
PICALM	-2.21	TMEM261	-1.87	ADCK2	-1.70
EFCAB4A	-2.20	ABI1	-1.87	SOX21	-1.70
USH1C	-2.19	TMEM45A	-1.86	GIMAP7	-1.70
CHCHD3	-2.18	ACYP1	-1.86	OARD1	-1.70
PTRH2	-2.16	CHD1L	-1.86		
FUNDC2	-2.15	ACTR1A	-1.86	RAB11A	-1.68
PTPDC1	-2.11	PDE6G	-1.85	FBLIM1	-1.68
NOS1AP	-2.10	RPP25	-1.84	CSRP2BP	-1.68
SYCP1	-2.09	USP49	-1.84	GGT1	-1.67
MYH4	-2.08	PLEKHF1	-1.83	MCM3	-1.67
PDXK	-2.07	OSGIN1	-1.83	PPA1	-1.67
AQR	-2.07	USP16	-1.82	DKC1	-1.67
GALNT18	-2.06	MS4A8	-1.82	TRIM37	-1.66
TMEM5	-2.05	RGS9BP	-1.81	PACSIN2	-1.66
CC2D1B	-2.04	SLC16A3	-1.81	ATHL1	-1.66
OAZ2	-2.02	PLSCR5	-1.81	RAC1	-1.66
TMEM30B	-2.02	KLHL25	-1.80	TFB1M	-1.66
DHX32	-2.00	SS18L2	-1.80	ZNF235	-1.66
CPA1	-2.00	AKIP1	-1.79	PRTG	-1.65
RLTPR	-1.99	SFT2D2	-1.78	DUT	-1.65
GLB1	-1.99	CPEB1	-1.78	PRDX1	-1.65
TLDC1	-1.97	GALNT14	-1.78	LGALS9	-1.64
DHX33	-1.96	DAPK2	-1.78	STK16	-1.64
HSPA9	-1.95	MAK16	-1.78	PLP1	-1.64

TCBPA	FI	TCBPA	FI	TCBPA	FI
DBX1	-1.64	P2RY11	-1.57	SLC30A10	1.50
FITM1	-1.64	MPL	-1.57	PTRF	1.50
C11orf63	-1.63	A2M	-1.57	TECPR2	1.50
TRIM35	-1.63	FRMD8	-1.56	SIX2	1.50
UBE2C	-1.63	RFC5	-1.56	COL10A1	1.50
QDPR	-1.63	EXOC1	-1.56	C6	1.50
IRS2	-1.62	ACTA1	-1.56	MEF2D	1.51
TTLL1	-1.62	TSGA10	-1.56	PKM	1.51
PWP2	-1.62	RBM44	-1.56	AMY2A	1.51
TBX20	-1.62	RBCK1	-1.56	EGFR	1.51
OR2AT4	-1.62	NCAPD2	-1.55	KLHDC3	1.51
TONSL	-1.62	C8orf33	-1.55	QKI	1.51
ATP1A1	-1.62	ARL10	-1.55	CLUL1	1.51
PSMB10	-1.62	NLE1	-1.55	ASB10	1.51
SRSF5	-1.61	UNC119	-1.55	ELAVL3	1.51
PSMA5	-1.61	TTF2	-1.55	SERPINA9	1.51
CYP26A1	-1.61	TRAM2	-1.55	ACTC1	1.51
IQCA1	-1.61	RRP9	-1.55	STAU1	1.51
EHD4	-1.61	E2F5	-1.55	PDE6H	1.51
CD97	-1.61	ALOXE3	-1.54	OGN	1.51
RBM17	-1.61	ANKFY1	-1.54	TFAP2C	1.51
CUZD1	-1.61	ZC3H6	-1.54	PDK3	1.51
CTRB2	-1.60	CHD8	-1.54	C2	1.52
HIST1H1E	-1.60	ZBTB8A	-1.54	DGAT2	1.52
NDUFA2	-1.60	SH2D4B	-1.53	KLF6	1.52
SYNE1	-1.59	CCND3	-1.53	ASB2	1.52
TMEM126A	-1.59	OLFM4	-1.53	BACH1	1.52
ZNF337	-1.59	EIF4G2	-1.53	LRP1	1.52
CEP44	-1.59	GNAI1	-1.53	OAT	1.52
HAPLN4	-1.58	GLB1L2	-1.53	FGFBP2	1.52
TRIM36	-1.58	ZNF814	-1.53	MST1	1.52
LIG1	-1.58	RFESD	-1.53	LCN15	1.52
RIC8B	-1.58	GNL3	-1.52	MGP	1.52
ST3GAL5	-1.58	DTWD1	-1.52	NFKBIA	1.52
HTRA2	-1.58	AANAT	-1.52	SSPN	1.52
ELF3	-1.58	GHR	-1.52	MMEL1	1.52
RTP3	-1.58	SYNE3	-1.52	ATP2B1	1.52
LGALS3BP	-1.58	APOM	1.50	MBLAC1	1.52
FAM115C	-1.58	BHLHE41	1.50	TP53INP1	1.52
GPNMB	-1.58	GADD45A	1.50	ZBTB16	1.53

TCBPA	FI	TCBPA	FI	TCBPA	FI
GATA2	1.53	ABHD14B	1.55	METTL11B	1.59
CTSK	1.53	CETP	1.56	TRIM54	1.59
WDR45B	1.53	CACNG6	1.56	CAV1	1.59
CFHR2	1.53	TMPRSS13	1.56	SELK	1.60
DSG2	1.53	GABARAPL3	1.56	ELAVL4	1.60
SLC26A5	1.53	FGA	1.56	GPR39	1.60
SGK2	1.53	CRABP1	1.56	ATP2A2	1.60
ENPP6	1.53	ANKRD9	1.56	NET1	1.60
PROZ	1.53	HBZ	1.56	TMEM154	1.60
PKP1	1.53	SLC1A2	1.56	ENDOD1	1.60
EIF4A2	1.53	IGFN1	1.56	NR5A2	1.60
PCDHB3	1.53	PDK4	1.56	TSPAN17	1.60
TMEM240	1.53	ARL5C	1.56	EGR3	1.60
PTPRC	1.53	HBP1	1.56	FOXO3	1.60
HIGD2A	1.53	P4HA2	1.56	ATP2A1	1.60
JUN	1.54	KLF13	1.57	SLC38A4	1.61
SLC2A5	1.54	CYP2W1	1.57	PNP	1.61
COX8BP	1.54	SLC27A1	1.57	LYRM5	1.61
MTOR	1.54	DPYSL5	1.57	ZFP36L1	1.61
C5	1.54	CLDN6	1.57	MAN1A2	1.61
DMRT1	1.54	MBNL2	1.57	OGDH	1.62
SP5	1.54	SERPING1	1.57	DNAJB13	1.62
GIMAP5	1.54	FBP1	1.58	TAT	1.62
STEAP4	1.54	KLHL21	1.58	METTL20	1.62
SLC5A8	1.54	IGFBP7	1.58	CITED4	1.62
EPGN	1.54	TSC22D2	1.58	OMG	1.62
FAM172A	1.54	CLDN1	1.58	SLC38A2	1.62
ACBD4	1.54	NFIX	1.58	MUC5B	1.62
CD36	1.54	PANX3	1.58	GPR156	1.62
RASD1	1.54	ZNF410	1.58	LIAS	1.62
CLDN4	1.54	MMP14	1.58	G0S2	1.63
CYP1A1	1.54	TNS1	1.58	FN1	1.63
KXD1	1.54	CPE	1.58	HDAC4	1.63
PDZK1IP1	1.54	FA2H	1.58	CUX1	1.63
LOXL3	1.55	SPATA2L	1.58	ARL4A	1.63
MATN1	1.55	RPLP0	1.58	GLB1L	1.63
FGD3	1.55	MGAM	1.59	XKR9	1.63
FAM96A	1.55	ITGB1	1.59	LPIN1	1.63
IGFBP5	1.55	HOMER2	1.59	LOX	1.63
CNKSR1	1.55	STX11	1.59	AHSG	1.63

TCBPA	FI	TCBPA	FI	TCBPA	FI
DIABLO	1.63	HSPB9	1.68	CAPN5	1.76
LAMA3	1.64	ABRA	1.68	UCP1	1.76
ALPK2	1.64	GPM6B	1.68	BMP1	1.76
GJB3	1.64	HAMP	1.68	MID1IP1	1.76
USP28	1.64	CSDC2	1.68	MKNK2	1.77
BGLAP	1.64	PLOD1	1.69	SQRDL	1.77
EGR2	1.65	GMDS	1.69	MYBPC2	1.77
SEC23B	1.65	F5	1.69	MYOD1	1.77
ANKRD16	1.65	TFCP2L1	1.69	C4B	1.77
NBL1	1.65	POLL	1.69	C7	1.77
SEMA3D	1.65	NR4A1	1.69	SOAT2	1.78
VGLL2	1.65	NT5C2	1.70	PLK2	1.78
KANK2	1.65	ENTPD8	1.70	GPD1	1.78
PIM1	1.66	TRIB3	1.70	VWA5A	1.78
FAXDC2	1.66	BBS4	1.70	CUBN	1.79
GBP6	1.66	COL1A1	1.70	SLC43A2	1.79
ABCA1	1.66	TTN	1.70	BCAR1	1.79
PKP3	1.66	USP8	1.71	CRYGS	1.80
TMEM59L	1.66	CXCR4	1.71	SP8	1.80
SLC6A19	1.66	SLC43A1	1.71	HLA-DQA2	1.80
KLF9	1.66	KLF4	1.72	PRSS48	1.80
MYL7	1.66	ANXA4	1.72	NT5E	1.80
LUM	1.66	RPL36	1.72	LYRM2	1.80
BTG1	1.66	KLHL32	1.72	EXT2	1.80
SMYD2	1.66	ZNF277	1.72	RBP2	1.80
WBP2	1.66	APBA2	1.73	MICA	1.81
DUSP2	1.66	METTL21B	1.73	UMOD	1.81
SLC25A34	1.66	SREBF2	1.73	VPS16	1.81
F8	1.66	MMP13	1.73	ADCY8	1.81
DNASE1L3	1.66	CTGF	1.73	DNAJC19	1.81
PARP12	1.67	GSTK1	1.73	SULT1A1	1.82
SLC34A2	1.67	PODNL1	1.74	DUSP6	1.82
PDF	1.67	HPX	1.74	BRF2	1.82
BFSP2	1.67	COL8A1	1.75	FAM213A	1.82
PRMT3	1.67	ATF6B	1.75	TMEM43	1.83
SLC10A3	1.67	TMPRSS2	1.75	TNNI1	1.83
CFB	1.67	KEAP1	1.75	PFKFB3	1.83
ZYG11B	1.67	HLA-DMB	1.76	TUBA3D	1.83
SLC16A12	1.68	UFL1	1.76	CCNG2	1.83
RGCC	1.68	TOB1	1.76	PI16	1.83

TCBPA	FI	TCBPA	FI	TCBPA	FI
PELI3	1.84	CD38	2.02	TRIM47	2.50
FAM43A	1.84	RBM39	2.03	APCS	2.55
BID	1.84	EVA1C	2.03	RBBP8	2.61
NMRK2	1.84	TCAP	2.04	NKX3-1	2.64
EEF2K	1.85	CRP	2.06	NPTN	2.68
AGXT	1.85	MAFA	2.06	GGACT	2.72
ESAM	1.85	CAPN2	2.06	CEBPB	2.79
NTAN1	1.88	NUDT18	2.07	TTC18	2.79
CHRNB3	1.88	IGFBP1	2.07	CCR9	2.82
SH3GL3	1.88	MS4A4	2.07	C8orf4	2.82
GBP3	1.89	C6orf58	2.08	PBDC1	2.89
CHIA	1.89	TIMP2	2.08	PCK1	2.96
YTHDC1	1.90	FAM160B2	2.11	JDP2	3.16
APP	1.90	CYB5B	2.12	FKBP5	3.28
KIF1A	1.90	CP	2.12	FOS	3.46
DHDH	1.90	DUSP11	2.13	ALDH2	3.49
SLC27A2	1.90	KIAA1279	2.13	LCT	3.51
BRF2	1.90	ADAL	2.14	SLC44A5	3.66
DHRS13	1.91	HIF3A	2.16	EGR4	4.10
NR1D2	1.91	DNAJC16	2.16	SOCS3	5.12
HBE1	1.92	G6PC	2.16	NPAS4	5.29
MAF	1.94	SAA1	2.19	FOSB	5.43
SRD5A2	1.94	PLXNB2	2.20	TCTEX1D2	5.43
PTGS2	1.94	C6orf58	2.20	MPV17	130.37
TRIM29	1.94	CFH	2.22		
CAPN8	1.95	RGS13	2.24		
MFSD1	1.96	PDLIM5	2.26		
HOXC6	1.96	ALOX5	2.28		
HIST2H2AB	1.96	CYP24A1	2.29		
ID1	1.97	ACE	2.30		
C3	1.97	KLF2	2.33		
IER2	1.98	FOXQ1	2.34		
ERRFI1	1.98	CEBPD	2.36		
ATP5J	1.98	GADD45B	2.37		
HTATIP2	1.99	JUNB	2.39		
TSC22D3	1.99	SIK1	2.39		
MIDN	2.00	PRX	2.42		
TUFT1	2.00	SPTSSB	2.46		
SLC13A2	2.01	PPP1R3A	2.47		
SLC15A1	2.02	SCRN3	2.48		
BLVRB	2.02	IARS	2.49		

TBT	FI	TBT	FI	TBT	FI
MED13	-15.95	AQR	-2.53	MFSD10	-2.15
CSF3	-5.66	CLCNKB	-2.52	TONSL	-2.15
IQCA1	-5.63	NOTCH1	-2.50	ACYP1	-2.15
PCNA	-5.61	GALNT14	-2.49	FUNDC2	-2.15
FAT3	-5.12	BOLA1	-2.49	ITPA	-2.14
NOA1	-5.00	SLC29A2	-2.48	B4GALNT1	-2.12
GTF2A2	-4.74	PYCRL	-2.48	MYH4	-2.12
WNT8A	-4.10	HSPA9	-2.47	C2orf44	-2.11
UFL1	-3.78	TDRD9	-2.47	PDSS2	-2.11
EXOC1	-3.71	RWDD2B	-2.45	KIAA0825	-2.10
ALDH3A1	-3.70	PHC3	-2.43	FPGS	-2.09
PANX1	-3.61	ANKDD1B	-2.41	NXPH1	-2.09
CPT1C	-3.59	GALNT18	-2.41	HES7	-2.08
PDLIM2	-3.52	IQCC	-2.39	CCDC157	-2.08
GPNMB	-3.18	GPC2	-2.39	USP49	-2.08
ALOX5	-3.17	C1D	-2.38	RNF146	-2.07
PRKG1	-3.09	RNMTL1	-2.37	ECHDC3	-2.07
TSGA10	-3.03	AHSA1	-2.35	THTPA	-2.07
RUNDC3A	-3.02	GNMT	-2.34	MCCC2	-2.05
FEN1	-2.99	PEX2	-2.33	ERO1L	-2.05
RAB15	-2.99	ARL10	-2.33	ATP6AP1	-2.04
MYCL	-2.97	OIP5	-2.33	STIM2	-2.03
DBR1	-2.97	DHX33	-2.32	GTPBP2	-2.03
HSD17B13	-2.97	TRAM1	-2.32	C14orf169	-2.03
PPT1	-2.97	DOCK5	-2.30	AMOTL2	-2.02
DCK	-2.94	TFB1M	-2.30	ZNF235	-2.02
PTPDC1	-2.84	CYP11A1	-2.28	CCND3	-2.01
DBX1	-2.83	CSRP2BP	-2.28	CAMSAP1	-2.01
ACRC	-2.81	GRIK1	-2.27	OPA3	-2.01
CENPT	-2.76	P2RY11	-2.24	CBR4	-2.00
DHX32	-2.72	B3GNT5	-2.23	PIWIL1	-2.00
TRAM2	-2.68	FRRS1	-2.21	CC2D1B	-1.99
POLR3G	-2.64	TRIM47	-2.21	CCNA1	-1.99
METTL13	-2.64	SMN1	-2.20	ST6GAL1	-1.98
EXOC8	-2.62	SF3A1	-2.20	WDR35	-1.98
UBXN2A	-2.60	ALOXE3	-2.20	TBL3	-1.98
KCNS3	-2.60	ALDH3A2	-2.18	XYLB	-1.97
SLC2A3	-2.58	CCKAR	-2.16	ACTR1A	-1.97
AMY2A	-2.58	CSAD	-2.16	ALKBH6	-1.97
TPH1	-2.56	SYCE3	-2.15	NIT1	-1.96

TBT	FI	TBT	FI	TBT	FI
HRASLS	-1.95	LBX1	-1.86	NELL2	-1.78
TUBB4A	-1.95	CETN3	-1.86	NSF	-1.78
DTWD1	-1.94	KDELC1	-1.85	RCL1	-1.78
ZP3	-1.94	OARD1	-1.85	ZNF214	-1.78
PRPF19	-1.93	UBE2C	-1.85	GGCT	-1.78
ORC3	-1.93	PABPC1L	-1.85	MSRA	-1.78
DDX55	-1.93	GRAP	-1.84	DNMT1	-1.77
AUH	-1.93	SCFD2	-1.84	DOPEY2	-1.77
ORC4	-1.92	EXOSC4	-1.84	PTPRB	-1.77
GLRX	-1.92	C11orf63	-1.83	DND1	-1.77
PTGER3	-1.92	WDR6	-1.83	TRMT2B	-1.77
POC1A	-1.91	ACOT1	-1.83	HIRIP3	-1.77
RCCD1	-1.91	ICA1L	-1.82	CHM	-1.77
TECRL	-1.91	SERPINH1	-1.82	KPNA7	-1.77
CDK2AP2	-1.91	A2M	-1.82	SCLT1	-1.77
RTKN2	-1.90	HEATR1	-1.82	OVCH1	-1.77
KCNN1	-1.90	QTRTD1	-1.82	IFI27L2	-1.76
FANCL	-1.90	ELAVL2	-1.82	RNF17	-1.76
SRSF5	-1.90	UBE2T	-1.82	C4orf29	-1.76
DNAJC2	-1.90	SALL4	-1.82	UCHL5	-1.76
TSR2	-1.90	TACO1	-1.82	GLOD4	-1.76
CNIH1	-1.90	FAM117A	-1.81	PPP2R2A	-1.76
CPA1	-1.90	PWP1	-1.81	PDLIM7	-1.75
FAM19A3	-1.89	CPEB1	-1.81	LSM14B	-1.75
GPR21	-1.89	ALDH9A1	-1.81	DCLRE1A	-1.75
MEGF10	-1.89	NHP2L1	-1.81	C12orf29	-1.75
GTF2A1L	-1.89	ZAR1	-1.81	CDC45	-1.75
AP4B1	-1.89	C12orf5	-1.81	CTU2	-1.75
TRIT1	-1.88	HENMT1	-1.80	FTCDNL1	-1.75
MLH3	-1.88	VPS9D1	-1.80	GINS4	-1.75
ZNF131	-1.88	RAD51	-1.80	PLCXD1	-1.75
PGLYRP2	-1.87	SAAL1	-1.80	SLMAP	-1.74
GDF3	-1.87	GAD1	-1.80	C9orf41	-1.74
FBXO16	-1.87	ATIC	-1.80	POLH	-1.74
FUT10	-1.87	UNCX	-1.80	SPATA18	-1.74
NAPA	-1.86	APTX	-1.79	TEX30	-1.74
TBX20	-1.86	RAB11A	-1.79	SLC30A1	-1.74
USP14	-1.86	TNNT1	-1.79	HBA1	-1.74
LARGE	-1.86	PREP	-1.79	KIAA0101	-1.74
VDAC3	-1.86	ELF3	-1.79	DUT	-1.74

TBT	FI	TBT	FI	TBT	FI
CENPU	-1.73	CST7	-1.69	TRIM36	-1.66
TMEM184B	-1.73	PPIG	-1.69	CCNB1	-1.66
B4GALNT2	-1.73	SHD	-1.69	DISP1	-1.66
PHOX2B	-1.73	SHISA6	-1.69	HYOU1	-1.66
SSX2IP	-1.73	INADL	-1.69	RAD21L1	-1.66
CCNB2	-1.73	GRHL3	-1.69	SELM	-1.66
MMACHC	-1.73	SYNCRIP	-1.69	GKAP1	-1.66
GTF2F1	-1.72	CNOT8	-1.69	KIAA1407	-1.66
STT3A	-1.72	PYCR1	-1.69	PRDM8	-1.66
WDR25	-1.72	RHBDL2	-1.68	SYT9	-1.66
SS18L2	-1.72	BCL2L13	-1.68	TRIM16	-1.66
KRT5	-1.72	MCM3	-1.68	AP1G2	-1.66
SH3D19	-1.72	HSPA14	-1.68	LGALS8	-1.66
GTF3A	-1.72	ERI1	-1.68	MTX1	-1.66
NR2F1	-1.72	TAF1A	-1.68	CDC42EP2	-1.66
AFMID	-1.72	ANGEL1	-1.68	METTL25	-1.66
TXNDC17	-1.72	RADIL	-1.68	GTF2A1	-1.66
DNMT3B	-1.72	ULK4	-1.68	SMPDL3A	-1.66
TOP1MT	-1.71	NINL	-1.68	TUBB4B	-1.66
ST3GAL1	-1.71	POLR1A	-1.68	TUT1	-1.65
SOCS5	-1.71	GPAT2	-1.68	TXNDC5	-1.65
RNF20	-1.71	ASCC2	-1.68	TRPC4AP	-1.65
NPM2	-1.71	LAMP2	-1.67	ACP5	-1.65
GIMAP7	-1.71	CWC22	-1.67	POU2F1	-1.65
DAZL	-1.71	CENPO	-1.67	NEK2	-1.65
RGS9BP	-1.71	RBM44	-1.67	FANCE	-1.65
RHOG	-1.71	BMPR1B	-1.67	CHTF18	-1.65
APOA4	-1.71	HAUS5	-1.67	JMJD6	-1.65
LARP6	-1.71	SLX4IP	-1.67	SERP1	-1.65
RASSF8	-1.71	APEX1	-1.67	NPM1	-1.65
PYGL	-1.70	ALG2	-1.67	ALKBH2	-1.65
RIF1	-1.70	ST3GAL5	-1.67	TDGF1	-1.65
SLC38A6	-1.70	ALPI	-1.67	UBA2	-1.65
MVK	-1.70	DIEXF	-1.67	APCS	-1.65
C8orf76	-1.70	KIF14	-1.67	YRDC	-1.65
SNX21	-1.70	PCOLCE2	-1.67	DCAF13	-1.65
PHEX	-1.70	PEX11B	-1.67	KIF23	-1.65
PIGS	-1.70	NUP37	-1.67	LBR	-1.65
HIP1R	-1.69	MEI4	-1.67	ERLIN2	-1.65
DENND2D	-1.69	SYNRG	-1.67	CPM	-1.65

TBT	FI	TBT	FI	TBT	FI
HOMER3	-1.65	CD6	-1.63	MCM2	-1.60
MTFR1L	-1.65	UNG	-1.63	PODXL2	-1.60
PAQR3	-1.65	ZP3	-1.63	TRMT5	-1.60
PPOX	-1.65	NEU1	-1.63	EEF2	-1.60
ZBTB40	-1.64	NAP1L1	-1.63	C2H1orf27	-1.60
ANAPC7	-1.64	ADAD1	-1.63	CDC6	-1.60
TRA2B	-1.64	RNLS	-1.62	EIF4G2	-1.60
LIG1	-1.64	SLC35A3	-1.62	LMO7	-1.60
CSE1L	-1.64	ERAP1	-1.62	ORC1	-1.60
EXOSC6	-1.64	GPR180	-1.62	TDRD7	-1.60
SPICE1	-1.64	ILF2	-1.62	SUMF1	-1.60
QARS	-1.64	PATL2	-1.62	ZNF740	-1.60
SEL1L2	-1.64	RPP25	-1.62	IDH3G	-1.60
PLA2G4C	-1.64	TPM1	-1.62	PFN2	-1.60
TBC1D19	-1.64	TTLL12	-1.62	CLK2	-1.60
TCTN2	-1.64	MCM10	-1.62	CTSS	-1.60
NRF1	-1.64	ZMAT1	-1.62	FAAH2	-1.60
ARHGEF39	-1.64	POFUT1	-1.62	TRAF1	-1.60
WEE2	-1.64	TKT	-1.62	OCLN	-1.60
PRDX1	-1.64	NODAL	-1.62	ESCO2	-1.60
KRR1	-1.64	RLIM	-1.62	GLB1L2	-1.60
GYG1	-1.64	EAPP	-1.62	TBPL2	-1.60
GBGT1	-1.64	ELOVL3	-1.62	NAA40	-1.60
MED21	-1.64	ZCCHC17	-1.62	DDX26B	-1.60
SART3	-1.64	IQCK	-1.61	ZC3H15	-1.60
TYMS	-1.64	TRIM14	-1.61	SLC2A7	-1.60
KCNT2	-1.64	IFI27	-1.61	HSPA5	-1.59
OR2AT4	-1.63	TRMT2A	-1.61	SLC25A10	-1.59
EBPL	-1.63	BCL7B	-1.61	ABCB5	-1.59
KIF11	-1.63	PRKG2	-1.61	FKBP6	-1.59
SLC46A1	-1.63	PCM1	-1.61	PIWIL2	-1.59
CTNNA1	-1.63	PPP1R26	-1.61	SYCN	-1.59
GTF3C2	-1.63	NSMCE4A	-1.61	CLDN17	-1.59
SLC12A8	-1.63	SLBP	-1.61	PGAP2	-1.59
CIRH1A	-1.63	CCDC57	-1.61	BORA	-1.59
CHAF1A	-1.63	FAM84B	-1.61	FIGLA	-1.59
NR4A2	-1.63	E2F5	-1.61	FBXL14	-1.59
SASH1	-1.63	ADAM21	-1.61	BMS1	-1.59
TMPO	-1.63	P4HB	-1.61	MCMBP	-1.59
NOL6	-1.63	FANCG	-1.61	SPTAN1	-1.59

TBT	FI	TBT	FI	TBT	FI
FOXR1	-1.59	TTC31	-1.57	ADAT2	-1.56
UNC119	-1.59	TDRD5	-1.57	NF2	-1.56
EIF4A1	-1.59	FKBP1A	-1.57	PDCL3	-1.56
ARL15	-1.58	IGF2BP3	-1.57	FKRP	-1.56
RYR2	-1.58	RHOV	-1.57	OVCA2	-1.56
FAM221A	-1.58	TUBA3C	-1.57	PLK1	-1.56
SUV39H1	-1.58	EML2	-1.57	TRMT6	-1.56
TRIM55	-1.58	MOS	-1.57	TCEA1	-1.56
ZP4	-1.58	PLCD1	-1.57	STARD8	-1.56
BRD8	-1.58	HSDL1	-1.57	RFC4	-1.56
TIMM44	-1.58	BAX	-1.57	PRKAR1B	-1.56
GFRA4	-1.58	TMEM106C	-1.57	DCAF4	-1.56
HMX3	-1.58	CCDC34	-1.57	LDLRAP1	-1.56
NASP	-1.58	ALDH2	-1.57	DDX4	-1.55
KIAA0020	-1.58	DDX3X	-1.57	DNTTIP2	-1.55
HAPLN4	-1.58	THOP1	-1.57	QDPR	-1.55
PIP5K1A	-1.58	WNT11	-1.57	PDIA6	-1.55
TINF2	-1.58	FNBP1L	-1.57	MFSD6	-1.55
UVRAG	-1.58	LPCAT4	-1.57	MCOLN3	-1.55
IRX4	-1.58	ALDH18A1	-1.57	WBSCR22	-1.55
TAF4B	-1.58	TOMM22	-1.57	BBS4	-1.55
DFFA	-1.58	ABCE1	-1.57	CSNK1D	-1.55
CITED2	-1.58	C17orf104	-1.57	FAM65C	-1.55
MTERFD1	-1.58	KLHL35	-1.57	PIAS4	-1.55
IMPDH2	-1.58	TTLL4	-1.57	TRPT1	-1.55
SPSB1	-1.58	MCM4	-1.57	MPND	-1.55
CCDC132	-1.58	TSEN2	-1.56	GDPGP1	-1.55
HMGA1	-1.58	TMEM209	-1.56	LACE1	-1.55
GGNBP2	-1.58	TM9SF4	-1.56	HPS3	-1.55
KIF20A	-1.58	C6orf211	-1.56	MUS81	-1.55
DNAJC9	-1.58	SMARCAD1	-1.56	ESF1	-1.55
TOP2A	-1.57	PACSIN2	-1.56	ATP1A1	-1.55
EFTUD2	-1.57	GRIP2	-1.56	METTL3	-1.55
C2CD4A	-1.57	NOP16	-1.56	C19orf55	-1.55
RAC1	-1.57	TRIP13	-1.56	KPTN	-1.55
DYNLL2	-1.57	FGF8	-1.56	RDH14	-1.55
SLC47A1	-1.57	RFX6	-1.56	DCUN1D1	-1.55
SPINT1	-1.57	UMPS	-1.56	ERAS	-1.55
LRRC42	-1.57	HERC5	-1.56	DPM1	-1.55
TTC39B	-1.57	AP3B1	-1.56	SLC35C2	-1.54

TBT	FI	TBT	FI	TBT	FI
CTSV	-1.54	POLR3D	-1.53	METAP1D	-1.52
CLDN7	-1.54	PTGS1	-1.53	TSPAN13	-1.52
PTTG1	-1.54	NCL	-1.53	TMEM244	-1.52
XPC	-1.54	TMTC3	-1.53	GNL2	-1.52
PRMT2	-1.54	SHQ1	-1.53	ALPL	-1.52
MGAT5	-1.54	NCAPG	-1.53	TRNAU1AP	-1.52
C15orf41	-1.54	SAMD14	-1.53	ATF7IP2	-1.52
FAM136A	-1.54	CXXC1	-1.53	KIAA1211L	-1.52
EMC9	-1.54	WDR75	-1.53	PCF11	-1.52
NMS	-1.54	NIF3L1	-1.53	HTRA2	-1.52
BZW1	-1.54	TMED1	-1.53	AURKA	-1.52
KIAA1919	-1.54	C15orf27	-1.53	PTS	-1.52
FBXO10	-1.54	FRMD7	-1.53	PSAT1	-1.52
CEP78	-1.54	METTL15	-1.53	TTC1	-1.52
PPIL3	-1.54	NCAPD2	-1.53	ZNF346	-1.52
PKIG	-1.54	PRC1	-1.53	SYNGR1	-1.52
FASTKD2	-1.54	EGLN3	-1.53	CPA2	-1.52
BDP1	-1.54	PLEKHF1	-1.53	USP39	-1.52
TMEM54	-1.54	CTPS1	-1.53	SYNE1	-1.52
MAP7	-1.54	DDX56	-1.53	PYGO1	-1.52
UCHL1	-1.54	MYOF	-1.53	PUS3	-1.52
ETF1	-1.54	DNAJC5G	-1.53	CENPE	-1.52
TRMT1	-1.54	URB1	-1.53	FTSJ1	-1.52
IGF1R	-1.54	RNASEH2C	-1.53	MED20	-1.52
SLC16A3	-1.54	RACGAP1	-1.53	ELAVL3	1.50
NUPL1	-1.54	ADO	-1.53	TMEM251	1.50
RIOK2	-1.54	NAT10	-1.53	MUL1	1.50
MED28	-1.54	USF1	-1.53	BGN	1.50
SLC37A3	-1.54	CDC16	-1.52	SYNGR2	1.50
DKC1	-1.54	EIF4A3	-1.52	STAU2	1.50
PDCD2	-1.54	FANCF	-1.52	KIAA1147	1.50
TPI1	-1.54	NRDE2	-1.52	SUN1	1.50
TARS	-1.54	IPO5	-1.52	COMTD1	1.50
TDRKH	-1.53	HNRNPAB	-1.52	CRX	1.50
SNX10	-1.53	HNRNPC	-1.52	ASPDH	1.50
KCNH8	-1.53	GOPC	-1.52	PCDHB3	1.50
ALKBH4	-1.53	RRM2	-1.52	SLC51A	1.50
NKIRAS1	-1.53	PNKP	-1.52	GCDH	1.50
CEBPZ	-1.53	CBX5	-1.52	MTMR3	1.50
MED24	-1.53	PES1	-1.52	ACTN3	1.51

TBT	FI	TBT	FI	TBT	FI
PRDM1	1.51	MOB2	1.52	CREM	1.53
VPS18	1.51	FGFRL1	1.52	SLC6A8	1.53
PPP1CB	1.51	PEX14	1.52	IFI44L	1.53
HLA-DQA2	1.51	NEFH	1.52	VSTM2L	1.53
CATIP	1.51	PLEKHS1	1.52	CYP2J2	1.53
ANKRD49	1.51	GHR	1.52	FGFR3	1.53
ACY3	1.51	H1FX	1.52	PTEN	1.54
CNKSR1	1.51	DNASE2	1.52	PAK7	1.54
GRHPR	1.51	AADACL4	1.52	TM4SF4	1.54
RGS2	1.51	HIP1	1.52	PTPRS	1.54
DAZAP2	1.51	CYYR1	1.52	TBCEL	1.54
SCN4B	1.51	RPS27	1.52	NCCRP1	1.54
METTL9	1.51	COG5	1.52	SLC43A2	1.54
CYP51A1	1.51	STAT5B	1.52	TXNIP	1.54
HSF1	1.51	PPP1R3C	1.52	CUL4A	1.54
TMEM81	1.51	MYBPC3	1.52	SNX12	1.54
ZNF609	1.51	SEC24D	1.52	TFE3	1.54
ATP8B5P	1.51	RASL12	1.52	SLC5A12	1.54
TXLNB	1.51	MUSTN1	1.52	BTG2	1.54
SLC16A2	1.51	ROBO1	1.52	ACMSD	1.54
ZFPM2	1.51	SPSB3	1.53	GPM6B	1.54
SLC39A3	1.51	SKI	1.53	CREBL2	1.54
F3	1.51	KCNJ1	1.53	GNE	1.54
LPIN2	1.51	RNF44	1.53	TNS1	1.54
CCRN4L	1.51	KMT2E	1.53	HSPB8	1.54
TAB2	1.51	POTEE	1.53	IRX1	1.54
ASB14	1.51	HOMER2	1.53	FAM172A	1.54
FOXF1	1.51	KY	1.53	LUM	1.54
ZDHHC3	1.51	ALLC	1.53	POSTN	1.54
ZBTB20	1.51	SLC25A38	1.53	OLFML2A	1.54
CTSB	1.52	ASB10	1.53	TAP2	1.54
TBX15	1.52	DEPTOR	1.53	CYP2W1	1.54
NAALADL1	1.52	FZD3	1.53	DENND2A	1.54
COL6A3	1.52	GPD1	1.53	RASD1	1.55
SGK2	1.52	FLI1	1.53	HPN	1.55
CRYBB3	1.52	NOTCH2	1.53	SLC25A48	1.55
LRP1	1.52	THBS2	1.53	TEK	1.55
ATF6B	1.52	GMPR	1.53	COL15A1	1.55
OBSCN	1.52	DTX1	1.53	MEGF8	1.55
ROM1	1.52	CHD3	1.53	CPEB4	1.55

TBT	FI	TBT	FI	TBT	FI
GRN	1.55	PER1	1.56	C9orf116	1.58
PLAC8	1.55	HIST1H1C	1.56	SLC2A5	1.58
CGA	1.55	SGK1	1.56	NPTX2	1.58
CREB3L3	1.55	MORN3	1.56	CFHR2	1.58
ATP1A3	1.55	EZR	1.56	SLC25A32	1.58
CXCL12	1.55	AP1S3	1.56	UROC1	1.58
MICA	1.55	CDON	1.57	MEF2C	1.58
SMOX	1.55	THBS1	1.57	SIX2	1.58
PLXNB2	1.55	ASB2	1.57	STOM	1.58
ENPP6	1.55	COBL	1.57	MEF2A	1.58
BAZ2B	1.55	CRYBA1	1.57	MYOD1	1.58
RHO	1.55	FILIP1L	1.57	CLRN3	1.59
SP5	1.55	BNIP3	1.57	PAPL	1.59
ATG4A	1.55	F8	1.57	CALCOCO2	1.59
ZMIZ1	1.55	COL11A2	1.57	AGPAT9	1.59
COL8A1	1.55	PDHX	1.57	ACKR3	1.59
CRTC2	1.56	MYL7	1.57	RGS4	1.59
SAMD11	1.56	STOML3	1.57	KLF6	1.59
ATP2B1	1.56	PDZK1IP1	1.57	NFIX	1.59
FBXO36	1.56	GABARAPL	1.57	SMAD9	1.59
HAMP	1.56	CENPV	1.57	SH3PXD2A	1.59
BHLHE41	1.56	MMP14	1.57	DDIT4	1.59
SLC52A1	1.56	CLDN5	1.57	FOXA3	1.59
EDN1	1.56	GP1BB	1.57	CCNF	1.59
WBP11	1.56	SH3GL3	1.57	CFH	1.59
PARP9	1.56	SESN1	1.57	USP2	1.59
DCST1	1.56	CEBPA	1.57	NDFIP2	1.59
HLF	1.56	HDGFRP3	1.57	SERPING1	1.59
SLC16A10	1.56	LCN15	1.57	RUNX3	1.60
AMFR	1.56	SLC7A8	1.57	SYNPO2L	1.60
TRAF4	1.56	MKNK2	1.57	CLIC5	1.60
STEAP4	1.56	RGMB	1.58	CCDC77	1.60
TTC28	1.56	AKT2	1.58	FTCD	1.60
DNAJC22	1.56	PLXND1	1.58	CIART	1.60
GSTT1	1.56	SLC22A2	1.58	NFIL3	1.60
MATN1	1.56	NR5A1	1.58	MGP	1.60
S1PR4	1.56	ASS1	1.58	RBM47	1.60
LIMS2	1.56	UPP2	1.58	NDRG2	1.60
SOX6	1.56	DYX1C1	1.58	KLHDC3	1.60
TOB1	1.56	ZNRF1	1.58	MAFA	1.60

TBT	FI	TBT	FI	TBT	FI
ATP2A1	1.60	CPE	1.63	CFB	1.66
FGB	1.60	TXLNB	1.63	IGFBP5	1.66
AR	1.60	APP	1.63	TCTE1	1.66
SLC12A7	1.60	ADCK3	1.63	ADRB2	1.66
SNAP23	1.60	UMOD	1.63	CKMT2	1.66
SEC23B	1.60	NANS	1.63	PABPC1	1.66
ANGPTL1	1.60	SST	1.63	SLC10A3	1.66
HTRA1	1.60	FABP1	1.63	VIL1	1.66
ATP2A2	1.61	ITIH3	1.63	APBB1IP	1.66
FGFR1OP2	1.61	C21orf33	1.63	NFIA	1.66
COL6A1	1.61	F10	1.63	KLHL32	1.66
CPPED1	1.61	ARRDC2	1.63	GHR	1.66
ARG2	1.61	MXRA8	1.64	KLHL21	1.66
ORAI1	1.61	H1F0	1.64	PIK3R1	1.66
PLAGL2	1.61	CEP19	1.64	PDK2	1.66
NUAK2	1.61	SMC1B	1.64	MBNL2	1.66
AQP12A	1.61	RUSC2	1.64	CLDN9	1.67
BPHL	1.61	PPAP2C	1.64	LCP1	1.67
MMP9	1.61	IP6K2	1.64	USP8	1.67
SLC34A2	1.61	CFHR1	1.64	GCNT3	1.67
FA2H	1.61	GIMAP5	1.64	ZFP36L1	1.67
COMMD5	1.61	RAB11FIP1	1.64	STXBP1	1.67
SPRY4	1.61	IRS1	1.64	C19H5orf49	1.67
DOCK6	1.61	FAM96A	1.64	STMN2	1.67
DPYSL5	1.61	TPRKB	1.64	ELAVL4	1.67
PROZ	1.62	RYK	1.64	C18orf21	1.67
TBX1	1.62	TF	1.65	MTIF2	1.67
OAZ2	1.62	KLF13	1.65	ANPEP	1.67
P4HA2	1.62	TBX22	1.65	OAT	1.67
NAIF1	1.62	MARK2	1.65	WNK1	1.67
FGFR2	1.62	EXT2	1.65	MSGN1	1.68
LGMN	1.62	GATA2	1.65	RIN2	1.68
HAND1	1.62	SLC26A2	1.65	ENDOD1	1.68
SLC38A2	1.62	GPT	1.65	NT5C2	1.68
BCO2	1.62	SESN3	1.65	PDLIM5	1.68
CYR61	1.62	OGN	1.65	AQP7	1.68
PROC	1.62	FAM46B	1.65	PLK2	1.68
LPHN2	1.62	MYZAP	1.65	GADD45A	1.68
RTN4	1.63	ROPN1L	1.65	TAT	1.68
MYO7B	1.63	VTN	1.65	DDC	1.68

TBT	FI	TBT	FI	TBT	FI
LGALS3BP	1.68	FETUB	1.70	MIXL1	1.72
COL10A1	1.68	OGFR	1.70	COL11A1	1.72
ACTB	1.68	PDE6H	1.70	PLEKHN1	1.72
SYNJ1	1.69	DUSP27	1.70	MYOG	1.72
PKP3	1.69	SERPINA7	1.71	DIO2	1.73
AGXT	1.69	PTRF	1.71	ROR1	1.73
KLHL31	1.69	GIT2	1.71	F7	1.73
DLL4	1.69	SULF2	1.71	COL2A1	1.73
NME5	1.69	FBXO6	1.71	TRMT10B	1.73
DTX3	1.69	CYP7A1	1.71	MAFB	1.73
SLC16A6	1.69	HIPK3	1.71	SLCO2A1	1.73
PNP	1.69	ENDOU	1.71	TMEM43	1.73
PEF1	1.69	GAS6	1.71	SLC38A4	1.73
CYP3A7	1.69	TMEM59L	1.71	COL6A2	1.74
CETP	1.69	CAPSL	1.72	ADAM23	1.74
RBP4	1.70	F2RL1	1.72	BBC3	1.74
CD36	1.70	TNNT2	1.72	ZFR2	1.74
FN1	1.70	MLF1	1.72	DDIT3	1.74
USP28	1.70	SLC27A2	1.72	SAT1	1.74
C8A	1.70	HPX	1.72	SLC40A1	1.74
MFAP4	1.70	SLC1A2	1.72	GIMAP4	1.74
SLC6A19	1.70	ABCA1	1.72	PAPLN	1.74
ZNF385B	1.70	TTYH3	1.72	PHC1	1.74
DSCAM	1.70	RGS3	1.72	CD93	1.74
FOSL2	1.70	TCF7L1	1.72	SLC2A8	1.74
ESR2	1.70	CLDN4	1.72	BCAR1	1.74
ZRANB1	1.70	C4B	1.72	MMP13	1.74
FASN	1.70	CLDN1	1.72	AGT	1.74

TBT	FI	TBT	FI	TBT	FI
HIST1H1E	1.74	HSD11B2	1.78	DIRAS3	1.81
PTPRC	1.74	DIO1	1.78	DUPD1	1.81
APOE	1.74	B3GNTL1	1.78	CCDC113	1.82
PTH	1.75	CLEC4E	1.78	DMRT1	1.82
NYAP2	1.75	HSPB11	1.78	NBL1	1.82
LYRM2	1.75	DCDC2B	1.78	SLC2A4RG	1.82
NET1	1.75	KLHL24	1.78	SMTNL1	1.82
ATP5L	1.75	VGLL2	1.78	C19orf10	1.82
NACA	1.75	BGLAP	1.78	DYNLRB2	1.82
IRF2BP2	1.75	OXT	1.78	EGR3	1.82
FLT1	1.75	TSC22D2	1.79	AMH	1.82
HAPLN1	1.75	MEF2D	1.79	VAV3	1.82
SAA1	1.76	TMPRSS2	1.79	CD38	1.82
SYCP3	1.76	POLL	1.79	NR5A2	1.83
TNS1	1.76	NR1D1	1.79	SMOX	1.83
TTN	1.76	ACTC1	1.79	ARRDC3	1.83
TSPAN17	1.76	IARS	1.79	CTGF	1.83
PELI3	1.76	C9orf9	1.79	WBP2	1.84
MGRN1	1.76	TAGAP	1.79	BTG1	1.84
METTL11B	1.76	JUN	1.80	RAB36	1.84
HBP1	1.76	ACTA2	1.80	BMP1	1.84
HDAC3	1.76	ANTXR2	1.80	MFSD1	1.84
RNF4	1.77	MGAM	1.80	EXOC3L2	1.85
IL15	1.77	ABHD14B	1.80	ANXA4	1.85
ARID5B	1.77	NRP2	1.81	ABRA	1.85
TAGLN	1.77	TIMP2	1.81	SQLE	1.85
ORAOV1	1.77	FAM213A	1.81	COL1A1	1.85
GJB3	1.77	OTP	1.81	RNF207	1.85

TBT	FI	TBT	FI	TBT	FI
SERPINA9	1.86	INSL3	1.91	ZDHHC16	1.98
TLN1	1.86	CHST14	1.91	CFL2	1.99
SLC25A34	1.86	ACE	1.91	SRD5A2	1.99
CAPN8	1.86	CCDC83	1.92	ZFP36L2	1.99
ACBD4	1.86	AHSG	1.92	TNNI1	2.00
HIGD2A	1.86	RIBC1	1.93	SLC25A14	2.00
ADAM28	1.87	CAPN5	1.93	CXCR4	2.00
SIK3	1.87	MID1IP1	1.93	EPGN	2.00
F5	1.87	CYP4F3	1.93	CYTL1	2.00
DIABLO	1.87	SLC16A9	1.93	IER5	2.01
ITIH4	1.87	SPAG6	1.93	KANK2	2.02
HSPB9	1.87	TRIB3	1.94	MS4A4	2.02
IGFN1	1.88	C3	1.94	MAF	2.03
ETS2	1.88	SLC20A2	1.94	ARL4A	2.04
SLC16A12	1.88	NFKBIA	1.94	PRSS48	2.04
TEKT1	1.88	DHDH	1.95	HLA-DMB	2.04
CREG1	1.88	NMRK2	1.95	SPAG1	2.04
DAW1	1.88	TUBA3D	1.95	ZYG11B	2.04
CDH2	1.88	KIF1A	1.96	PIM1	2.04
KRT8	1.88	NR4A1	1.96	STAU1	2.05
FGA	1.88	HSF5	1.97	HORMAD2	2.05
ADD1	1.88	ZC3H12A	1.97	SPON2	2.05
BRF2	1.89	SLC52A3	1.97	ANKRD9	2.06
COL1A2	1.89	PHLDA2	1.97	C22H1orf53	2.06
SLC43A1	1.90	UCP3	1.98	C2	2.06
C4orf22	1.90	CITED4	1.98	TP53INP1	2.07
LPIN1	1.91	TMEM240	1.98	STX11	2.07
ENTPD8	1.91	DMC1	1.98	DNALI1	2.08

TBT	FI	TBT	FI	TBT	FI	TBT	FI
DNAJB13	2.08	SLC13A2	2.31	ERRFI1	2.63	CYP24A1	3.24
DHRS13	2.09	PTGS2	2.33	UHRF1	2.66	DNAI1	3.33
ULK2	2.09	NPTN	2.33	CP	2.67	LIPI	3.37
NOTCH3	2.10	CCNG2	2.34	SULT2B1	2.67	G6PC	3.57
DNASE1L3	2.10	HSD17B7	2.35	CCR9	2.70	FKBP5	3.65
SMYD2	2.11	UCP1	2.37	SCRN3	2.71	C8orf4	3.77
MYBPC2	2.11	IER2	2.38	SIK1	2.73	EGR4	3.78
C4BPA	2.11	DUSP2	2.38	RGS13	2.74	SFXN2	3.87
CRYGS	2.14	CUBN	2.39	ID1	2.75	CEBPB	3.98
IGFBP7	2.15	BID	2.39	CCM2L	2.75	JUNB	4.15
KEAP1	2.17	FAM43A	2.40	CRP	2.76	CYP8B1	4.33
TCAP	2.17	PIGX	2.40	HIF3A	2.88	PCK1	4.41
TALDO1	2.18	DUSP6	2.41	GGACT	2.89	KLF2	4.88
PARP12	2.20	CCL19	2.41	CYB5B	2.92	FOS	5.55
GMNN	2.21	PODNL1	2.43	XKR9	2.95	HBE1	5.75
LCT	2.22	HTATIP2	2.43	GADD45B	2.98	NPAS4	6.00
DUSP5	2.22	NR1D2	2.45	TRIM54	3.01	ITIH2	6.78
SLC15A1	2.24	TSC22D3	2.48	ZNRF2	3.04	JDP2	6.78
KLF4	2.24	MFSD2A	2.49	CHRNB3	3.05	FOSB	7.40
NR0B2	2.24	NKX3-1	2.49	ALDOB	3.05	TCTEX1D2	7.75
ESAM	2.25	ARL5C	2.51	CEBPD	3.07	SOCS3	8.05
KLF9	2.25	DUSP11	2.51	GTF2H1	3.08	MPV17	414.90
NTAN1	2.25	ECHDC1	2.52	FOXQ1	3.08		
OPN1LW	2.26	MIDN	2.53	KRT15	3.13		
SP8	2.26	TTC18	2.53	ADSSL1	3.13		
EGR2	2.29	CYP19A1	2.55	PBDC1	3.13		
TUFT1	2.30	ASPG	2.56	GJB1	3.19		
GSTK1	2.30	C6orf58	2.59	IGFBP1	3.23		

REFERENCES

Abraham E, Palevitch O, Gothilf Y, Zohar Y. 2010. Targeted gonadotropin-releasing hormone-3 neuron ablation in zebrafish: Effects on neurogenesis, neuronal migration, and reproduction. Endocrinology 151:332-340.

Adams M, Reginato MJ, Shao D, Lazar MA, Chatterjee VK. 1997. Transcriptional activation by peroxisome proliferator-activated receptor gamma is inhibited by phosphorylation at a consensus mitogen-activated protein kinase site. The Journal of biological chemistry 272:5128-5132.

Adams MD, Celniker SE, Holt RA, Evans CA, Gocayne JD, Amanatides PG, et al. 2000. The genome sequence of drosophila melanogaster. Science 287:2185-2195.

Adewale HB, Jefferson WN, Newbold RR, Patisaul HB. 2009. Neonatal bisphenol-a exposure alters rat reproductive development and ovarian morphology without impairing activation of gonadotropin-releasing hormone neurons. Biology of reproduction 81:690-699.

Ahdieh HB, Wade GN. 1982. Effects of hysterectomy on sexual receptivity, food intake, running wheel activity, and hypothalamic estrogen and progestin receptors in rats. Journal of comparative and physiological psychology 96:886-892.

Ainslie DA, Morris MJ, Wittert G, Turnbull H, Proietto J, Thorburn AW. 2001. Estrogen deficiency causes central leptin insensitivity and increased hypothalamic neuropeptide y. International journal of obesity and related metabolic disorders : journal of the International Association for the Study of Obesity 25:1680-1688.

Akahori Y, Nakai M, Yamasaki K, Takatsuki M, Shimohigashi Y, Ohtaki M. 2008. Relationship between the results of in vitro receptor binding assay to human estrogen receptor alpha and in vivo uterotrophic assay: Comparative study with 65 selected chemicals. Toxicology in vitro : an international journal published in association with BIBRA 22:225-231.

Aktar MW, Sengupta D, Purkait S, Ganguly M, Paramasivam M. 2008. Degradation dynamics and dissipation kinetics of an imidazole fungicide (prochloraz) in aqueous medium of varying ph. Interdisciplinary toxicology 1:203-205.

Anand BK, Brobeck JR. 1951. Hypothalamic control of food intake in rats and cats. The Yale journal of biology and medicine 24:123-140.

Andersen HR, Vinggaard AM, Rasmussen TH, Gjermandsen IM, Bonefeld-Jorgensen EC. 2002. Effects of currently used pesticides in assays for estrogenicity, androgenicity, and aromatase activity in vitro. Toxicology and applied pharmacology 179:1-12.

Andersen HR, Bonefeld-Jorgensen EC, Nielsen F, Jarfeldt K, Jayatissa MN, Vinggaard AM. 2006. Estrogenic effects in vitro and in vivo of the fungicide fenarimol. Toxicology letters 163:142-152.

Ankley GT, Johnson RD. 2004. Small fish models for identifying and assessing the effects of endocrine-disrupting chemicals. ILAR journal / National Research Council, Institute of Laboratory Animal Resources 45:469-483.

Ankley GT, Jensen KM, Durhan EJ, Makynen EA, Butterworth BC, Kahl MD, et al. 2005. Effects of two fungicides with multiple modes of action on reproductive endocrine function in the fathead minnow (pimephales promelas). Toxicological sciences : an official journal of the Society of Toxicology 86:300-308.

Asakawa K, Suster ML, Mizusawa K, Nagayoshi S, Kotani T, Urasaki A, et al. 2008. Genetic dissection of neural circuits by tol2 transposon-mediated gal4 gene and enhancer trapping in zebrafish. Proc Natl Acad Sci U S A 105:1255-1260.

Asarian L, Geary N. 2006. Modulation of appetite by gonadal steroid hormones. Philosophical transactions of the Royal Society of London Series B, Biological sciences 361:1251-1263.
Ashby J, Tinwell H. 1998. Uterotrophic activity of bisphenol a in the immature rat. Environmental health perspectives 106:719-720.
Ashby J, Tinwell H, Haseman J. 1999. Lack of effects for low dose levels of bisphenol a and diethylstilbestrol on the prostate gland of cf1 mice exposed in utero. Regulatory toxicology and pharmacology : RTP 30:156-166.
Ashby J, Tinwell H, Stevens J, Pastoor T, Breckenridge CB. 2002. The effects of atrazine on the sexual maturation of female rats. Regulatory toxicology and pharmacology : RTP 35:468-473.
Ashby J, Odum J, Burns A, Lefevre P. 2005. The reported in vitro anti-estrogen pentachloronitrobenzene enhances the estrogenic activity of estradiol in vivo in the rat. Environmental toxicology and pharmacology 20:199-208.
Baillie-Hamilton PF. 2002. Chemical toxins: A hypothesis to explain the global obesity epidemic. Journal of alternative and complementary medicine 8:185-192.
Baraban SC, Dinday MT, Hortopan GA. 2013. Drug screening in scn1a zebrafish mutant identifies clemizole as a potential dravet syndrome treatment. Nature communications 4:2410.
Bardet PL, Horard B, Robinson-Rechavi M, Laudet V, Vanacker JM. 2002. Characterization of oestrogen receptors in zebrafish (danio rerio). Journal of molecular endocrinology 28:153-163.
Barros RP, Gustafsson JA. 2011. Estrogen receptors and the metabolic network. Cell metabolism 14:289-299.
Beato M. 1989. Gene regulation by steroid hormones. Cell 56:335-344.
Beggel S, Connon R, Werner I, Geist J. 2011. Changes in gene transcription and whole organism responses in larval fathead minnow (pimephales promelas) following short-term exposure to the synthetic pyrethroid bifenthrin. Aquatic toxicology (Amsterdam, Netherlands) 105:180-188.
Bellet EM, van Ravenzwaay B, Hellwig J, Pigott G. 2001. Reproductive toxicity of mcpa (4-chloro-2-methylphenoxyacetic acid) in the rat. International journal of toxicology 20:29-38.
Berger RG, Foster WG, deCatanzaro D. 2010. Bisphenol-a exposure during the period of blastocyst implantation alters uterine morphology and perturbs measures of estrogen and progesterone receptor expression in mice. Reproductive toxicology (Elmsford, NY) 30:393-400.
Biales AD, Bencic DC, Villeneuve DL, Ankley GT, Lattier DL. 2011. Proteomic analysis of zebrafish brain tissue following exposure to the pesticide prochloraz. Aquatic toxicology 105:618-628.
Birsoy K, Chen Z, Friedman J. 2008. Transcriptional regulation of adipogenesis by klf4. Cell metabolism 7:339-347.
Boekelheide K, Campion SN. 2010. Toxicity testing in the 21st century: Using the new toxicity testing paradigm to create a taxonomy of adverse effects. Toxicological sciences : an official journal of the Society of Toxicology 114:20-24.
Bouchard C, Tremblay A, Despres JP, Nadeau A, Lupien PJ, Theriault G, et al. 1990. The response to long-term overfeeding in identical twins. The New England journal of medicine 322:1477-1482.
Bouchard C, Tremblay A, Despres JP, Nadeau A, Lupien PJ, Moorjani S, et al. 1996. Overfeeding in identical twins: 5-year postoverfeeding results. Metabolism: clinical and experimental 45:1042-1050.
Brander SM, He G, Smalling KL, Denison MS, Cherr GN. 2012. The in vivo estrogenic and in vitro anti-estrogenic activity of permethrin and bifenthrin. Environmental toxicology and chemistry / SETAC 31:2848-2855.

Bringolf RB, Belden JB, Summerfelt RC. 2004. Effects of atrazine on fathead minnow in a short-term reproduction assay. Environmental toxicology and chemistry / SETAC 23:1019-1025.
Brobeck JR, Tepperman J, Long CN. 1943. Experimental hypothalamic hyperphagia in the albino rat. The Yale journal of biology and medicine 15:831-853.
Brobeck JR. 1946. Mechanism of the development of obesity in animals with hypothalamic lesions. Physiological reviews 26:541-559.
Brooks CM, Lambert HF. 1946. A study of the effect of limitation of food intake and the method of feeding on the rate of weight gain during hypothalamic obesity in the albino rat. The American journal of physiology 147:695-707.
Brox S, Ritter AP, Kuster E, Reemtsma T. 2014. A quantitative hplc-ms/ms method for studying internal concentrations and toxicokinetics of 34 polar analytes in zebrafish (danio rerio) embryos. Analytical and bioanalytical chemistry 406:4831-4840.
Bryzgalova G, Gao H, Ahren B, Zierath JR, Galuska D, Steiler TL, et al. 2006. Evidence that oestrogen receptor-alpha plays an important role in the regulation of glucose homeostasis in mice: Insulin sensitivity in the liver. Diabetologia 49:588-597.
Bulger WH, Muccitelli RM, Kupfer D. 1978. Studies on the in vivo and in vitro estrogenic activities of methoxychlor and its metabolites. Role of hepatic mono-oxygenase in methoxychlor activation. Biochemical pharmacology 27:2417-2423.
Callard GV, Tarrant AM, Novillo A, Yacci P, Ciaccia L, Vajda S, et al. 2011. Evolutionary origins of the estrogen signaling system: Insights from amphioxus. The Journal of steroid biochemistry and molecular biology 127:176-188.
Calle EE, Rodriguez C, Walker-Thurmond K, Thun MJ. 2003. Overweight, obesity, and mortality from cancer in a prospectively studied cohort of u.S. Adults. The New England journal of medicine 348:1625-1638.
Campfield LA, Smith FJ, Guisez Y, Devos R, Burn P. 1995. Recombinant mouse ob protein: Evidence for a peripheral signal linking adiposity and central neural networks. Science 269:546-549.
Cariou R, Antignac JP, Zalko D, Berrebi A, Cravedi JP, Maume D, et al. 2008. Exposure assessment of french women and their newborns to tetrabromobisphenol-a: Occurrence measurements in maternal adipose tissue, serum, breast milk and cord serum. Chemosphere 73:1036-1041.
Carow B, Rottenberg ME. 2014. Socs3, a major regulator of infection and inflammation. Frontiers in immunology 5:58.
Carrera I, Janody F, Leeds N, Duveau F, Treisman JE. 2008. Pygopus activates wingless target gene transcription through the mediator complex subunits med12 and med13. Proceedings of the National Academy of Sciences of the United States of America 105:6644-6649.
Carvalho L, Heisenberg CP. 2010. The yolk syncytial layer in early zebrafish development. Trends in cell biology 20:586-592.
Cavieres MF, Jaeger J, Porter W. 2002. Developmental toxicity of a commercial herbicide mixture in mice: I. Effects on embryo implantation and litter size. Environmental health perspectives 110:1081-1085.
Cecil JE, Tavendale R, Watt P, Hetherington MM, Palmer CN. 2008. An obesity-associated fto gene variant and increased energy intake in children. The New England journal of medicine 359:2558-2566.
Chan JL, Heist K, DePaoli AM, Veldhuis JD, Mantzoros CS. 2003. The role of falling leptin levels in the neuroendocrine and metabolic adaptation to short-term starvation in healthy men. Journal of Clinical Investigation 111:1409-1421.

Chau P, Fielding PE, Fielding CJ. 2007. Bone morphogenetic protein-1 (bmp-1) cleaves human proapolipoprotein a1 and regulates its activation for lipid binding. Biochemistry 46:8445-8450.
Chen SX, Bogerd J, Garcia-Lopez A, de Jonge H, de Waal PP, Hong WS, et al. 2010. Molecular cloning and functional characterization of a zebrafish nuclear progesterone receptor. Biology of reproduction 82:171-181.
Church C, Moir L, McMurray F, Girard C, Banks GT, Teboul L, et al. 2010. Overexpression of fto leads to increased food intake and results in obesity. Nature genetics 42:1086-1092.
Clifton JD, Lucumi E, Myers MC, Napper A, Hama K, Farber SA, et al. 2010. Identification of novel inhibitors of dietary lipid absorption using zebrafish. PloS one 5:e12386.
Cobb JE, Blanchard SG, Boswell EG, Brown KK, Charifson PS, Cooper JP, et al. 1998. N-(2-benzoylphenyl)-l-tyrosine ppargamma agonists. 3. Structure-activity relationship and optimization of the n-aryl substituent. Journal of medicinal chemistry 41:5055-5069.
Coleman DL, Hummel KP. 1969. Effects of parabiosis of normal with genetically diabetic mice. The American journal of physiology 217:1298-1304.
Coleman DL. 1973. Effects of parabiosis of obese with diabetes and normal mice. Diabetologia 9:294-298.
Connor K, Howell J, Chen I, Liu H, Berhane K, Sciarretta C, et al. 1996. Failure of chloro-s-triazine-derived compounds to induce estrogen receptor-mediated responses in vivo and in vitro. Fundamental and applied toxicology : official journal of the Society of Toxicology 30:93-101.
Coutellier L, Beraki S, Ardestani PM, Saw NL, Shamloo M. 2012. Npas4: A neuronal transcription factor with a key role in social and cognitive functions relevant to developmental disorders. PloS one 7:e46604.
Cray C, Zaias J, Altman NH. 2009. Acute phase response in animals: A review. Comparative medicine 59:517-526.
de Waal PP, Wang DS, Nijenhuis WA, Schulz RW, Bogerd J. 2008. Functional characterization and expression analysis of the androgen receptor in zebrafish (danio rerio) testis. Reproduction (Cambridge, England) 136:225-234.
DeGroot BC, Brander SM. 2014. The role of p450 metabolism in the estrogenic activity of bifenthrin in fish. Aquatic toxicology (Amsterdam, Netherlands) 156:17-20.
DeSesso JM, Scialli AR, White TE, Breckenridge CB. 2014. Multigeneration reproduction and male developmental toxicity studies on atrazine in rats. Birth defects research Part B, Developmental and reproductive toxicology 101:237-253.
Dichtl W, Moraga F, Ares MP, Crisby M, Nilsson J, Lindgren S, et al. 2000. The carboxyl-terminal fragment of alpha1-antitrypsin is present in atherosclerotic plaques and regulates inflammatory transcription factors in primary human monocytes. Molecular cell biology research communications : MCBRC 4:50-61.
Diel P, Schulz T, Smolnikar K, Strunck E, Vollmer G, Michna H. 2000. Ability of xeno- and phytoestrogens to modulate expression of estrogen-sensitive genes in rat uterus: Estrogenicity profiles and uterotropic activity. The Journal of steroid biochemistry and molecular biology 73:1-10.
Diel P, Schmidt S, Vollmer G, Janning P, Upmeier A, Michna H, et al. 2004. Comparative responses of three rat strains (da/han, sprague-dawley and wistar) to treatment with environmental estrogens. Archives of toxicology 78:183-193.
Dina C, Meyre D, Gallina S, Durand E, Korner A, Jacobson P, et al. 2007. Variation in fto contributes to childhood obesity and severe adult obesity. Nature genetics 39:724-726.

Domingues I, Oliveira R, Musso C, Cardoso M, Soares AM, Loureiro S. 2013. Prochloraz effects on biomarkers activity in zebrafish early life stages and adults. Environmental toxicology 28:155-163.
Dreyer C, Krey G, Keller H, Givel F, Helftenbein G, Wahli W. 1992. Control of the peroxisomal beta-oxidation pathway by a novel family of nuclear hormone receptors. Cell 68:879-887.
Du G, Huang H, Hu J, Qin Y, Wu D, Song L, et al. 2013. Endocrine-related effects of perfluorooctanoic acid (pfoa) in zebrafish, h295r steroidogenesis and receptor reporter gene assays. Chemosphere 91:1099-1106.
Dubuc PU. 1985. Effects of estrogen on food intake, body weight, and temperature of male and female obese mice. Proceedings of the Society for Experimental Biology and Medicine Society for Experimental Biology and Medicine (New York, NY) 180:468-473.
Eastwood H, Brown KM, Markovic D, Pieri LF. 2002. Variation in the esr1 and esr2 genes and genetic susceptibility to anorexia nervosa. Molecular psychiatry 7:86-89.
Eddy EM, Washburn TF, Bunch DO, Goulding EH, Gladen BC, Lubahn DB, et al. 1996. Targeted disruption of the estrogen receptor gene in male mice causes alteration of spermatogenesis and infertility. Endocrinology 137:4796-4805.
Eldridge JC, Tennant MK, Wetzel LT, Breckenridge CB, Stevens JT. 1994. Factors affecting mammary tumor incidence in chlorotriazine-treated female rats: Hormonal properties, dosage, and animal strain. Environmental health perspectives 102 Suppl 11:29-36.
Escriva H, Delaunay F, Laudet V. 2000. Ligand binding and nuclear receptor evolution. BioEssays : news and reviews in molecular, cellular and developmental biology 22:717-727.
Evans RM. 1988. The steroid and thyroid hormone receptor superfamily. Science 240:889-895.
Fagot-Campagna A. 2000. Emergence of type 2 diabetes mellitus in children: Epidemiological evidence. Journal of pediatric endocrinology & metabolism : JPEM 13 Suppl 6:1395-1402.
Faulds MH, Zhao C, Dahlman-Wright K, Gustafsson JA. 2012. The diversity of sex steroid action: Regulation of metabolism by estrogen signaling. The Journal of endocrinology 212:3-12.
Feige JN, Gelman L, Rossi D, Zoete V, Metivier R, Tudor C, et al. 2007. The endocrine disruptor monoethyl-hexyl-phthalate is a selective peroxisome proliferator-activated receptor gamma modulator that promotes adipogenesis. The Journal of biological chemistry 282:19152-19166.
Fernandez M, Bianchi M, Lux-Lantos V, Libertun C. 2009. Neonatal exposure to bisphenol a alters reproductive parameters and gonadotropin releasing hormone signaling in female rats. Environmental health perspectives 117:757-762.
Fernandez M, Bourguignon N, Lux-Lantos V, Libertun C. 2010. Neonatal exposure to bisphenol a and reproductive and endocrine alterations resembling the polycystic ovarian syndrome in adult rats. Environmental health perspectives 118:1217-1222.
Fernandez MF, Arrebola JP, Taoufiki J, Navalon A, Ballesteros O, Pulgar R, et al. 2007. Bisphenol-a and chlorinated derivatives in adipose tissue of women. Reproductive toxicology 24:259-264.
Finkelstein EA, Trogdon JG, Cohen JW, Dietz W. 2009. Annual medical spending attributable to obesity: Payer-and service-specific estimates. Health affairs (Project Hope) 28:w822-831.
Fischer J, Koch L, Emmerling C, Vierkotten J, Peters T, Bruning JC, et al. 2009. Inactivation of the fto gene protects from obesity. Nature 458:894-898.
Food and Agriculture Organization of the United Nations. 1978. Pesticide residues in food : 1977, report of the joint meeting of the fao panel of experts on pesticide residues and environment and the who expert committee on pesticide residues held in geneva, 6-15 december 1977 In: FAO plant production and protection paper ; 10 Rev.

Forman BM, Tontonoz P, Chen J, Brun RP, Spiegelman BM, Evans RM. 1995. 15-deoxy-delta 12, 14-prostaglandin j2 is a ligand for the adipocyte determination factor ppar gamma. Cell 83:803-812.
Forsgren KL, Riar N, Schlenk D. 2013. The effects of the pyrethroid insecticide, bifenthrin, on steroid hormone levels and gonadal development of steelhead (oncorhynchus mykiss) under hypersaline conditions. General and comparative endocrinology 186:101-107.
Frayling TM, Timpson NJ, Weedon MN, Zeggini E, Freathy RM, Lindgren CM, et al. 2007. A common variant in the fto gene is associated with body mass index and predisposes to childhood and adult obesity. Science 316:889-894.
Gerken T, Girard CA, Tung YC, Webby CJ, Saudek V, Hewitson KS, et al. 2007. The obesity-associated fto gene encodes a 2-oxoglutarate-dependent nucleic acid demethylase. Science 318:1469-1472.
Gesta S, Bluher M, Yamamoto Y, Norris AW, Berndt J, Kralisch S, et al. 2006. Evidence for a role of developmental genes in the origin of obesity and body fat distribution. Proceedings of the National Academy of Sciences of the United States of America 103:6676-6681.
Gibert Y, Trengove MC, Ward AC. 2013. Zebrafish as a genetic model in pre-clinical drug testing and screening. Current medicinal chemistry 20:2458-2466.
Gluckman PD, Hanson MA, Beedle AS. 2007. Early life events and their consequences for later disease: A life history and evolutionary perspective. American journal of human biology : the official journal of the Human Biology Council 19:1-19.
Goldman JM, Stoker TE, Cooper RL, McElroy WK, Hein JF. 1994. Blockade of ovulation in the rat by the fungicide sodium n-methyldithiocarbamate: Relationship between effects on the luteinizing hormone surge and alterations in hypothalamic catecholamines. Neurotoxicology and teratology 16:257-268.
Goldman JM, Cooper RL, Murr AS. 2007. Reproductive functions and hypothalamic catecholamines in response to the soil fumigant metam sodium: Adaptations to extended exposures. Neurotoxicology and teratology 29:368-376.
Goloubkova T, Ribeiro MF, Rodrigues LP, Cecconello AL, Spritzer PM. 2000. Effects of xenoestrogen bisphenol a on uterine and pituitary weight, serum prolactin levels and immunoreactive prolactin cells in ovariectomized wistar rats. Archives of toxicology 74:92-98.
Gorelick DA, Halpern ME. 2011. Visualization of estrogen receptor transcriptional activation in zebrafish. Endocrinology 152:2690-2703.
Graves RA, Tontonoz P, Spiegelman BM. 1992. Analysis of a tissue-specific enhancer: Arf6 regulates adipogenic gene expression. Molecular and cellular biology 12:1202-1208.
Green S, Chambon P. 1988. Nuclear receptors enhance our understanding of transcription regulation. Trends in genetics : TIG 4:309-314.
Gronemeyer H, Gustafsson JA, Laudet V. 2004. Principles for modulation of the nuclear receptor superfamily. Nature reviews Drug discovery 3:950-964.
Grun F, Blumberg B. 2006. Environmental obesogens: Organotins and endocrine disruption via nuclear receptor signaling. Endocrinology 147:S50-55.
Guerra MT, de Toledo FC, Kempinas Wde G. 2011. In utero and lactational exposure to fenvalerate disrupts reproductive function in female rats. Reproductive toxicology (Elmsford, NY) 32:298-303.
Gutierrez A, Pan L, Groen RW, Baleydier F, Kentsis A, Marineau J, et al. 2014. Phenothiazines induce pp2a-mediated apoptosis in t cell acute lymphoblastic leukemia. The Journal of clinical investigation 124:644-655.

Hagenaars A, Vergauwen L, Benoot D, Laukens K, Knapen D. 2013. Mechanistic toxicity study of perfluorooctanoic acid in zebrafish suggests mitochondrial dysfunction to play a key role in pfoa toxicity. Chemosphere 91:844-856.
Halaas JL, Gajiwala KS, Maffei M, Cohen SL, Chait BT, Rabinowitz D, et al. 1995. Weight-reducing effects of the plasma protein encoded by the obese gene. Science 269:543-546.
Hallakou S, Doare L, Foufelle F, Kergoat M, Guerre-Millo M, Berthault MF, et al. 1997. Pioglitazone induces in vivo adipocyte differentiation in the obese zucker fa/fa rat. Diabetes 46:1393-1399.
Hanna RN, Daly SC, Pang Y, Anglade I, Kah O, Thomas P, et al. 2010. Characterization and expression of the nuclear progestin receptor in zebrafish gonads and brain. Biology of reproduction 82:112-122.
Hao R, Bondesson M, Singh AV, Riu A, McCollum CW, Knudsen TB, et al. 2013. Identification of estrogen target genes during zebrafish embryonic development through transcriptomic analysis. PloS one 8:e79020.
Hardwick JP, Song BJ, Huberman E, Gonzalez FJ. 1987. Isolation, complementary DNA sequence, and regulation of rat hepatic lauric acid omega-hydroxylase (cytochrome p-450la omega). Identification of a new cytochrome p-450 gene family. The Journal of biological chemistry 262:801-810.
Hatch EE, Nelson JW, Qureshi MM, Weinberg J, Moore LL, Singer M, et al. 2008. Association of urinary phthalate metabolite concentrations with body mass index and waist circumference: A cross-sectional study of nhanes data, 1999-2002. Environmental health : a global access science source 7:27.
Hawkins MB, Thornton JW, Crews D, Skipper JK, Dotte A, Thomas P. 2000. Identification of a third distinct estrogen receptor and reclassification of estrogen receptors in teleosts. Proceedings of the National Academy of Sciences of the United States of America 97:10751-10756.
Heine PA, Taylor JA, Iwamoto GA, Lubahn DB, Cooke PS. 2000. Increased adipose tissue in male and female estrogen receptor-alpha knockout mice. Proceedings of the National Academy of Sciences of the United States of America 97:12729-12734.
Herzog W, Sonntag C, Walderich B, Odenthal J, Maischein HM, Hammerschmidt M. 2004. Genetic analysis of adenohypophysis formation in zebrafish. Molecular endocrinology (Baltimore, Md) 18:1185-1195.
Hess RA, Bunick D, Lee KH, Bahr J, Taylor JA, Korach KS, et al. 1997. A role for oestrogens in the male reproductive system. Nature 390:509-512.
Hetherington AW, Ranson SW. 1983. Nutrition classics. The anatomical record, volume 78, 1940: Hypothalamic lesions and adiposity in the rat. Nutrition reviews 41:124-127.
Hirsch KS, Weaver DE, Black LJ, Falcone JF, MacLusky NJ. 1987. Inhibition of central nervous system aromatase activity: A mechanism for fenarimol-induced infertility in the male rat. Toxicology and applied pharmacology 91:235-245.
Holtta-Vuori M, Salo VT, Nyberg L, Brackmann C, Enejder A, Panula P, et al. 2010. Zebrafish: Gaining popularity in lipid research. The Biochemical journal 429:235-242.
Horvath TL. 2005. The hardship of obesity: A soft-wired hypothalamus. Nature neuroscience 8:561-565.
Hossain MS, Larsson A, Scherbak N, Olsson PE, Orban L. 2008. Zebrafish androgen receptor: Isolation, molecular, and biochemical characterization. Biology of reproduction 78:361-369.

Houseknecht KL, Cole BM, Steele PJ. 2002. Peroxisome proliferator-activated receptor gamma (ppargamma) and its ligands: A review. Domestic animal endocrinology 22:1-23.
Hovey RC, Coder PS, Wolf JC, Sielken RL, Jr., Tisdel MO, Breckenridge CB. 2011. Quantitative assessment of mammary gland development in female long evans rats following in utero exposure to atrazine. Toxicological sciences : an official journal of the Society of Toxicology 119:380-390.
Howdeshell KL, Hotchkiss AK, Thayer KA, Vandenbergh JG, vom Saal FS. 1999. Exposure to bisphenol a advances puberty. Nature 401:763-764.
Howe K, Clark MD, Torroja CF, Torrance J, Berthelot C, Muffato M, et al. 2013. The zebrafish reference genome sequence and its relationship to the human genome. Nature 496:498-503.
Hu E, Kim JB, Sarraf P, Spiegelman BM. 1996. Inhibition of adipogenesis through map kinase-mediated phosphorylation of ppargamma. Science 274:2100-2103.
Inadera H, Shimomura A. 2005. Environmental chemical tributyltin augments adipocyte differentiation. Toxicology letters 159:226-234.
Issemann I, Green S. 1990. Activation of a member of the steroid hormone receptor superfamily by peroxisome proliferators. Nature 347:645-650.
Jorgensen A, Andersen O, Bjerregaard P, Rasmussen LJ. 2007. Identification and characterisation of an androgen receptor from zebrafish danio rerio. Comparative biochemistry and physiology Toxicology & pharmacology : CBP 146:561-568.
Jung EM, An BS, Choi KC, Jeung EB. 2012. Potential estrogenic activity of triclosan in the uterus of immature rats and rat pituitary gh3 cells. Toxicology letters 208:142-148.
Kalasekar SM, Zacharia E, Kessler N, Ducharme NA, Gustafsson JA, Kakadiaris IA, et al. 2014. Identification of environmental chemicals that induce yolk malabsorption in zebrafish using automated image segmentation. Reproductive toxicology.
Kang JS, Krauss RS. 2010. Muscle stem cells in developmental and regenerative myogenesis. Current opinion in clinical nutrition and metabolic care 13:243-248.
Kanno J, Onyon L, Peddada S, Ashby J, Jacob E, Owens W. 2003. The oecd program to validate the rat uterotrophic bioassay. Phase 2: Dose-response studies. Environmental health perspectives 111:1530-1549.
Kanoski SE, Davidson TL. 2011. Western diet consumption and cognitive impairment: Links to hippocampal dysfunction and obesity. Physiology & behavior 103:59-68.
Kato H, Ota T, Furuhashi T, Ohta Y, Iguchi T. 2003. Changes in reproductive organs of female rats treated with bisphenol a during the neonatal period. Reproductive toxicology (Elmsford, NY) 17:283-288.
Kendig EL, Buesing DR, Christie SM, Cookman CJ, Gear RB, Hugo ER, et al. 2012. Estrogen-like disruptive effects of dietary exposure to bisphenol a or 17alpha-ethinyl estradiol in cd1 mice. International journal of toxicology 31:537-550.
Kennedy GC. 1950. The hypothalamic control of food intake in rats. Proceedings of the Royal Society of London Series B, Biological sciences 137:535-549.
Kim HS, Han SY, Yoo SD, Lee BM, Park KL. 2001. Potential estrogenic effects of bisphenol-a estimated by in vitro and in vivo combination assays. The Journal of toxicological sciences 26:111-118.
Kim HS, Kang TS, Kang IH, Kim TS, Moon HJ, Kim IY, et al. 2005. Validation study of oecd rodent uterotrophic assay for the assessment of estrogenic activity in sprague-dawley immature female rats. Journal of toxicology and environmental health Part A 68:2249-2262.

Kimmel CB, Ballard WW, Kimmel SR, Ullmann B, Schilling TF. 1995. Stages of embryonic development of the zebrafish. Developmental dynamics : an official publication of the American Association of Anatomists 203:253-310.
Kimura K, Yokoyama K, Sato H, Nordin RB, Naing L, Kimura S, et al. 2005. Effects of pesticides on the peripheral and central nervous system in tobacco farmers in malaysia: Studies on peripheral nerve conduction, brain-evoked potentials and computerized posturography. Industrial health 43:285-294.
Kitamura S, Suzuki T, Sanoh S, Kohta R, Jinno N, Sugihara K, et al. 2005. Comparative study of the endocrine-disrupting activity of bisphenol a and 19 related compounds. Toxicological sciences : an official journal of the Society of Toxicology 84:249-259.
Kliewer SA, Lenhard JM, Willson TM, Patel I, Morris DC, Lehmann JM. 1995. A prostaglandin j2 metabolite binds peroxisome proliferator-activated receptor gamma and promotes adipocyte differentiation. Cell 83:813-819.
Kliewer SA, Sundseth SS, Jones SA, Brown PJ, Wisely GB, Koble CS, et al. 1997. Fatty acids and eicosanoids regulate gene expression through direct interactions with peroxisome proliferator-activated receptors alpha and gamma. Proceedings of the National Academy of Sciences of the United States of America 94:4318-4323.
Kobayashi K, Kubota H, Ohtani K, Hojo R, Miyagawa M. 2012. Lack of effects for dietary exposure of bisphenol a during in utero and lactational periods on reproductive development in rat offspring. The Journal of toxicological sciences 37:565-573.
Koda T, Umezu T, Kamata R, Morohoshi K, Ohta T, Morita M. 2005. Uterotrophic effects of benzophenone derivatives and a p-hydroxybenzoate used in ultraviolet screens. Environmental research 98:40-45.
Kokel D, Bryan J, Laggner C, White R, Cheung CY, Mateus R, et al. 2010. Rapid behavior-based identification of neuroactive small molecules in the zebrafish. Nature chemical biology 6:231-237.
Kokel D, Cheung CY, Mills R, Coutinho-Budd J, Huang L, Setola V, et al. 2013. Photochemical activation of trpa1 channels in neurons and animals. Nature chemical biology 9:257-263.
Krey G, Braissant O, L'Horset F, Kalkhoven E, Perroud M, Parker MG, et al. 1997. Fatty acids, eicosanoids, and hypolipidemic agents identified as ligands of peroxisome proliferator-activated receptors by coactivator-dependent receptor ligand assay. Molecular endocrinology 11:779-791.
Kuiper GG, Enmark E, Pelto-Huikko M, Nilsson S, Gustafsson JA. 1996. Cloning of a novel receptor expressed in rat prostate and ovary. Proceedings of the National Academy of Sciences of the United States of America 93:5925-5930.
Kuiper GG, Carlsson B, Grandien K, Enmark E, Haggblad J, Nilsson S, et al. 1997. Comparison of the ligand binding specificity and transcript tissue distribution of estrogen receptors alpha and beta. Endocrinology 138:863-870.
Kunimatsu T, Yamada T, Ose K, Sunami O, Kamita Y, Okuno Y, et al. 2002. Lack of (anti-) androgenic or estrogenic effects of three pyrethroids (esfenvalerate, fenvalerate, and permethrin) in the hershberger and uterotrophic assays. Regulatory toxicology and pharmacology : RTP 35:227-237.
Laignelet L, Riviere JL, Lhuguenot JC. 1992. Metabolism of an imidazole fungicide (prochloraz) in the rat after oral administration. Food and chemical toxicology : an international journal published for the British Industrial Biological Research Association 30:575-583.

Lalwani ND, Fahl WE, Reddy JK. 1983. Detection of a nafenopin-binding protein in rat liver cytosol associated with the induction of peroxisome proliferation by hypolipidemic compounds. Biochemical and biophysical research communications 116:388-393.
Lalwani ND, Alvares K, Reddy MK, Reddy MN, Parikh I, Reddy JK. 1987. Peroxisome proliferator-binding protein: Identification and partial characterization of nafenopin-, clofibric acid-, and ciprofibrate-binding proteins from rat liver. Proceedings of the National Academy of Sciences of the United States of America 84:5242-5246.
Lamon-Fava S, Asztalos BF, Howard TD, Reboussin DM, Horvath KV, Schaefer EJ, et al. 2010. Association of polymorphisms in genes involved in lipoprotein metabolism with plasma concentrations of remnant lipoproteins and hdl subpopulations before and after hormone therapy in postmenopausal women. Clinical endocrinology 72:169-175.
Lassiter CS, Kelley B, Linney E. 2002. Genomic structure and embryonic expression of estrogen receptor beta a (erbetaa) in zebrafish (danio rerio). Gene 299:141-151.
Laudenslager ML, Wilkinson CW, Carlisle HJ, Hammel HT. 1980. Energy balance in ovariectomized rats with and without estrogen replacement. The American journal of physiology 238:R400-405.
Laws SC, Carey SA, Ferrell JM, Bodman GJ, Cooper RL. 2000. Estrogenic activity of octylphenol, nonylphenol, bisphenol a and methoxychlor in rats. Toxicological sciences : an official journal of the Society of Toxicology 54:154-167.
Lee SG, Kim JY, Chung JY, Kim YJ, Park JE, Oh S, et al. 2013. Bisphenol a exposure during adulthood causes augmentation of follicular atresia and luteal regression by decreasing 17beta-estradiol synthesis via downregulation of aromatase in rat ovary. Environmental health perspectives 121:663-669.
Lee SS, Pineau T, Drago J, Lee EJ, Owens JW, Kroetz DL, et al. 1995. Targeted disruption of the alpha isoform of the peroxisome proliferator-activated receptor gene in mice results in abolishment of the pleiotropic effects of peroxisome proliferators. Molecular and cellular biology 15:3012-3022.
Li X, Ycaza J, Blumberg B. 2011. The environmental obesogen tributyltin chloride acts via peroxisome proliferator activated receptor gamma to induce adipogenesis in murine 3t3-l1 preadipocytes. The Journal of steroid biochemistry and molecular biology 127:9-15.
Linossi EM, Babon JJ, Hilton DJ, Nicholson SE. 2013. Suppression of cytokine signaling: The socs perspective. Cytokine & growth factor reviews 24:241-248.
Liu Y, Yuan C, Chen S, Zheng Y, Zhang Y, Gao J, et al. 2014. Global and cyp19a1a gene specific DNA methylation in gonads of adult rare minnow gobiocypris rarus under bisphenol a exposure. Aquatic toxicology (Amsterdam, Netherlands) 156:10-16.
Liu YJ, Fan HB, Jin Y, Ren CG, Jia XE, Wang L, et al. 2013. Cannabinoid receptor 2 suppresses leukocyte inflammatory migration by modulating the jnk/c-jun/alox5 pathway. The Journal of biological chemistry 288:13551-13562.
Locke AE, Kahali B, Berndt SI, Justice AE, Pers TH, Day FR, et al. 2015. Genetic studies of body mass index yield new insights for obesity biology. Nature 518:197-206.
Long M, Laier P, Vinggaard AM, Andersen HR, Lynggaard J, Bonefeld-Jorgensen EC. 2003. Effects of currently used pesticides in the ahr-calux assay: Comparison between the human tv101l and the rat h4iie cell line. Toxicology 194:77-93.
Loos RJ, Lindgren CM, Li S, Wheeler E, Zhao JH, Prokopenko I, et al. 2008. Common variants near mc4r are associated with fat mass, weight and risk of obesity. Nature genetics 40:768-775.

Louis GW, Hallinger DR, Stoker TE. 2013. The effect of triclosan on the uterotrophic response to extended doses of ethinyl estradiol in the weanling rat. Reproductive toxicology (Elmsford, NY) 36:71-77.
Lubahn DB, Moyer JS, Golding TS, Couse JF, Korach KS, Smithies O. 1993. Alteration of reproductive function but not prenatal sexual development after insertional disruption of the mouse estrogen receptor gene. Proceedings of the National Academy of Sciences of the United States of America 90:11162-11166.
Lubis AR, Widia F, Soegondo S, Setiawati A. 2008. The role of socs-3 protein in leptin resistance and obesity. Acta medica Indonesiana 40:89-95.
Manson JE, Colditz GA, Stampfer MJ, Willett WC, Rosner B, Monson RR, et al. 1990. A prospective study of obesity and risk of coronary heart disease in women. The New England journal of medicine 322:882-889.
Marcus MD, Wildes JE. 2014. Disordered eating in obese individuals. Current opinion in psychiatry 27:443-447.
Mathias JR, Saxena MT, Mumm JS. 2012. Advances in zebrafish chemical screening technologies. Future medicinal chemistry 4:1811-1822.
Matthews JB, Twomey K, Zacharewski TR. 2001. In vitro and in vivo interactions of bisphenol a and its metabolite, bisphenol a glucuronide, with estrogen receptors alpha and beta. Chemical research in toxicology 14:149-157.
McCollum CW, Ducharme NA, Bondesson M, Gustafsson JA. 2011. Developmental toxicity screening in zebrafish. Birth defects research Part C, Embryo today : reviews 93:67-114.
McGonnell IM, Fowkes RC. 2006. Fishing for gene function--endocrine modelling in the zebrafish. The Journal of endocrinology 189:425-439.
McMillen IC, MacLaughlin SM, Muhlhausler BS, Gentili S, Duffield JL, Morrison JL. 2008. Developmental origins of adult health and disease: The role of periconceptional and foetal nutrition. Basic & clinical pharmacology & toxicology 102:82-89.
Mehmood Z, Smith AG, Tucker MJ, Chuzel F, Carmichael NG. 2000. The development of methods for assessing the in vivo oestrogen-like effects of xenobiotics in cd-1 mice. Food and chemical toxicology : an international journal published for the British Industrial Biological Research Association 38:493-501.
Mendoza-Rodriguez CA, Garcia-Guzman M, Baranda-Avila N, Morimoto S, Perrot-Applanat M, Cerbon M. 2011. Administration of bisphenol a to dams during perinatal period modifies molecular and morphological reproductive parameters of the offspring. Reproductive toxicology (Elmsford, NY) 31:177-183.
Menuet A, Pellegrini E, Anglade I, Blaise O, Laudet V, Kah O, et al. 2002. Molecular characterization of three estrogen receptor forms in zebrafish: Binding characteristics, transactivation properties, and tissue distributions. Biology of reproduction 66:1881-1892.
Milan DJ, Peterson TA, Ruskin JN, Peterson RT, MacRae CA. 2003. Drugs that induce repolarization abnormalities cause bradycardia in zebrafish. Circulation 107:1355-1358.
Milligan SR, Balasubramanian AV, Kalita JC. 1998. Relative potency of xenobiotic estrogens in an acute in vivo mammalian assay. Environmental health perspectives 106:23-26.
Miscevic F, Rotstein O, Wen XY. 2012. Advances in zebrafish high content and high throughput technologies. Combinatorial chemistry & high throughput screening 15:515-521.
Moniz AC, Cruz-Casallas PE, Salzgeber SA, Varoli FM, Spinosa HS, Bernardi MM. 2005. Behavioral and endocrine changes induced by perinatal fenvalerate exposure in female rats. Neurotoxicology and teratology 27:609-614.

Moon HJ, Han SY, Shin JH, Kang IH, Kim TS, Hong JH, et al. 2007. Gestational exposure to nonylphenol causes precocious mammary gland development in female rat offspring. The Journal of reproduction and development 53:333-344.
Mukherjee R, Hoener PA, Jow L, Bilakovics J, Klausing K, Mais DE, et al. 2000. A selective peroxisome proliferator-activated receptor-gamma (ppargamma) modulator blocks adipocyte differentiation but stimulates glucose uptake in 3t3-l1 adipocytes. Molecular endocrinology 14:1425-1433.
Muto N, Hirai H, Tanaka T, Itoh N, Tanaka K. 1997. Induction and inhibition of cytochrome p450 isoforms by imazalil, a food contaminant, in mouse small intestine and liver. Xenobiotica; the fate of foreign compounds in biological systems 27:1215-1223.
Nagel SC, Hagelbarger JL, McDonnell DP. 2001. Development of an er action indicator mouse for the study of estrogens, selective er modulators (serms), and xenobiotics. Endocrinology 142:4721-4728.
Nah WH, Park MJ, Gye MC. 2011. Effects of early prepubertal exposure to bisphenol a on the onset of puberty, ovarian weights, and estrous cycle in female mice. Clinical and experimental reproductive medicine 38:75-81.
Nakade K, Pan J, Yoshiki A, Ugai H, Kimura M, Liu B, et al. 2007. Jdp2 suppresses adipocyte differentiation by regulating histone acetylation. Cell death and differentiation 14:1398-1405.
Newbold RR, Bullock BC, McLachlan JA. 1990. Uterine adenocarcinoma in mice following developmental treatment with estrogens: A model for hormonal carcinogenesis. Cancer research 50:7677-7681.
Newbold RR, McLachlan JA. 1996. Transplacental hormonal carcinogenesis: Diethylstilbestrol as an example. Progress in clinical and biological research 394:131-147.
Newbold RR, Jefferson WN, Padilla-Banks E, Walker VR, Pena DS, Developmental Endocrinology Studies G. 2001. Cell response endpoints enhance sensitivity of the immature mouse uterotropic assay. Reproductive toxicology (Elmsford, NY) 15:245-252.
Newbold RR. 2004. Lessons learned from perinatal exposure to diethylstilbestrol. Toxicology and applied pharmacology 199:142-150.
Newbold RR, Padilla-Banks E, Snyder RJ, Jefferson WN. 2005. Developmental exposure to estrogenic compounds and obesity. Birth defects research Part A, Clinical and molecular teratology 73:478-480.
Newbold RR, Padilla-Banks E, Snyder RJ, Phillips TM, Jefferson WN. 2007. Developmental exposure to endocrine disruptors and the obesity epidemic. Reproductive toxicology 23:290-296.
Newbold RR, Padilla-Banks E, Jefferson WN, Heindel JJ. 2008. Effects of endocrine disruptors on obesity. International journal of andrology 31:201-208.
Newbold RR, Padilla-Banks E, Jefferson WN. 2009. Environmental estrogens and obesity. Molecular and cellular endocrinology 304:84-89.
Ng AN, de Jong-Curtain TA, Mawdsley DJ, White SJ, Shin J, Appel B, et al. 2005. Formation of the digestive system in zebrafish: Iii. Intestinal epithelium morphogenesis. Developmental biology 286:114-135.
Nikaido Y, Yoshizawa K, Danbara N, Tsujita-Kyutoku M, Yuri T, Uehara N, et al. 2004. Effects of maternal xenoestrogen exposure on development of the reproductive tract and mammary gland in female cd-1 mouse offspring. Reproductive toxicology 18:803-811.
Nilsson S, Gustafsson JA. 2011. Estrogen receptors: Therapies targeted to receptor subtypes. Clinical pharmacology and therapeutics 89:44-55.

Ogden CL, Carroll MD, Kit BK, Flegal KM. 2012. Prevalence of obesity in the united states, 2009-2010. NCHS data brief:1-8.
Ogden CL, Carroll MD, Kit BK, Flegal KM. 2014. Prevalence of childhood and adult obesity in the united states, 2011-2012. JAMA : the journal of the American Medical Association 311:806-814.
Ohta R, Takagi A, Ohmukai H, Marumo H, Ono A, Matsushima Y, et al. 2012. Ovariectomized mouse uterotrophic assay of 36 chemicals. The Journal of toxicological sciences 37:879-889.
Okuda K, Takiguchi M, Yoshihara S. 2010. In vivo estrogenic potential of 4-methyl-2,4-bis(4-hydroxyphenyl)pent-1-ene, an active metabolite of bisphenol a, in uterus of ovariectomized rat. Toxicology letters 197:7-11.
Papaconstantinou AD, Umbreit TH, Fisher BR, Goering PL, Lappas NT, Brown KM. 2000. Bisphenol a-induced increase in uterine weight and alterations in uterine morphology in ovariectomized b6c3f1 mice: Role of the estrogen receptor. Toxicological sciences : an official journal of the Society of Toxicology 56:332-339.
Papaconstantinou AD, Fisher BR, Umbreit TH, Brown KM. 2002. Increases in mouse uterine heat shock protein levels are a sensitive and specific response to uterotrophic agents. Environmental health perspectives 110:1207-1212.
Papoulias DM, Tillitt DE, Talykina MG, Whyte JJ, Richter CA. 2014. Atrazine reduces reproduction in japanese medaka (oryzias latipes). Aquatic toxicology (Amsterdam, Netherlands) 154:230-239.
Park M, Han J, Ko JJ, Lee WS, Yoon TK, Lee K, et al. 2011. Maternal exposure to fenarimol promotes reproductive performance in mouse offspring. Toxicology letters 205:241-249.
Peal DS, Mills RW, Lynch SN, Mosley JM, Lim E, Ellinor PT, et al. 2011. Novel chemical suppressors of long qt syndrome identified by an in vivo functional screen. Circulation 123:23-30.
Pelleymounter MA, Cullen MJ, Baker MB, Hecht R, Winters D, Boone T, et al. 1995. Effects of the obese gene product on body weight regulation in ob/ob mice. Science 269:540-543.
Peter I, Shearman AM, Vasan RS, Zucker DR, Schmid CH, Demissie S, et al. 2005. Association of estrogen receptor beta gene polymorphisms with left ventricular mass and wall thickness in women. American journal of hypertension 18:1388-1395.
Pine MD, Hiney JK, Lee B, Dees WL. 2008. The pyrethroid pesticide esfenvalerate suppresses the afternoon rise of luteinizing hormone and delays puberty in female rats. Environmental health perspectives 116:1243-1247.
Pinto C, Grimaldi M, Boulahtouf A, Pakdel F, Brion F, Ait-Aissa S, et al. 2014. Selectivity of natural, synthetic and environmental estrogens for zebrafish estrogen receptors. Toxicology and applied pharmacology 280:60-69.
Pogrmic K, Fa S, Dakic V, Kaisarevic S, Kovacevic R. 2009. Atrazine oral exposure of peripubertal male rats downregulates steroidogenesis gene expression in leydig cells. Toxicological sciences : an official journal of the Society of Toxicology 111:189-197.
Poupard G, Andre M, Durliat M, Ballagny C, Boeuf G, Babin PJ. 2000. Apolipoprotein e gene expression correlates with endogenous lipid nutrition and yolk syncytial layer lipoprotein synthesis during fish development. Cell and tissue research 300:251-261.
Prossnitz ER, Barton M. 2011. The g-protein-coupled estrogen receptor gper in health and disease. Nature reviews Endocrinology 7:715-726.
Raldua D, Andre M, Babin PJ. 2008. Clofibrate and gemfibrozil induce an embryonic malabsorption syndrome in zebrafish. Toxicology and applied pharmacology 228:301-314.

Raldua D, Pina B. 2014. In vivo zebrafish assays for analyzing drug toxicity. Expert opinion on drug metabolism & toxicology 10:685-697.
Raubenheimer D, Machovsky-Capuska GE, Gosby AK, Simpson S. 2015. Nutritional ecology of obesity: From humans to companion animals. The British journal of nutrition 113 Suppl:S26-39.
Rayssiguier Y, Gueux E, Nowacki W, Rock E, Mazur A. 2006. High fructose consumption combined with low dietary magnesium intake may increase the incidence of the metabolic syndrome by inducing inflammation. Magnesium research : official organ of the International Society for the Development of Research on Magnesium 19:237-243.
Reddy JK, Goel SK, Nemali MR, Carrino JJ, Laffler TG, Reddy MK, et al. 1986. Transcription regulation of peroxisomal fatty acyl-coa oxidase and enoyl-coa hydratase/3-hydroxyacyl-coa dehydrogenase in rat liver by peroxisome proliferators. Proceedings of the National Academy of Sciences of the United States of America 83:1747-1751.
Reeves GK, Pirie K, Beral V, Green J, Spencer E, Bull D. 2007. Cancer incidence and mortality in relation to body mass index in the million women study: Cohort study. BMJ (Clinical research ed) 335:1134.
Rennekamp AJ, Peterson RT. 2015. 15 years of zebrafish chemical screening. Current Opinion in Chemical Biology 24:58-70.
Rihel J, Prober DA, Arvanites A, Lam K, Zimmerman S, Jang S, et al. 2010. Zebrafish behavioral profiling links drugs to biological targets and rest/wake regulation. Science 327:348-351.
Riu A, Grimaldi M, le Maire A, Bey G, Phillips K, Boulahtouf A, et al. 2011. Peroxisome proliferator-activated receptor gamma is a target for halogenated analogs of bisphenol a. Environmental health perspectives 119:1227-1232.
Riu A, McCollum CW, Pinto CL, Grimaldi M, Hillenweck A, Perdu E, et al. 2014a. Halogenated bisphenol-a analogs act as obesogens in zebrafish larvae (danio rerio). Toxicological sciences : an official journal of the Society of Toxicology.
Riu A, McCollum CW, Pinto CL, Grimaldi M, Hillenweck A, Perdu E, et al. 2014b. Halogenated bisphenol-a analogs act as obesogens in zebrafish larvae (danio rerio). Toxicological sciences : an official journal of the Society of Toxicology 139:48-58.
Rivera OE, Varayoud J, Rodriguez HA, Munoz-de-Toro M, Luque EH. 2011. Neonatal exposure to bisphenol a or diethylstilbestrol alters the ovarian follicular dynamics in the lamb. Reproductive toxicology (Elmsford, NY) 32:304-312.
Robertson AL, Holmes GR, Bojarczuk AN, Burgon J, Loynes CA, Chimen M, et al. 2014. A zebrafish compound screen reveals modulation of neutrophil reverse migration as an anti-inflammatory mechanism. Science translational medicine 6:225ra229.
Robinson-Rechavi M, Carpentier AS, Duffraisse M, Laudet V. 2001. How many nuclear hormone receptors are there in the human genome? Trends in genetics : TIG 17:554-556.
Robinson-Rechavi M, Laudet V. 2003. Bioinformatics of nuclear receptors. Methods in enzymology 364:95-118.
Rodriguez PE, Sanchez MS. 2010. Maternal exposure to triclosan impairs thyroid homeostasis and female pubertal development in wistar rat offspring. Journal of toxicology and environmental health Part A 73:1678-1688.
Rosen ED, Sarraf P, Troy AE, Bradwin G, Moore K, Milstone DS, et al. 1999. Ppar gamma is required for the differentiation of adipose tissue in vivo and in vitro. Molecular cell 4:611-617.
Ross SE, Hemati N, Longo KA, Bennett CN, Lucas PC, Erickson RL, et al. 2000. Inhibition of adipogenesis by wnt signaling. Science 289:950-953.

Ryan BC, Hotchkiss AK, Crofton KM, Gray LE, Jr. 2010. In utero and lactational exposure to bisphenol a, in contrast to ethinyl estradiol, does not alter sexually dimorphic behavior, puberty, fertility, and anatomy of female le rats. Toxicological sciences : an official journal of the Society of Toxicology 114:133-148.
Sabatini PV, Krentz NA, Zarrouki B, Westwell-Roper CY, Nian C, Uy RA, et al. 2013. Npas4 is a novel activity-regulated cytoprotective factor in pancreatic beta-cells. Diabetes 62:2808-2820.
Salaberria I, Hansen BH, Asensio V, Olsvik PA, Andersen RA, Jenssen BM. 2009. Effects of atrazine on hepatic metabolism and endocrine homeostasis in rainbow trout (oncorhynchus mykiss). Toxicology and applied pharmacology 234:98-106.
Schiller V, Zhang X, Hecker M, Schafers C, Fischer R, Fenske M. 2014. Species-specific considerations in using the fish embryo test as an alternative to identify endocrine disruption. Aquatic toxicology (Amsterdam, Netherlands) 155:62-72.
Schlegel A, Stainier DY. 2006. Microsomal triglyceride transfer protein is required for yolk lipid utilization and absorption of dietary lipids in zebrafish larvae. Biochemistry 45:15179-15187.
Schmidt S, Degen GH, Seibel J, Hertrampf T, Vollmer G, Diel P. 2006. Hormonal activity of combinations of genistein, bisphenol a and 17beta-estradiol in the female wistar rat. Archives of toxicology 80:839-845.
Schoonjans K, Staels B, Auwerx J. 1996. Role of the peroxisome proliferator-activated receptor (ppar) in mediating the effects of fibrates and fatty acids on gene expression. Journal of lipid research 37:907-925.
Schopfer FJ, Lin Y, Baker PR, Cui T, Garcia-Barrio M, Zhang J, et al. 2005. Nitrolinoleic acid: An endogenous peroxisome proliferator-activated receptor gamma ligand. Proceedings of the National Academy of Sciences of the United States of America 102:2340-2345.
Schuit SC, Oei HH, Witteman JC, Geurts van Kessel CH, van Meurs JB, Nijhuis RL, et al. 2004. Estrogen receptor alpha gene polymorphisms and risk of myocardial infarction. Jama 291:2969-2977.
Seth A, Stemple DL, Barroso I. 2013. The emerging use of zebrafish to model metabolic disease. Disease models & mechanisms 6:1080-1088.
Shanthalatha A, Madhuranath BN, Yajurvedi HN. 2012. Effect of methomyl formulation, a carbamate pesticide on ovarian follicular development and fertility in albino mice. Journal of environmental biology / Academy of Environmental Biology, India 33:33-37.
Shelby MD, Newbold RR, Tully DB, Chae K, Davis VL. 1996. Assessing environmental chemicals for estrogenicity using a combination of in vitro and in vivo assays. Environmental health perspectives 104:1296-1300.
Shibata T, Matsui K, Nagao K, Shinkai H, Yonemori F, Wakitani K. 1999. Pharmacological profiles of a novel oral antidiabetic agent, jtt-501, an isoxazolidinedione derivative. European journal of pharmacology 364:211-219.
Shibayama H, Kotera T, Shinoda Y, Hanada T, Kajihara T, Ueda M, et al. 2009. Collaborative work on evaluation of ovarian toxicity. 14) two- or four-week repeated-dose studies and fertility study of atrazine in female rats. The Journal of toxicological sciences 34 Suppl 1:SP147-155.
Shim WS, Do MY, Kim SK, Kim HJ, Hur KY, Kang ES, et al. 2006. The long-term effects of rosiglitazone on serum lipid concentrations and body weight. Clinical endocrinology 65:453-459.
Shimizu H, Shimomura Y, Nakanishi Y, Futawatari T, Ohtani K, Sato N, et al. 1997. Estrogen increases in vivo leptin production in rats and human subjects. The Journal of endocrinology 154:285-292.

Silverstein RL, Febbraio M. 2009. Cd36, a scavenger receptor involved in immunity, metabolism, angiogenesis, and behavior. Science signaling 2:re3.
Sisman T, Turkez H. 2010. Toxicologic evaluation of imazalil with particular reference to genotoxic and teratogenic potentials. Toxicology and industrial health 26:641-648.
Sluder AE, Mathews SW, Hough D, Yin VP, Maina CV. 1999. The nuclear receptor superfamily has undergone extensive proliferation and diversification in nematodes. Genome research 9:103-120.
Smemo S, Tena JJ, Kim KH, Gamazon ER, Sakabe NJ, Gomez-Marin C, et al. 2014. Obesity-associated variants within fto form long-range functional connections with irx3. Nature 507:371-375.
Smyth GK, Michaud J, Scott HS. 2005. Use of within-array replicate spots for assessing differential expression in microarray experiments. Bioinformatics 21:2067-2075.
Soloff MS, Szego CM. 1969. Purification of estradiol receptor from rat uterus and blockade of its estrogen-binding function by specific antibody. Biochemical and biophysical research communications 34:141-147.
Somm E, Schwitzgebel VM, Toulotte A, Cederroth CR, Combescure C, Nef S, et al. 2009. Perinatal exposure to bisphenol a alters early adipogenesis in the rat. Environmental health perspectives 117:1549-1555.
Song YM, Sung J, Davey Smith G, Ebrahim S. 2004. Body mass index and ischemic and hemorrhagic stroke: A prospective study in korean men. Stroke; a journal of cerebral circulation 35:831-836.
Stahlhut RW, van Wijngaarden E, Dye TD, Cook S, Swan SH. 2007. Concentrations of urinary phthalate metabolites are associated with increased waist circumference and insulin resistance in adult u.S. Males. Environmental health perspectives 115:876-882.
Steven C, Lehnen N, Kight K, Ijiri S, Klenke U, Harris WA, et al. 2003. Molecular characterization of the gnrh system in zebrafish (danio rerio): Cloning of chicken gnrh-ii, adult brain expression patterns and pituitary content of salmon gnrh and chicken gnrh-ii. General and comparative endocrinology 133:27-37.
Stoker TE, Gibson EK, Zorrilla LM. 2010. Triclosan exposure modulates estrogen-dependent responses in the female wistar rat. Toxicological sciences : an official journal of the Society of Toxicology 117:45-53.
Stouten H, Bessems JG. 1998. Toxicological profile for o-benzyl-p-chlorophenol. Journal of applied toxicology : JAT 18:271-279.
Stratigopoulos G, Padilla SL, LeDuc CA, Watson E, Hattersley AT, McCarthy MI, et al. 2008. Regulation of fto/ftm gene expression in mice and humans. American journal of physiology Regulatory, integrative and comparative physiology 294:R1185-1196.
Suh N, Wang Y, Williams CR, Risingsong R, Gilmer T, Willson TM, et al. 1999. A new ligand for the peroxisome proliferator-activated receptor-gamma (ppar-gamma), gw7845, inhibits rat mammary carcinogenesis. Cancer research 59:5671-5673.
Tabb MM, Blumberg B. 2006. New modes of action for endocrine-disrupting chemicals. Molecular endocrinology 20:475-482.
Talwar GP, Segal SJ, Evans A, Davidson OW. 1964. The binding of estradiol in the uterus: A mechanism for depression of rna synthesis. Proceedings of the National Academy of Sciences of the United States of America 52:1059-1066.

Tan W, Huang H, Wang Y, Wong TY, Wang CC, Leung LK. 2013. Bisphenol a differentially activates protein kinase c isoforms in murine placental tissue. Toxicology and applied pharmacology 269:163-168.
Tan Y, Wang H, Song Y, Yang H, Jia X, Li N. 2012. [potential endocrine disrupting effects of bifenthrin in rats]. Wei sheng yan jiu = Journal of hygiene research 41:399-404.
Tang QQ, Lane MD. 2012. Adipogenesis: From stem cell to adipocyte. Annual review of biochemistry 81:715-736.
Tennant MK, Hill DS, Eldridge JC, Wetzel LT, Breckenridge CB, Stevens JT. 1994. Possible antiestrogenic properties of chloro-s-triazines in rat uterus. Journal of toxicology and environmental health 43:183-196.
Thorpe KL, Hutchinson TH, Hetheridge MJ, Scholze M, Sumpter JP, Tyler CR. 2001. Assessing the biological potency of binary mixtures of environmental estrogens using vitellogenin induction in juvenile rainbow trout (oncorhynchus mykiss). Environmental science & technology 35:2476-2481.
Thorpe KL, Benstead R, Hutchinson TH, Tyler CR. 2007. Associations between altered vitellogenin concentrations and adverse health effects in fathead minnow (pimephales promelas). Aquatic toxicology (Amsterdam, Netherlands) 85:176-183.
Tillitt DE, Papoulias DM, Whyte JJ, Richter CA. 2010. Atrazine reduces reproduction in fathead minnow (pimephales promelas). Aquatic toxicology (Amsterdam, Netherlands) 99:149-159.
Tingaud-Sequeira A, Ouadah N, Babin PJ. 2011. Zebrafish obesogenic test: A tool for screening molecules that target adiposity. Journal of lipid research 52:1765-1772.
Tinwell H, Joiner R, Pate I, Soames A, Foster J, Ashby J. 2000. Uterotrophic activity of bisphenol a in the immature mouse. Regulatory toxicology and pharmacology : RTP 32:118-126.
Tinwell H, Haseman J, Lefevre PA, Wallis N, Ashby J. 2002. Normal sexual development of two strains of rat exposed in utero to low doses of bisphenol a. Toxicological sciences : an official journal of the Society of Toxicology 68:339-348.
Tontonoz P, Hu E, Spiegelman BM. 1994. Stimulation of adipogenesis in fibroblasts by ppar gamma 2, a lipid-activated transcription factor. Cell 79:1147-1156.
Tontonoz P, Spiegelman BM. 2008. Fat and beyond: The diverse biology of ppargamma. Annual review of biochemistry 77:289-312.
Tordjman J. 2003. Regulation of glyceroneogenesis and phosphoenolpyruvate carboxykinase by fatty acids, retinoic acids and thiazolidinediones: Potential relevance to type 2 diabetes. Biochimie 85:1213-1218.
Tzameli I, Fang H, Ollero M, Shi H, Hamm JK, Kievit P, et al. 2004. Regulated production of a peroxisome proliferator-activated receptor-gamma ligand during an early phase of adipocyte differentiation in 3t3-l1 adipocytes. The Journal of biological chemistry 279:36093-36102.
Urasaki A, Asakawa K, Kawakami K. 2008. Efficient transposition of the tol2 transposable element from a single-copy donor in zebrafish. Proc Natl Acad Sci U S A 105:19827-19832.
van der Klaauw AA, Farooqi IS. 2015. The hunger genes: Pathways to obesity. Cell 161:119-132.
Varayoud J, Ramos JG, Bosquiazzo VL, Lower M, Munoz-de-Toro M, Luque EH. 2011. Neonatal exposure to bisphenol a alters rat uterine implantation-associated gene expression and reduces the number of implantation sites. Endocrinology 152:1101-1111.
Vierke L, Staude C, Biegel-Engler A, Drost W, Schulte C. 2012. Perfluorooctanoic acid (pfoa) — main concerns and regulatory developments in europe from an environmental point of view. Environmental Sciences Europe 24.

Vinggaard AM, Hnida C, Breinholt V, Larsen JC. 2000. Screening of selected pesticides for inhibition of cyp19 aromatase activity in vitro. Toxicology in vitro : an international journal published in association with BIBRA 14:227-234.
Vinggaard AM, Nellemann C, Dalgaard M, Jorgensen EB, Andersen HR. 2002. Antiandrogenic effects in vitro and in vivo of the fungicide prochloraz. Toxicological sciences : an official journal of the Society of Toxicology 69:344-353.
Vinggaard AM, Hass U, Dalgaard M, Andersen HR, Bonefeld-Jorgensen E, Christiansen S, et al. 2006. Prochloraz: An imidazole fungicide with multiple mechanisms of action. International journal of andrology 29:186-192.
Wang Y, Porter WW, Suh N, Honda T, Gribble GW, Leesnitzer LM, et al. 2000. A synthetic triterpenoid, 2-cyano-3,12-dioxooleana-1,9-dien-28-oic acid (cddo), is a ligand for the peroxisome proliferator-activated receptor gamma. Molecular endocrinology 14:1550-1556.
Wardle J, Carnell S, Haworth CM, Farooqi IS, O'Rahilly S, Plomin R. 2008. Obesity associated genetic variation in fto is associated with diminished satiety. The Journal of clinical endocrinology and metabolism 93:3640-3643.
Weber GJ, Sepulveda MS, Peterson SM, Lewis SS, Freeman JL. 2013. Transcriptome alterations following developmental atrazine exposure in zebrafish are associated with disruption of neuroendocrine and reproductive system function, cell cycle, and carcinogenesis. Toxicological sciences : an official journal of the Society of Toxicology 132:458-466.
Werner I, Geist J, Okihiro M, Rosenkranz P, Hinton DE. 2002. Effects of dietary exposure to the pyrethroid pesticide esfenvalerate on medaka (oryzias latipes). Marine environmental research 54:609-614.
Whitlock G, Lewington S, Sherliker P, Clarke R, Emberson J, Halsey J, et al. 2009. Body-mass index and cause-specific mortality in 900 000 adults: Collaborative analyses of 57 prospective studies. Lancet 373:1083-1096.
Wolman MA, Jain RA, Liss L, Granato M. 2011. Chemical modulation of memory formation in larval zebrafish. Proceedings of the National Academy of Sciences of the United States of America 108:15468-15473.
Wright HM, Clish CB, Mikami T, Hauser S, Yanagi K, Hiramatsu R, et al. 2000. A synthetic antagonist for the peroxisome proliferator-activated receptor gamma inhibits adipocyte differentiation. The Journal of biological chemistry 275:1873-1877.
Wu G, Bazer FW, Wallace JM, Spencer TE. 2006. Board-invited review: Intrauterine growth retardation: Implications for the animal sciences. Journal of animal science 84:2316-2337.
Wu Z, Rosen ED, Brun R, Hauser S, Adelmant G, Troy AE, et al. 1999. Cross-regulation of c/ebp alpha and ppar gamma controls the transcriptional pathway of adipogenesis and insulin sensitivity. Molecular cell 3:151-158.
Xi W, Lee CK, Yeung WS, Giesy JP, Wong MH, Zhang X, et al. 2011. Effect of perinatal and postnatal bisphenol a exposure to the regulatory circuits at the hypothalamus-pituitary-gonadal axis of cd-1 mice. Reproductive toxicology (Elmsford, NY) 31:409-417.
Xu HE, Lambert MH, Montana VG, Parks DJ, Blanchard SG, Brown PJ, et al. 1999. Molecular recognition of fatty acids by peroxisome proliferator-activated receptors. Molecular cell 3:397-403.
Yajnik CS, Deshmukh US. 2008. Maternal nutrition, intrauterine programming and consequential risks in the offspring. Reviews in endocrine & metabolic disorders 9:203-211.
Yamasaki K, Sawaki M, Takatsuki M. 2000. Immature rat uterotrophic assay of bisphenol a. Environmental health perspectives 108:1147-1150.

Yamasaki K, Sawaki M, Noda S, Imatanaka N, Takatsuki M. 2002a. Subacute oral toxicity study of ethynylestradiol and bisphenol a, based on the draft protocol for the "enhanced oecd test guideline no. 407". Archives of toxicology 76:65-74.
Yamasaki K, Takeyoshi M, Yakabe Y, Sawaki M, Imatanaka N, Takatsuki M. 2002b. Comparison of reporter gene assay and immature rat uterotrophic assay of twenty-three chemicals. Toxicology 170:21-30.
Yeh JR, Munson KM, Elagib KE, Goldfarb AN, Sweetser DA, Peterson RT. 2009. Discovering chemical modifiers of oncogene-regulated hematopoietic differentiation. Nature chemical biology 5:236-243.
Yoshihara R, Utsunomiya K, Gojo A, Ishizawa S, Kanazawa Y, Matoba K, et al. 2009. Association of polymorphism of estrogen receptor-alpha gene with circulating levels of adiponectin in postmenopausal women with type 2 diabetes. Journal of atherosclerosis and thrombosis 16:250-255.
You L, Casanova M, Bartolucci EJ, Fryczynski MW, Dorman DC, Everitt JI, et al. 2002. Combined effects of dietary phytoestrogen and synthetic endocrine-active compound on reproductive development in sprague-dawley rats: Genistein and methoxychlor. Toxicological sciences : an official journal of the Society of Toxicology 66:91-104.
Yu B, Chen QF, Liu ZP, Xu HF, Zhang XP, Xiang Q, et al. 2010. Estrogen receptor alpha and beta expressions in hypothalamus-pituitary-ovary axis in rats exposed lactationally to soy isoflavones and bisphenol a. Biomedical and environmental sciences : BES 23:357-362.
Zhang C, Baker DL, Yasuda S, Makarova N, Balazs L, Johnson LR, et al. 2004. Lysophosphatidic acid induces neointima formation through ppargamma activation. The Journal of experimental medicine 199:763-774.
Zhang Y, Proenca R, Maffei M, Barone M, Leopold L, Friedman JM. 1994. Positional cloning of the mouse obese gene and its human homologue. Nature 372:425-432.
Zhang Y, Gao J, Xu P, Yuan C, Qin F, Liu S, et al. 2014. Low-dose bisphenol a disrupts gonad development and steroidogenic genes expression in adult female rare minnow gobiocypris rarus. Chemosphere 112:435-442.
Zhu Y, Alvares K, Huang Q, Rao MS, Reddy JK. 1993. Cloning of a new member of the peroxisome proliferator-activated receptor gene family from mouse liver. The Journal of biological chemistry 268:26817-26820.
Zou KH, Warfield SK, Bharatha A, Tempany CM, Kaus MR, Haker SJ, et al. 2004. Statistical validation of image segmentation quality based on a spatial overlap index. Academic radiology 11:178-189.
Zuo Z, Chen S, Wu T, Zhang J, Su Y, Chen Y, et al. 2011. Tributyltin causes obesity and hepatic steatosis in male mice. Environmental toxicology 26:79-85.